

---

# A

---

## Accumulation

- ▶ [Deposition](#)
- ▶ [Particle Deposition](#)

---

## Adhesion

- ▶ [Deposition](#)
- ▶ [Particle Deposition](#)

---

## Adhesive

Tharwat Tadros  
Wokingham, Berkshire, UK

---

## Definition

An adhesive is a material capable of holding materials together by surface attachment. Valence forces are not required in order that excellent adhesion be obtained since the van der Waals forces are in themselves sufficient to cause excellent adhesion. The early adhesives were natural products (e.g., glues, starch, natural resins), but most modern adhesives are based on synthetic polymers (e.g., polyacrylates). For an adhesive joint to be formed, the adhesive must

move into the bond area and remain there until the bond is completely established. The rheology of the polymer systems used as adhesives plays a significant part in adhesion. For adhesion to occur, intimate interaction of the adhesive and substrate must occur, and this requires adequate wetting and spreading of the adhesive.

---

## Cross-References

- ▶ [Particle Deposition](#)
- ▶ [Polyelectrolyte Dynamics](#)
- ▶ [Polymers](#)
- ▶ [Rheology](#)
- ▶ [Van der Waals Forces](#)
- ▶ [Wetting](#)

---

## Adsorption

- ▶ [Deposition](#)
- ▶ [Particle Deposition](#)

---

## Adsorption Amount and Adsorption Isotherm

- ▶ [Adsorption Isotherm](#)

## Adsorption Isotherm

Tharwat Tadros  
Wokingham, Berkshire, UK

### Synonyms

[Adsorption amount and adsorption isotherm](#)

### Definition

An adsorption isotherm is a representation of the amount of material (in  $\text{mg m}^{-2}$  or  $\text{mol m}^{-2}$ ) adsorbed on a substrate (solid, liquid, or gas) as a function of the equilibrium concentration (in  $\text{mg m}^{-2}$  or  $\text{mol m}^{-2}$ ) remaining after adsorption, at constant temperature. With materials consisting of small molecules (e.g., alcohol), the adsorption isotherm follows the Freundlich equation ( $w = \alpha C^n$ , where  $w$  is the weight of solute adsorbed per unit mass of solid,  $C$  is the concentration of solute in solution at equilibrium),  $\alpha$  and  $n$  are constants). For surface-active materials (surfactants), the adsorption isotherm follows the Langmuir equation,

$$\frac{\theta}{1 - \theta} = \frac{C_1}{55.51} \exp\left(-\frac{\Delta G_{ads}}{kT}\right)$$

where  $\theta$  is the surface coverage,  $C_1$  is the surfactant concentration ( $\text{mol dm}^{-3}$ ),  $\Delta G$  is the free energy of adsorption,  $k$  is the Boltzmann constant, and  $T$  is the absolute temperature. More complex adsorption isotherms may be obtained with surfactants. With polymers, the adsorption isotherm is of high affinity (first added molecules are completely adsorbed).

### Cross-References

- ▶ [Gibbs Adsorption Isotherm](#)
- ▶ [Polymer Adsorption](#)
- ▶ [Surfactants](#)

## Adsorption of Surfactants

- ▶ [Surfactant Adsorption](#)

## Adsorption Parameters

Tharwat Tadros  
Wokingham, Berkshire, UK

### Synonyms

[Adsorption parameters from adsorption isotherms](#)

### Definition

The adsorption parameters that are obtained from the adsorption isotherms are the following: the amount of adsorption  $\Gamma$  (in  $\text{mg m}^{-2}$  or  $\text{mol m}^{-2}$ ) obtained at various equilibrium concentrations  $C_2$ , the saturation adsorption (the plateau value)  $\Gamma_\infty$ , and the free energy of adsorption  $\Delta G$ . For surfactant adsorption at the air/liquid and liquid/liquid interface,  $\Gamma$  and  $\Gamma_\infty$  are obtained from the variation of surface or interfacial tension  $\gamma$  with surfactant concentration  $C$  and application of the Gibbs adsorption isotherm equation ( $d\gamma/d\ln C = -\Gamma RT$ , where  $R$  is the gas constant and  $T$  is the absolute temperature). For surfactant adsorption at the solid/liquid interface, the adsorption parameters are obtained by fitting the data to the Langmuir equation,  $\Gamma = (\Gamma_\infty b C_2)/(1 + b C_2)$ , where  $b$  is a constant that is related to the free energy of adsorption,  $b = -\Delta G/RT$ .

### Cross-References

- ▶ [Surfactant Adsorption](#)

---

## Adsorption Parameters from Adsorption Isotherms

### ► Adsorption Parameters

---

## Agrochemical Formulations

Tharwat Tadros  
Wokingham, Berkshire, UK

### Synonyms

Colloid aspects of agrochemical formulations

### Keywords

Agrochemicals; Controlled release; Emulsions; Interaction forces; Microemulsions; Microencapsulation; Surfactants; Suspensions; Suspoemulsions

### Definition

Agrochemicals are formulated as emulsions, suspensions, microemulsions, and various controlled-release systems. Control of the interaction forces between the droplets or particles is essential in achieving the long-term physical stability of the formulation as well as optimum application. Various interaction forces must be considered: attractive van der Waals, repulsive electrostatic, or steric forces. Combination of these interaction forces results in various energy-distance curves that determine the state of the system on storage. It is necessary to control the various processes such as creaming or sedimentation, flocculation, Ostwald ripening, coalescence, and phase inversions. This requires the use of effective emulsifiers and dispersants. Methods must be designed to assess and predict the long-term physical stability of the formulation.

### Overview

The formulations of agrochemicals cover a wide range of systems that are prepared to suit a specific application. Agrochemicals are usually effective at several grams to hundreds of grams of active ingredient per 1,000 m<sup>2</sup>. It is, therefore, difficult to apply such a small amount uniformly to the crop. In all cases, the active ingredient is first formulated in a suitable diluent such as water or an organic solvent, and when the formulation is applied, it is further diluted in the spray tank to ensure uniform deposition on spraying. In some cases, an agrochemical is a water soluble compound of which paraquat and glyphosate (both are herbicides) are probably the most familiar. Paraquat is a 2,2 bipyridium salt, and the counterions are normally chloride. It is formulated as a 20 % aqueous solution which on application is simply diluted into water at various ratios (1:50 up to 1:200 depending on the application). To such an aqueous solution, surface active agents (sometimes referred to as wetters) are added which are essential for a number of reasons. The most obvious reason for adding surfactants is to enable the spray solution to adhere to the target surface and spread over it to cover a large area. However, such picture is an oversimplification since the surface active agent plays a more subtle role in the optimization of the biological efficacy. Thus, the choice of the surfactant system in an agrochemical formulation is crucial since it has to perform a number of functions. To date, such a choice is made by a trial-and-error procedure due to the complex nature of application and lack of understanding of the mode of action of the chemical. It is the objective of this essay to apply the basic principle of colloid and interface science in agrochemical formulations, subsequent application, and optimization of biological efficacy.

Most agrochemicals are water-insoluble compounds with various physical properties, which have first to be determined in order to decide on the type of formulation. One of the earliest types of formulations are wettable powders (WP) which are suitable for formulating solid water-insoluble compounds that can be produced in

a powder form. The chemical (which may be micronized) is mixed with a filler such as china clay and a solid surfactant such as sodium alkyl or alkyl aryl sulfate or sulfonate is added. When the powder is added to water, the particles are spontaneously wetter by the medium and an agitation dispersion of the particles takes place. It is clear that the particles should remain suspended in the continuous medium for a period of time depending on the application. Some physical testing methods are available to evaluate the suspensibility of the WP. Clearly, the surfactant system plays a crucial role in wettable powders. In the first place, it enables spontaneous wetting and dispersion of the particles. Secondly, by adsorption on the particle surface, it provides a repulsive force that prevents aggregation of the particles. Such process of aggregation will enhance the settling of the particles and may also cause problems on application such as nozzle blockage.

The second and most familiar type of agrochemical formulations is the emulsifiable concentrates (ECs). This is produced by mixing an agrochemical oil with another one such as xylene or trimethylbenzene or a mixture of various hydrocarbon solvents. Alternatively, a solid pesticide could be dissolved in a specific oil to produce a concentrated solution. In some cases, the pesticide oil may be used without any extra addition of oils. In all cases, a surfactant system (usually a mixture of two or three components) is added for a number of purposes. Firstly, the surfactant enables self-emulsification of the oil on addition to water. This occurs by a complex mechanism that involves a number of physical changes such as lowering of the interfacial tension at the oil/water interface, enhancement of turbulence at that interface with the result of spontaneous production of droplets. Secondly, the surfactant film that adsorbs at the oil/water interface stabilizes the produced emulsion against flocculation and/or coalescence. As we will see in later sections, emulsion breakdown must be prevented; otherwise, excessive creaming or sedimentation or oil separation may take place during application. This results in an inhomogeneous application of the agrochemical on the one hand

and possible losses on the other. The third role of the surfactant system in agrochemicals is in the enhancement of biological efficacy.

In recent years, there has been great demand to replace ECs with concentrated aqueous oil-in-water (o/w) emulsions. Several advantages may be envisaged for such replacements. In the first place, one is able to replace the added oil with water, which is of course much cheaper and environmentally acceptable. Secondly, removal of the oil could help in reducing undesirable effects such as phytotoxicity, skin irritation, etc. Thirdly, by formulating the pesticide as an o/w emulsion and be able to control the droplet size to an optimum value which may be crucial for biological efficacy. Fourthly, water soluble surfactants, which may be desirable for biological optimization, can be added to the aqueous continuous phase. As we will see later, the choice of a surfactant or a mixed surfactant system is crucial for preparation of a stable o/w emulsion. In recent years, macromolecular surfactants have been designed to produce very stable o/w emulsions which could be easily diluted into water and applied without any detrimental effects to the emulsion droplets.

A similar concept has been applied to replace wettable powders, namely with aqueous suspension concentrates (SCs). These systems are more familiar than ECs, and they have been introduced for several decades. Indeed, SCs are probably the most widely used systems in agrochemical formulations. Again, SCs are much more convenient to apply than WPs. Dust hazards are absent, and the formulation can be simply diluted in the spray tanks, without the need of any vigorous agitation. As we will see later, SCs are produced by a two- or three-stage process. The pesticide powder is first dispersed in an aqueous solution of a surfactant or a macromolecule (usually referred to as the dispersing agent) using a high-speed mixer. The resulting suspension is then subjected to a wet milling process (usually bead milling) to break any remaining aggregates or agglomerates and reduce the particle size to smaller values. One usually aims at a particle size distribution ranging from 0.1 to 5  $\mu\text{m}$ ., with an average of 1–2  $\mu\text{m}$ . The surfactant or polymer added adsorbs on the

particle surfaces, resulting in their colloidal stability. The particles need to be maintained stable over a long period of time, since any strong aggregation in the system may cause various problems. Firstly, the aggregates being larger than the primary particles tend to settle faster. Secondly, any gross aggregation may result in lack of dispersion on dilution. The large aggregates can block the spray nozzles and may reduce biological efficacy as a result of the inhomogeneous distribution of the particles on the target surface. Apart from their role in ensuring the colloidal stability of the suspension, surfactants are added to many SCs to enhance their biological efficacy. This is usually produced by solubilization of the insoluble compared in the surfactant micelles. This will be discussed in later entries. Another role, a surfactant may play in SCs is the reduction of crystal growth (Ostwald ripening). The latter process may occur when the solubility of the agrochemical is appreciable (say greater than 100 ppm) and when the SC is polydisperse. The smaller particles will have higher solubility than the larger ones. With time, the small particles dissolve and become deposited on the larger one. Surfactants may reduce this Ostwald ripening by adsorption on the crystal surfaces, thus preventing deposition of the molecules at the surface. This will be described in detail in the entry on SCs.

Very recently, microemulsions are being considered as potential systems for formulating agrochemicals. Microemulsions are isotropic, thermodynamically stable systems consisting of oil, water, and surfactant(s) whereby the free energy of formation of the system is zero or negative. It is obvious why such systems, if can be formulated, are very attractive since they will have an indefinite shelf life (within a certain temperature range). Since the droplet size of microemulsions is very small (usually less than 50 nm), they appear transparent. As we will see later, the microemulsion droplets may be considered as swollen micelles, and hence, they will solubilize the agrochemical. This may result in considerable enhancement of the biological efficacy.

An important application in agrochemicals is that of controlled-release formulations. Several methods are used for controlled release of which microcapsules (CS) are probably the most widely used. These are small particles with size range 1–1,000  $\mu\text{m}$  consisting of a core material and an outer wall. The latter isolates the core material from the environment and protects it from degradation and interaction with other materials. The core active ingredient is designed to be released in a controlled manner as required. Microencapsulation of agrochemicals is usually carried out by interfacial condensation, in situ polymerization or coacervation.

It can be seen from the above short discussion that agrochemical formulations are complex multiphase systems, and their preparation, stabilization, and subsequent application require the application of the basic principles of colloid and interface science, and this is the objective of the present entry (Tadros 1994, 2009). It will start with a section on surfactants and the physical properties of their solutions. This is followed by a section on the interfacial aspects of agrochemical formulations including adsorption of surfactants and polymeric surfactants at the air/liquid, liquid/liquid, and solid/liquid interfaces. The stabilization of dispersions, both electrostatic and steric, is discussed in the next section. The basic principles of colloid and interface science are illustrated in detail by considering emulsion concentrates (EWs) and suspension concentrates (SCs). A summary will be given on microemulsions and controlled release of agrochemical formulations.

## Theory

### Surfactants Used in Agrochemical Formulations

Three main classes may be distinguished, namely anionic, cationic, and amphoteric (Tadros 2005; Holmberg et al. 2003). A useful technical reference is McCutcheon (*Detergents and emulsifiers. Allied, New Jersey, published annually*), which is produced annually to update the list of available surfactants. A recent text by van Os et al.

(van Os et al. 1993) listing the physicochemical properties of selected anionic, cationic, and nonionic surfactants has been published by Elsevier. Another useful text is the Handbook of Surfactants by Porter (1994). It should be mentioned also that a fourth class of surfactants, usually referred to as polymeric surfactants, has been used for many years for preparation of EWs (emulsion concentrates) and SCs (suspension concentrates) and their stabilization.

### Anionic Surfactants

These are the most widely used class of surfactants in agrochemical applications (Linfield 1967; Lucasssen-Reynders 1981). This is due to their relatively low cost of manufacture, and they are practically used in every type of formulation. Linear chains are preferred since they are more effective and more degradable than the branched chains. The most commonly used hydrophilic groups are carboxylates, sulfates, sulfonates, and phosphates. A general formula may be ascribed to anionic surfactants as follows:

Carboxylates :  $C_nH_{2n+1}COO^-X$

Sulfates :  $C_nH_{2n+1}OSO_3^-X$

Sulfonates :  $C_nH_{2n+1}SO_3^-X$

Phosphates :  $C_nH_{2n+1}OPO(OH)O^-X$

with  $n$  being the range 8–16 atoms and the counterion  $X$  is usually  $Na^+$ .

Several other anionic surfactants are commercially available such as sulfosuccinates, isethionates, and taurates, and these are sometimes used for special applications. Below, a brief description of the above anionic classes is given with some of their applications.

### Cationic Surfactants

The most common cationic surfactants are the quaternary ammonium compounds (Jungerman 1970; Rubingh and Holland 1991) with the general formula  $R'R''R'''N^+X^-$ , where  $X^-$  is usually chloride ion and  $R$  represents alkyl groups. A common class of cationics is the alkyl trimethyl ammonium chloride, where  $R$  contains 8–18 C atoms, for example, dodecyl trimethyl ammonium chloride,  $C_{12}H_{25}(CH_3)_3NCl$ . Another cationic surfactant class is that containing two long-chain alkyl groups, that is, dialkyl dimethyl

ammonium chloride, with the alkyl groups having a chain length of 8–18 C atoms. These dialkyl surfactants are less soluble in water than the monoalkyl quaternary compounds, but they are sometimes used in agrochemical formulations as adjuvants and/or rheology modifiers. A special cationic surfactant is alkyl dimethyl benzyl ammonium chloride (sometimes referred to as benzalkonium chloride), which may be also used in some formulations as an adjuvant. Imidazolines can also form quaternaries, the most common product being the ditallow derivative quaternized with dimethyl sulfate.

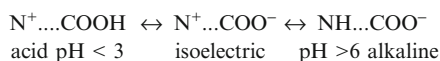
Cationic surfactants can also be modified by incorporating polyethylene oxide chains, for example, dodecyl methyl polyethylene oxide ammonium chloride. Cationic surfactants are generally water soluble when there is only one long alkyl group. They are generally compatible with most inorganic ions and hard water. Cationics are generally stable to pH changes, both acid and alkaline. They are incompatible with most anionic surfactants, but they are compatible with nonionics. These cationic surfactants are insoluble in hydrocarbon oils. In contrast, cationics with two or more long alkyl chains are soluble in hydrocarbon solvents, but they become only dispersible in water (sometimes forming bilayer vesicle type structures). They are generally chemically stable and can tolerate electrolytes. The cmc of cationic surfactants is close to that of anionics with the same alkyl chain length.

### Amphoteric (Zwitterionic) Surfactants

These are surfactants containing both cationic and anionic groups (Buestein and Hiliton 1982). The most common amphoteric are the N-alkyl betaines which are derivatives of trimethyl glycine  $(CH_3)_3NCH_2COOH$  (that was described as betaine). An example of betaine surfactant is lauryl amido propyl dimethyl betaine  $C_{12}H_{25}CON(CH_3)_2CH_2COOH$ . These alkyl betaines are sometimes described as alkyl dimethyl glycinate.

The main characteristic of amphoteric surfactants is their dependence on the pH of the solution in which they are dissolved. In acid pH solutions, the molecule acquires a positive charge and it

behaves like a cationic, whereas in alkaline pH solutions, they become negatively charged and behave like an anionic. A specific pH can be defined at which both ionic groups show equal ionization (the isoelectric point of the molecule). This can be described by the following scheme:



Amphoteric surfactants are sometimes referred to as zwitterionic molecules. They are soluble in water, but the solubility shows a minimum at the isoelectric point. Amphoteric surfactants show excellent compatibility with other surfactants, forming mixed micelles. They are chemically stable both in acids and alkalis. The surface activity of amphoteric surfactants varies widely, and it depends on the distance between the charged groups, and they show a maximum in surface activity at the isoelectric point. Another class of amphoteric surfactants are the N-alkyl amino propionates having the structure  $\text{R-NHCH}_2\text{CH}_2\text{COOH}$ . The NH group is reactive and can react with another acid molecule (e.g., acrylic) to form an amino dipropionate  $\text{R-N}(\text{CH}_2\text{CH}_2\text{COOH})_2$ . Alkyl imidazoline-based product can also be produced by reacting alkyl imidazoline with a chloro acid. However, the imidazoline ring breaks down during the formation of the amphoteric. The change in charge with pH of amphoteric surfactants affects their properties, such as wetting, foaming, etc. At the isoelectric point, the properties of amphoteric surfactants resemble those of nonionics very closely. Below and above the, that is, p, the properties shift toward those of cationic and anionic surfactants, respectively. Zwitterionic surfactants have excellent dermatological properties, and they also exhibit low eye irritation.

### Nonionic Surfactants

The most common nonionic surfactants are those based on ethylene oxide, referred to as ethoxylated surfactants (Schick 1966, 1987; Schonfeldt 1970). Several classes can be distinguished: alcohol ethoxylates, alkyl phenol ethoxylates, fatty acid ethoxylates, monoalkylamide ethoxylates, sorbitan ester ethoxylates, fatty amine ethoxylates, and ethylene oxide – propylene oxide copolymers

(sometimes referred to as polymeric surfactants). Another important class of nonionics are the multihydroxy products such as glycol esters, glycerol (and polyglycerol) esters, glucosides (and polyglucosides), and sucrose esters. Amine oxides and sulfinyl surfactants represent nonionics with a small head group.

### Alcohol Ethoxylates

These are generally produced by ethoxylation of a fatty chain alcohol such as dodecanol. Several generic names are given to this class of surfactants such as ethoxylated fatty alcohols, alkyl polyoxyethylene glycol, and monoalkyl polyethylene oxide glycol ethers. A typical example is dodecyl hexaoxyethylene glycol monoether with the chemical formula  $\text{C}_{12}\text{H}_{25}(\text{OCH}_2\text{CH}_2\text{O})_6\text{OH}$  (sometimes abbreviated as  $\text{C}_{12}\text{E}_6$ ). In practice, the starting alcohol will have a distribution of alkyl chain lengths and the resulting ethoxylate will have a distribution of ethylene oxide chain length. Thus, the numbers listed in the literature refer to average numbers.

The cmc of nonionic surfactants is about two orders of magnitude lower than the corresponding anionics with the same alkyl chain length. The solubility of the alcohol ethoxylates depends both on the alkyl chain length and the number of ethylene oxide units in the molecule. Molecules with an average alkyl chain length of 12 C atoms and containing more than 5 EO units are usually soluble in water at room temperature. However, as the temperature of the solution is gradually raised, the solution becomes cloudy (as a result of dehydration of the PEO chain), and the temperature at which this occurs is referred to as the cloud point (CP) of the surfactant. At a given alkyl chain length, the CP increases with increase in the EO chain of the molecule. The CP changes with change of concentration of the surfactant solution, and the trade literature usually quotes the CP of a 1 % solution. The CP is also affected by the presence of electrolyte in the aqueous solution. Most electrolytes lower the CP of a nonionic surfactant solution. Nonionics tend to have maximum surface activity near to the cloud point. The CP of most nonionics increases markedly on the addition of small quantities of



anionic surfactants. The surface tension of alcohol ethoxylate solutions decreases with decrease in the EO units of the chain. The viscosity of a nonionic surfactant solution increases gradually with increase in its concentration, but at a critical concentration (which depends on the alkyl and EO chain length), the viscosity shows a rapid increase and ultimately a gel-like structure appears. This results from the formation of liquid crystalline structure of the hexagonal type. In many cases, the viscosity reaches a maximum; after which, it shows a decrease due to the formation of other structures (e.g., lamellar phases).

#### Alkyl Phenol Ethoxylates

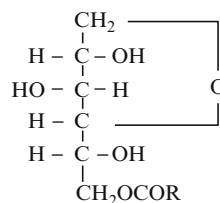
These are prepared by reaction of ethylene oxide with the appropriate alkyl phenol. The most common surfactants of this type are those based on nonyl phenol. These surfactants are cheap to produce, but they suffer from the problem of biodegradability and potential toxicity (the byproduct of degradation is nonyl phenol which has considerable toxicity). In spite of these problems, nonyl phenol ethoxylates are still used in many agrochemical formulations, due to their advantageous properties, such as their solubility both in aqueous and nonaqueous media, their good emulsification and dispersion properties, etc.

#### Fatty Acid Ethoxylates

These are produced by reaction of ethylene oxide with a fatty acid or a polyglycol, and they have the general formula  $\text{RCOO}-(\text{CH}_2\text{CH}_2\text{O})_n\text{H}$ . When a polyglycol is used, a mixture of mono- and diester ( $\text{RCOO}-(\text{CH}_2\text{CH}_2\text{O})_n-\text{OCOR}$ ) is produced. These surfactants are generally soluble in water provided there are enough EO units and the alkyl chain length of the acid is not too long. The monoesters are much more soluble in water than the diesters. In the latter case, a longer EO chain is required to render the molecule soluble. The surfactants are compatible with aqueous ions, provided there is not much unreacted acid. However, these surfactants undergo hydrolysis in highly alkaline solutions.

#### Sorbitan Esters and Their Ethoxylated Derivatives (Spans and Tweens)

The fatty acid esters of sorbitan (generally referred to as Spans, an Atlas commercial trade name) and their ethoxylated derivatives (generally referred to as Tweens) are perhaps one of the most commonly used nonionics. The sorbitan esters are produced by reaction of sorbitol with a fatty acid at a high temperature ( $> 200^\circ \text{C}$ ). The sorbitol dehydrates to 1,4-sorbitan and then esterification takes place. If one mole of fatty acid is reacted with one mole of sorbitol, one obtains a monoester (some diester is also produced as a byproduct). Thus, sorbitan monoester has the following general formula:



The free OH groups in the molecule can be esterified, producing di- and triesters. Several products are available depending on the nature of the alkyl group of the acid and whether the product is a mono-, di-, or triester. Some examples are given below:

Sorbitan monolaurate – Span 20

Sorbitan monopalmitate – Span 40

Sorbitan monostearate – Span 60

Sorbitan monooleate – Span 80

Sorbitan tristearate – Span 65

Sorbitan trioleate – Span 85

The ethoxylated derivatives of Spans (Tweens) are produced by reaction of ethylene oxide on any hydroxyl group remaining on the sorbitan ester group. Alternatively, the sorbitol is first ethoxylated and then esterified. However, the final product has different surfactant properties to the Tweens. Some examples of Tween surfactants are given below:

Polyoxyethylene (20) sorbitan monolaurate – Tween 20

Polyoxyethylene (20) sorbitan monopalmitate – Tween 40



Polyoxyethylene (20) sorbitan monostearate – Tween 60

Polyoxyethylene (20) sorbitan monooleate – Tween 80

Polyoxyethylene (20) sorbitan tristearate – Tween 65

Polyoxyethylene (20) sorbitan trioleate – Tween 85

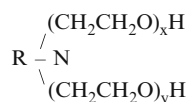
The sorbitan esters are insoluble in water but soluble in most organic solvents (low HLB number surfactants). The ethoxylated products are generally soluble in water, and they have relatively high HLB numbers. One of the main advantages of the sorbitan esters and their ethoxylated derivatives is their approval as food additives. They are also widely used in cosmetics and some pharmaceutical preparations.

#### Ethoxylated Fats and Oils

A number of natural fats and oils have been ethoxylated, for example, linolin (wool fat) and castor oil ethoxylates. These products are useful for application in agrochemical formulations, for example, as solubilizers.

#### Amine Ethoxylates

These are prepared by addition of ethylene oxide to primary or secondary fatty amines. With primary amines, both hydrogen atoms on the amine group react with ethylene oxide and, therefore, the resulting surfactant has the structure,



The above surfactants acquire a cationic character if the EO units are small in number and if the pH is low. However, at high EO levels and neutral pH, they behave very similarly to non-ionics. At low EO content, the surfactants are not soluble in water but become soluble in an acid solution. At high pH, the amine ethoxylates are water soluble provided the alkyl chain length of the compound is not long (usually a C<sub>12</sub> chain is adequate for reasonable solubility at sufficient EO content).

### Surfactants Derived from Mono- and Polysaccharides

Several surfactants were synthesized starting from mono- or oligosaccharides by reaction with the multifunctional hydroxyl groups. The technical problem is one of joining a hydrophobic group to the multihydroxyl structure. Several surfactants were made, for example, esterification of sucrose with fatty acids or fatty glycerides to produce sucrose esters. The most interesting sugar surfactants are the alkyl polyglucosides (APG). These molecules are produced from starch or glucose first by reaction with butanol in the presence of an acid catalyst to produce butyl oligoglycosides intermediate which then reacted with a fatty alcohol such as dodecanol (acid catalyst) to produce dodecyl polyglucoside with a low degree of polymerization  $n$  (1.1–3). The basic raw materials are glucose and fatty alcohols (which may be derived from vegetable oils), and hence these surfactants are sometimes referred to as “environmentally friendly.” A product with  $n = 2$  has two glucose residues with four OH groups on each molecule (i.e., total eight OH groups). The chemistry is more complex and commercial products are mixtures with  $n = 1.1$ –3. The properties of APG surfactants depend upon the alkyl chain length and the average degree of polymerization. APG surfactants have good solubility in water, and they have high cloud points ( $> 100$  °C). They are stable in neutral and alkaline solutions but are unstable in strong acid solutions. APG surfactants can tolerate high electrolyte concentrations, and they are compatible with most types of surfactants.

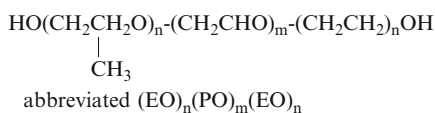
### Speciality Surfactants: Fluorocarbon and Silicone Surfactants

These surfactants can lower the surface tension of water to values below 20 mNm<sup>-1</sup> (most surfactants described above lower the surface tension of water to values above 20 mNm<sup>-1</sup>, typically in the region of 25–27 mNm<sup>-1</sup>). The fluorocarbon and silicone surfactants are sometimes referred to as

superwetters as they cause enhanced wetting and spreading of their aqueous solution. However, they are much more expensive than conventional surfactants and they are only applied for specific applications whereby the low surface tension is a desirable property. Fluorocarbon surfactants have been prepared with various structures consisting of perfluoroalkyl chains and anionic, cationic, amphoteric, and polyethylene oxide polar groups. These surfactants have good thermal and chemical stability, and they are excellent wetting agents for low-energy surfaces. Silicone surfactants, sometimes referred to as organosilicones, are those with polydimethylsiloxane backbone. The silicone surfactants are prepared by incorporation of a water soluble or hydrophilic group into a siloxane backbone. The latter can also be modified by incorporation of a paraffinic hydrophobic chain at the end or along the polysiloxane backbone. The most common hydrophilic groups are EO/PO, and the structures produced are rather complex, and most manufacturers of silicone surfactants do not reveal the exact structure. The mechanism by which these molecules lower the surface tension of water to low values is far from being well understood. The surfactants are widely applied as spreading agents on many hydrophobic surfaces. Incorporating organophilic groups into the backbone of the polydimethyl siloxane backbone can give products that exhibit surface active properties in organic solvents.

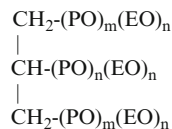
### Polymeric Surfactants: Ethylene Oxide-Propylene Oxide Copolymers (EO/PO)

These surfactants are sold under various trade names, namely, Pluronics (Wyandotte), Synperonic PE (ICI), Ploxomers, etc. Two types may be distinguished: The first type are prepared by reaction of polyoxypropylene glycol (dysfunctional) with EO or mixed EO/PO, giving block copolymers with the structure

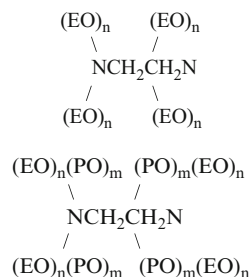


Various molecules are available, where  $n$  and  $m$  are varied systematically.

The second type of EO/PO copolymers are prepared by reaction of polyethylene glycol (difunctional) with PO or mixed EO/PO. These will have the structure  $(\text{PO})_n(\text{EO})_m(\text{PO})_n$ , and they are referred to as reverse Pluronics. Trifunctional products are also available where the starting material is glycerol. These have the structure



Tetrafunctional products are available where the starting material is ethylene diamine. These have the structures

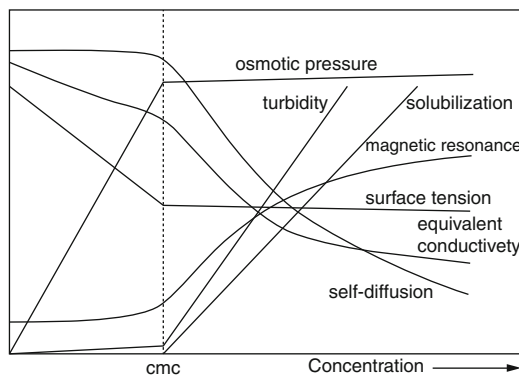


The recent development of speciality polymeric surfactants of the graft type (“comb” structures) has enabled one to obtain specific applications in dispersions. An example of such molecules is the graft copolymer of polymethyl methacrylate backbone with several PEO side chains which has excellent dispersing and stabilizing properties for concentrated dispersions of hydrophobic particles in water. Using such dispersant, one can obtain highly stable concentrated suspensions. These surfactants have been modified in several ways to produce molecules that are suitable as emulsifiers, dispersants in extreme conditions such as high or low pH values, high electrolyte concentrations, temperatures, etc. Other polymeric surfactants that are suitable for dispersing agrochemical particles in nonaqueous media have also been prepared, whereby the side chains were made oil soluble such as polyhydroxystearic acid.

## Properties of Surfactant Solutions

The physical properties of surface active agents differ from those of smaller or non-amphipathic molecules in one major aspect, namely the abrupt changes in their properties above a critical concentration (Lindman 1984). This is illustrated in Fig. 1 in which a number of physical properties (osmotic pressure, turbidity, solubilization, magnetic resonance, surface tension, equivalent conductivity, and self-diffusion) are plotted as a function of concentration for an ionic surfactant (Istraelachvili 1985).

At low concentrations, most properties are similar to those of a simple electrolyte. One notable exception is the surface tension which decreases rapidly with increase in surfactant concentration. However, all the properties (interfacial and bulk) show an abrupt change of a particular concentration that is consistent with the fact that at and above this concentration, surface active ions or molecules in solution associate to form larger units. These associated units are called micelles (self-assembled structures), and the first formed aggregates are generally approximately spherical in shape. The concentration at which this association phenomenon occurs is known as the critical micelle concentration (cmc). Each surfactant molecules has a characteristic cmc value at a given temperature and electrolyte concentration. The most common technique for measuring the cmc is surface tension,  $\gamma$ , which shows break at the cmc; after which,  $\gamma$  remains virtually constant with further increase in concentration. However, other techniques such as self-diffusion measurements, NMR, and fluorescence spectroscopy can be applied. A compilation of cmc values has been given in 1971 by Mukerjee and Mysels (1971), which is clearly not an up-to-date text but is an extremely valuable reference. Electrolytes and nonelectrolytes on the cmc can be very striking. For example, addition of 1:1 electrolyte to a solution of anionic surfactant gives a dramatic lowering of the cmc, which may amount to an order of magnitude. The effect is moderate for short-chain surfactants but is much larger for long-chain ones. At high electrolyte



**Agrochemical Formulations, Fig. 1** Variation of solution properties with concentration for surfactants

concentrations, the reduction in cmc with increase in number of carbon atoms in the alkyl chain is much stronger than without added electrolyte. This rate of decrease at high electrolyte concentrations is comparable to that of nonionics. The effect of added electrolyte also depends on the valency of the added counterions. In contrast, for nonionics, addition of electrolytes causes only small variation in the cmc. Nonelectrolytes such as alcohols can also cause a decrease in the cmc. The alcohols are less polar than water and are distributed between the bulk solution and the micelles. The more preference they have for the micelles, the more they stabilize them. A longer alkyl chain leads to a less favorable location in water and more favorable location in the micelles. The presence of micelles can account for many of the unusual properties of solutions of surface active agents (Elworthy et al. 1968; Shinoda et al. 1963). For example, it can account for the near constant surface tension value, above the cmc (see Fig. 1). It also accounts for the reduction in molar conductance of the surface active agent solution above the cmc, which is consistent with the reduction in mobility of the micelles as a result of counterion. The presence of micelles also accounts for the rapid increase in light scattering or turbidity above the cmc.

The presence of micelles was originally suggested by McBain (1913) who suggested that below the cmc, most of the surfactant molecules

are unassociated, whereas in the isotropic solutions immediately above the cmc, micelles and surfactant ions (molecules) are thought to coexist, the concentration of the latter changing very slightly as more surfactant is dissolved. Typically, the micelles have a closely spherical shape in a rather wide concentration range above the cmc. Originally, it was suggested by Adam (1925) and Hartley (1936) that micelles are spherical in shape and have the following properties: (1) the association unit is spherical with a radius approximately equal to the length of the hydrocarbon chain; (2) the micelle contains about 50–100 monomeric units – aggregation number generally increases with increase in alkyl chain length; (3) with ionic surfactants, most counterions are bound to the micelle surface, thus significantly reducing the mobility from the value to be expected from a micelle with non-counterion bonding; (4) micellization occurs over a narrow concentration range as a result of the high association number of surfactant micelles; (5) the interior of the surfactant micelle has essentially the properties of a liquid hydrocarbon. This is confirmed by the high mobility of the alkyl chains and the ability of the micelles to solubilize many water insoluble organic molecules, for example, dyes and agrochemicals.

Although, the spherical micelle model accounts for many of the physical properties of solutions of surfactants, a number of phenomena remain unexplained, without considering other shapes. For example, McBain (1950) suggested the presence of two types of micelles, spherical and lamellar, in order to account for the drop in molar conductance of surfactant solutions. The lamellar micelles are neutral, and hence they account for the reduction in the conductance. Later, Harkins et al. (1946) used McBain's model of lamellar micelles to interpret his x-ray results in soap solutions. Moreover, many modern techniques such as light scattering and neutron scattering indicate that in many systems, the micelles are not spherical. For example, Debye and Anacker (1951) proposed a cylindrical micelle to explain that light scattering results on hexadecyltrimethyl ammonium bromide in water.

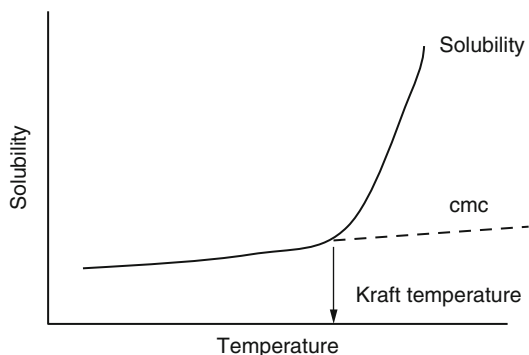
## Solubility–Temperature Relationship for Surfactants

Many ionic surfactants show dramatic temperature-dependent solubility. The solubility may be very low at low temperatures and then increases by orders of magnitude in a relatively narrow temperature range. This is illustrated in Fig. 2 which shows the change of solubility and cmc of sodium decyl sulfonate with temperature. This phenomenon is generally denoted as the Krafft phenomenon with the temperature for the onset of increasing solubility being known as the Krafft temperature. The cmc increases slowly with temperature, and at the Krafft temperature, the solubility is equal to the cmc. At this temperature, there is an equilibrium between hydrated surfactant solid, micelles, and monomers (triple point). The Krafft temperature may vary dramatically with subtle changes in the surfactant chemical structure. In general, the Krafft temperature increases rapidly as the alkyl chain length of the surfactant increases. It decreases with increase in the alkyl chain distribution of the surfactant. It also depends on the head group and counterion. Addition of electrolytes causes an increase in the Krafft temperature.

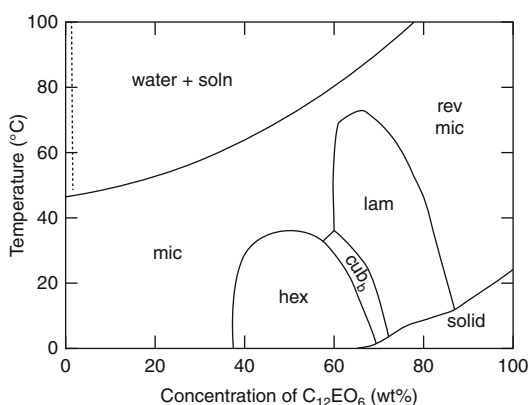
With nonionic surfactants of the ethoxylate type, increase of temperature for a solution at a given concentration causes dehydration of the polyethylene oxide (PEO) chains, and at a critical temperature, the solution becomes cloudy. This is illustrated in Fig. 3 which shows the phase diagram of  $C_{12}E_6$ . Below the cloud point (CP) curve, one can identify different liquid crystalline phases, Hexagonal – Cubic – Lamellar, which are schematically shown in Fig. 4.

## Interfacial Aspects of Agrochemical Formulations

Several interfacial aspects must be considered when dealing with agrochemical formulations: (1) Adsorption of surfactants at the air/liquid interface both equilibrium and dynamic aspects. These determine spray formation (spray droplet spectrum), impaction, and adhesion of droplets



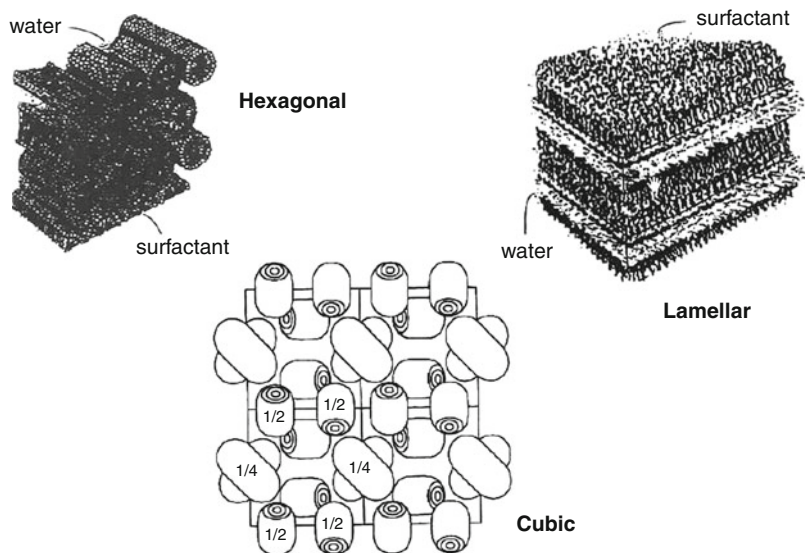
**Agrochemical Formulations, Fig. 2** Variation of solubility and critical micelle concentration (cmc) with temperature



**Agrochemical Formulations, Fig. 3** Phase diagram of nonionic surfactants

on leaf surfaces as well as the various wetting and spreading phenomena. (2) Adsorption of surfactants at the oil/water interface which determines emulsion formation and their stability. This subject is also important when dealing with microemulsions. (3) Adsorption of surfactants and polymeric at the solid/liquid interface. This is important when dealing with dispersion of agrochemical powders in liquids, preparation of suspension concentrates, and their stabilization.

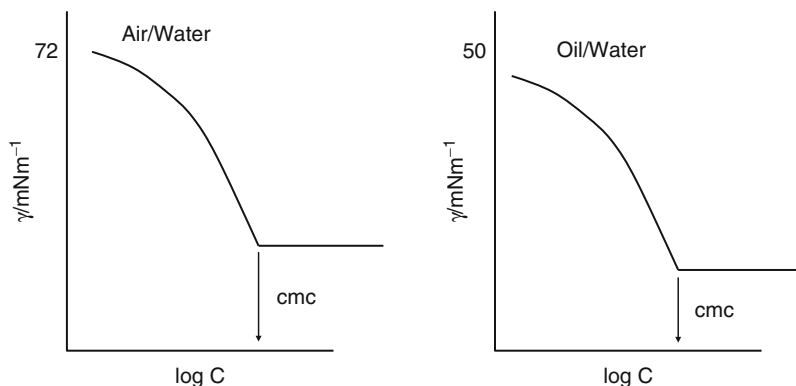
This section will deal with the above interfacial aspects starting with the equilibrium aspects of surfactant adsorption at the air/water and oil/water interfaces. Due to the equilibrium aspects of adsorption (rate of adsorption is equal to the rate of desorption), one can apply the second law of thermodynamics as analyzed by Gibbs (see below). This is followed by a section on dynamic aspects of surfactant adsorption, particularly the concept of dynamic surface tension and the techniques that can be applied in its measurement. The adsorption of surfactants both on hydrophobic surfaces (which represent the case of most agrochemical solids) as well as on hydrophilic surfaces (such as oxides) will be analyzed using the Langmuir adsorption isotherms. The structure of surfactant layers on solid surfaces will be described. The subject of polymeric surfactant adsorption will be dealt with separately due to its complex nature, namely



**Agrochemical Formulations, Fig. 4** Schematic picture of liquid crystalline phases

### Agrochemical Formulations,

**Fig. 5** Surface or interfacial tension – log C curves



irreversibility of adsorption and conformation of the polymer at the solid/liquid interface.

### Equilibrium Adsorption of Surfactants at the Air/Liquid and Liquid/Liquid Interface

There are generally two approaches for treating surfactant adsorption at the A/L and L/L interface. The first approach, adopted by Gibbs, treats adsorption as an equilibrium phenomenon whereby the second law of thermodynamics may be applied using surface quantities. The second approach, referred to as the equation of state approach, treats the surfactant film as a two-dimensional layer with a surface pressure  $\pi$  that may be related to the surface excess  $\Gamma$  (amount of surfactant adsorbed per unit area). Only the Gibbs approach will be described.

### The Gibbs Adsorption Isotherm

Gibbs (1928) derived a thermodynamic relationship between the surface or interfacial tension  $\gamma$  and the surface excess  $\Gamma$  (adsorption per unit area). At constant temperature, the Gibbs adsorption equation is given by

$$\Gamma_{2,1}^{\sigma} = -\frac{1}{RT} \left( \frac{d\gamma}{d \ln a_2^L} \right) \quad (1)$$

where  $R$  is the gas constant,  $T$  is the absolute temperature,  $\gamma$  is the surface or interfacial

tension, and  $a_2^L$  is the activity of the surfactant in bulk solution that is equal to  $C_2 f_2$  or  $x_2 f_2$ , where  $C_2$  is the concentration of the surfactant in moles  $\text{dm}^{-3}$  and  $x_2$  is its mole fraction. Equation 1 allows one to obtain the surface excess (abbreviated as  $\Gamma_2$ ) from the variation of surface or interfacial tension with surfactant concentration. Note that  $a_2 \sim C_2$  since in dilute solutions  $f_2 \sim 1$ . This approximation is valid since most surfactants have low cmc (usually less than  $10^{-3} \text{ mol dm}^{-3}$ ), but adsorption is complete at or just below the cmc. The surface excess  $\Gamma_2$  can be calculated from the linear portion of the  $\gamma - \log C_2$  curves before the cmc. Such  $\gamma - \log C$  curves are illustrated in Fig. 5 for the air/water and o/w interfaces;  $[C_{\text{SAA}}]$  denotes the concentration of surface active agent in bulk solution. It can be seen that for the A/W interface,  $\gamma$  decreases from the value for water ( $72 \text{ mNm}^{-1}$  at  $20^\circ \text{C}$ ) reaching about  $25\text{--}30 \text{ mNm}^{-1}$  near the cmc. This is clearly schematic since the actual values depend on the surfactant nature. For the o/w case,  $\gamma$  decreases from a value of about  $50 \text{ mNm}^{-1}$  (for a pure hydrocarbon-water interface) to  $\sim 1\text{--}5 \text{ mNm}^{-1}$  near the cmc (again depending on the nature of the surfactant).  $\Gamma_2$  can be calculated from the slope of the linear position of the curves shown in Fig. 2 just before the cmc is reached. From  $\Gamma_2$ , the area per surfactant ion or molecule can be calculated since

$$\text{Area/molecule} = \frac{1}{\Gamma_2 N_{\text{av}}} \quad (2)$$

where  $N_{\text{av}}$  is the Avogadro's constant. Determining the area per surfactant molecule is very useful



since it gives information on surfactant orientation at the interface. For example, for ionic surfactants such as sodium dodecyl sulfate, the area per surfactant is determined by the area occupied by the alkyl chain and head group if these molecules lie flat at the interface, whereas for vertical orientation, the area per surfactant ion is determined by that occupied by the charged head group, which at low electrolyte concentration will be in the region of  $0.40 \text{ nm}^2$ . Such area is larger than the geometrical area occupied by a sulfate group, as a result of the lateral repulsion between the head group. On addition of electrolytes, this lateral repulsion is reduced and the area/surfactant ion for vertical orientation will be lower than  $0.4 \text{ nm}^2$  (reaching in some case  $0.2 \text{ nm}^2$ ). On the other hand, if the molecules lie flat at the interface, the area per surfactant ion will be considerably higher than  $0.4 \text{ nm}^2$ . The hydrophilic head group may be unionized, for example, alcohols or poly(ethylene oxide) alkane or alkyl phenol compounds, weakly ionized such as carboxylic acids or strongly ionized such as sulfates, sulfonates, and quaternary ammonium salts. The adsorption of these different surfactants at the air/water and oil/water interface depends on the nature of the head group. With nonionic surfactants, repulsion between the head groups is small, and these surfactants are usually strongly adsorbed at the surface of water from very dilute solutions. As mentioned before, nonionic surfactants have much lower cmc values when compared with ionic surfactants with the same alkyl chain length. Typically, the cmc is in the region of  $10^{-5}$  to  $10^{-4} \text{ mol dm}^{-3}$ . Such nonionic surfactants form closely packed adsorbed layers at concentrations lower than their cmc values. The activity coefficient of such surfactants is close to unity and is only slightly affected by addition of moderate amounts of electrolytes (or change in the pH of the solution). Thus, nonionic surfactant adsorption is the simplest case since the solutions can be represented by a two-component system and the adsorption can be accurately calculated using Eq. 1. With ionic surfactants, on the other hand, the adsorption process is relatively more complicated since one has to consider the repulsion between the

head groups and the effect of presence of any indifferent electrolyte. Moreover, the Gibbs adsorption equation has to be solved taking into account the surfactant ions, the counterion, and any indifferent electrolyte ions present. For a strong surfactant electrolyte such as an  $\text{Na}^+ \text{R}^-$ ,

$$\Gamma_2 = \frac{1}{2RT} \frac{\partial \gamma}{\partial \ln a_{\pm}} \quad (3)$$

The factor of 2 in Eq. 3 arises because both surfactant ion and counter ion must be adsorbed to maintain neutrality, and  $d\gamma/d\ln a_{\pm}$  is twice as large as an unionized surfactant.

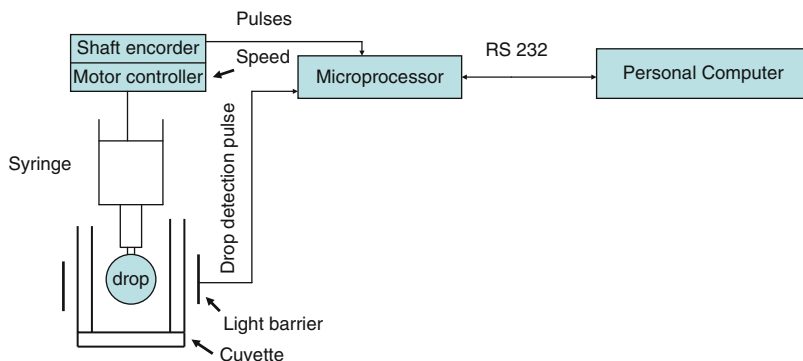
### Dynamic Processes of Adsorption

Most spraying processes work under dynamic conditions, and improvement of their efficiency requires the use of surfactants that lower the liquid surface tension  $\gamma_{LV}$  under these dynamic conditions. The interfaces involved (e.g., droplets formed in a spray or impacting on a surface) are freshly formed and have only a small effective age of some seconds or even less than a millisecond. The most frequently used parameter to characterize the dynamic properties of liquid adsorption layers is the dynamic surface tension (i.e., time-dependent quantity). Techniques should be available to measure  $\gamma_{LV}$  as a function of time (ranging from a fraction of a millisecond to minutes and hours or days). To optimize the use of surfactants, polymers, and mixtures, specific knowledge of their dynamic adsorption behavior rather than equilibrium properties is of great importance (Dukhin et al. 1995). It is, therefore, necessary to describe the dynamics of surfactant adsorption at a fundamental level. The first physically sound model for adsorption kinetics was derived by Ward and Tordai (1946). It is based on the assumption that the time dependence of surface or interfacial tension, which is directly proportional to the surface excess  $\Gamma$  (moles  $\text{m}^{-2}$ ), is caused by diffusion and transport of surfactant molecules to the interface. This is referred to as “the diffusion-controlled



### Agrochemical Formulations,

**Fig. 6** Representation of the drop-volume apparatus



adsorption kinetics model.” This diffusion-controlled model assumes transport by diffusion of the surface active molecules to be the rate-controlled step. The so-called kinetic-controlled model is based on the transfer mechanism of molecules from solution to the adsorbed state and vice versa (Dukhin et al. 1995).

In the presence of liquid flow, the situation becomes more complicated due to the creation of surface concentration gradients (Dukhin et al. 1995). These gradients, described by the Gibbs dilational elasticity (Dukhin et al. 1995), initiate a flow of mass along the interface in direction of the higher surface or interfacial tension (Marangoni effect). This situation can happen, for example, if an adsorption layer is compressed or stretched.

A qualitative model that can describe adsorption kinetics is given by Eq. 4:

$$\Gamma(t) = c_0 \left( \frac{Dt}{\pi} \right)^{1/2} \quad (4)$$

where  $c_0$  is the surfactant concentration,  $D$  is the diffusion coefficient, and  $t$  is the time.

As mentioned before, surfactant form micelles above the critical micelle concentration (cmc) of different sizes and shapes, depending on the nature of the molecule, temperature, electrolyte concentration, etc. The dynamic nature of micellization can be described by two main relaxation processes,  $\tau_1$  (the lifetime of a monomer in a micelle) and  $\tau_2$  (the lifetime of the micelle, i.e., complete dissolution into monomers). The presence of micelles in equilibrium with monomers influences the adsorption kinetics remarkably. After a fresh

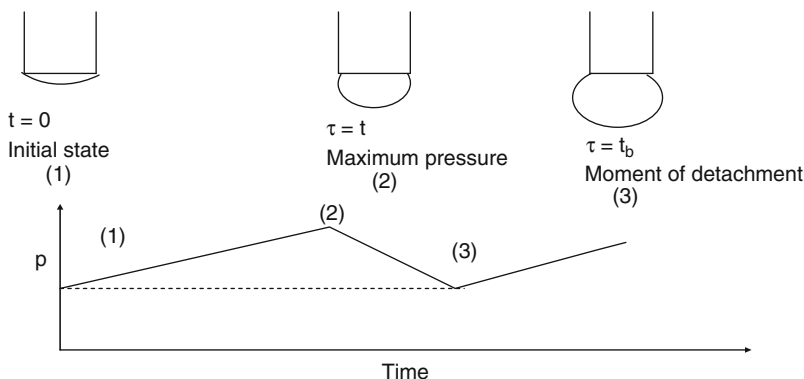
surface has been formed, surfactant monomers are adsorbed resulting in a concentration gradient of these monomers. This gradient will be equalized by diffusion to reestablish a homogeneous distribution. Simultaneously, the micelles are no longer in equilibrium with monomers within the range of concentration gradient. This leads to a net process of micelle dissolution or rearrangement to reestablish the local equilibrium. As a consequence, a concentration gradient of micelles results, which is equalized by diffusion of micelles (Dukhin et al. 1995).

The two most suitable techniques for studying adsorption kinetics are the drop-volume method and the maximum bubble pressure method. The first method can obtain information on adsorption kinetics in the range of seconds to some minutes. However, it has the advantage of measurement both at the air/liquid and liquid/liquid interfaces. The maximum bubble pressure method allows one to obtain measurements in the millisecond range, but it is restricted to the air/liquid interface. Below, a description of both techniques is given.

A schematic representation of the drop-volume apparatus (Miller et al. 1992) is given in Fig. 6. A metering system in the form of a motor-driven syringe allows the formation of the liquid drop at the tip of a capillary, which is positioned in a sealed cuvette. The cuvette is either filled with a small amount of the measuring liquid, to saturate the atmosphere, or with a second liquid in the case of interfacial studies. A light barrier arranged below the forming drop enables the detection of drop detachment from the capillary. Both the syringe and the light barriers are computer-controlled and allow a fully automatic operation

**Agrochemical Formulations,**

**Fig. 7** Scheme of bubble evolution and pressure change with time



of the setup. The syringe and the cuvette are temperature controlled by a water jacket which make interfacial tension measurements possible in the temperature range 10–90 °C. As mentioned above, the drop-volume method is of dynamic character, and it can be used for adsorption processes in the time interval of seconds up to some minutes. At small drop time, the so-called hydrodynamic effect has to be considered (Davies and Rideal 1969). This gives rise to apparently higher surface tension. Kloubek et al. (1976) used an empirical equation to account for this effect:

$$V_e = V(t) - \frac{K_v}{t} \quad (5)$$

$V_e$  is the unaffected drop volume and  $V(t)$  is the measured drop volume.  $K_v$  is a proportionality factor that depends on surface tension  $\gamma$ , density difference  $\Delta\rho$ , and tip radius  $r_{cap}$ .

Miller (1992) obtained the following equation for the variation of drop volume  $V(t)$  with time:

$$V(t) = V_e + t_0 F = V_e \left( 1 + \frac{t_0}{t - t_0} \right) \quad (6)$$

where  $F$  is the liquid flow per unit time that is given by

$$F = \frac{V(t)}{t} = \frac{V_e}{t - t_0} \quad (7)$$

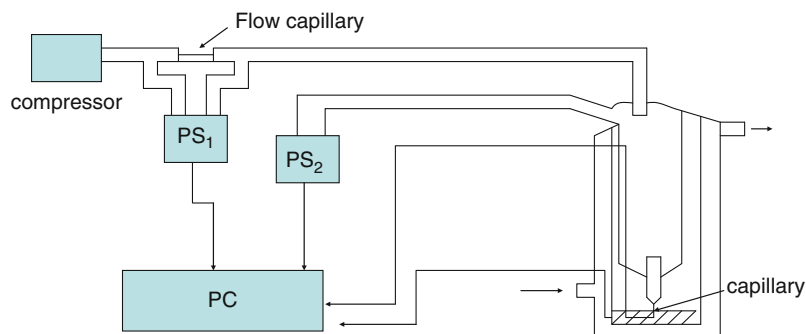
The drop-volume technique is limited in its application. Under conditions of fast drop

formation and larger tip radii, the drop formation shows irregular behavior.

The maximum bubble pressure technique is the most useful technique for measuring adsorption kinetics at short times, particularly if correction for the so-called dead time,  $\tau_d$ , is made. The dead time is simply the time required to detach the bubble after it has reached its hemispherical shape. A schematic representation of the principle of maximum bubble pressure is shown in Fig. 7, which shows the evolution of a bubble at the tip of a capillary. The figure also shows the variation of pressure  $p$  in the bubble with time. At  $t = 0$  (initial state), the pressure is low (note that the pressure is equal to  $2\gamma/r$ , since  $r$  of the bubble is large  $p$  is small). At  $t = \tau$  (smallest bubble radius that is equal to the tube radius),  $p$  reaches a maximum. At  $t = \tau_b$  (detachment time),  $p$  decreases since the bubble radius increases. The design of a maximum bubble pressure method for high bubble formation frequencies (short surface age) requires the following: (1) Measurement of bubble pressure, (2) measurement of bubble formation frequency, and (3) estimation of surface lifetime and effective surface age. The first problem can be easily solved if the system volume (which is connected to the bubble) is large enough in comparison with the bubble separating from the capillary. In this case, the system pressure is equal to the maximum bubble pressure. The use of an electric pressure transducer for measuring bubble formation frequency presumes that pressure oscillations in the measuring system are distinct enough, and this satisfies (2). Estimation of the

### Agrochemical Formulations,

**Fig. 8** Maximum bubble pressure apparatus



surface lifetime and effective surface age, that is, (3) requires estimation of the dead time  $\tau_d$ . A schematic representation of the setup for measuring the maximum bubble pressure and surface age is shown in Fig. 8. The air coming from a micro-compressor flows first through the flow capillary. The air flow rate is determined by measuring the pressure difference at both ends of the flow capillary with the electric transducer PS1. Thereafter, the air enters the measuring cell and the excess air pressure in the system is measured by a second electric sensor PS2. In the tube which leads the air to the measuring cell, a sensitive microphone is placed. The measuring cell is equipped with a water jacket for temperature control, which simultaneously holds the measuring capillary and two platinum electrodes, one of which is immersed in the liquid under study and the second is situated exactly opposite to the capillary and controls the size of the bubble. The electric signals from the gas flow sensor PS1 and pressure transducer PS2, the microphone and the electrodes, as well as the compressor are connected to a personal computer which operates the apparatus and acquires the data.

The value of  $\tau_d$ , equivalent to the time interval necessary to form a bubble of radius  $R$ , can be calculated using Poiseuille's law:

$$\tau_d = \frac{\tau_b L}{Kp} \left( 1 + \frac{3r_{ca}}{2R} \right) \quad (8)$$

$K$  is given by Poiseuille's law:

$$K = \frac{\pi r^4}{8\eta l} \quad (9)$$

$\eta$  is the gas viscosity,  $l$  is the length,  $L$  is the gas flow rate, and  $r_{ca}$  is the radius of the capillary.

The calculation of dead time  $\tau_d$  can be simplified when taking into account the existence of two gas flow regimes for the gas flow leaving the capillary: bubble flow regime when  $\tau > 0$  and jet regime when  $\tau = 0$  and hence  $\tau_b = \tau_d$ . A typical dependence of  $p$  on  $L$  is shown in Fig. 9.

On the right hand side of the critical point, the dependence of  $p$  on  $L$  is linear in accordance with Poiseuille's law. Under these conditions,

$$\tau_d = \tau_b \frac{L p_c}{L_c p} \quad (10)$$

where  $L_c$  and  $p_c$  are related to the critical point and  $L$  and  $p$  are the actual values of the dependence left from the critical point.

The surface lifetime can be calculated from

$$\tau = \tau_b - \tau_d = \tau_b \left( 1 - \frac{L p_c}{L_c p} \right) \quad (11)$$

The critical point in the dependence of  $p$  and  $L$  can be easily located and is included in the software of the computer program.

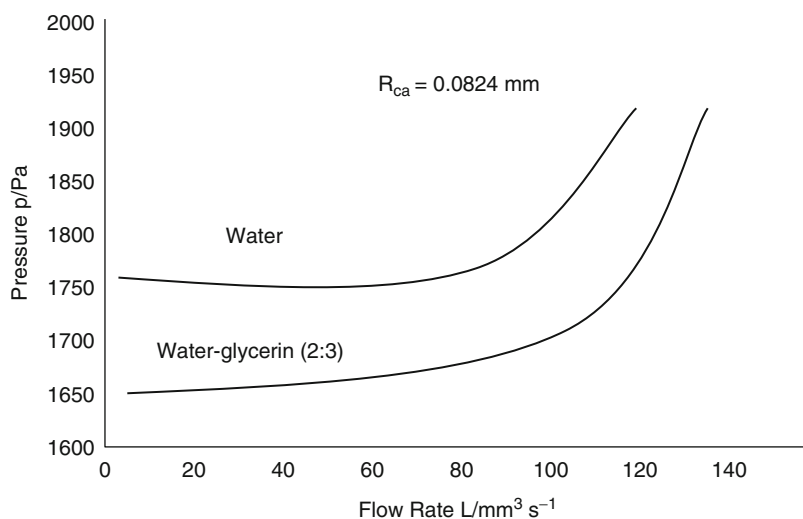
The surface tension value in the maximum bubble pressure method is calculated using the Laplace equation:

$$p = \frac{2\gamma}{r} + \rho hg + \Delta p \quad (12)$$

where  $\rho$  is the density of the liquid,  $g$  is the acceleration due to gravity,  $h$  is the depth the capillary is immersed in the liquid, and  $\Delta p$  is a correction factor to allow for hydrodynamic effects.

### Agrochemical Formulations,

**Fig. 9** Dependence of  $p$  on gas flow rate  $L$  at 30 °C



### Adsorption of Surfactants and Polymeric Surfactants at the Solid/Liquid Interface

The use of surfactants (ionic, nonionic, and zwitterionic) and polymers to control the stability behavior of suspension concentrates in agrochemical formulations is of considerable importance. They are particularly robust form of stabilization which is useful at high-disperse volume fractions and high electrolyte concentrations, as well as under extreme conditions of high temperature. In particular, surfactants and polymers are essential for the stabilization of suspensions in nonaqueous media, where electrostatic stabilization is less successful. The key to understanding how surfactants and polymers (to be referred to as polymeric surfactants) function as stabilizers is to know their adsorption and conformation at the solid/liquid interface. This is the objective of the present section which is a survey of the general trends observed and some of the theoretical treatments. Since surfactant and polymer adsorption processes are significantly different, the two subjects will be treated differently. Suffice to say at this stage is that surfactant adsorption is relatively more simple than polymer adsorption. This stems from the fact that surfactants consist of a small number of units and they mostly are reversibly adsorbed, allowing one to apply thermodynamic treatments. In this case, it

is possible to describe the adsorption in terms of the various interaction parameters, namely chain-surface, chain-solvent, and surface-solvent. Moreover, the conformation of the surfactant molecules at the interface can be deduced from these simple interaction parameters. In contrast, the process of polymer adsorption is fairly complicated. In addition to the usual adsorption considerations described above, one of the principle problems to be resolved is the conformation of the polymer molecule at the surface. This can acquire various possible ways depending on the number of segments and chain flexibility. This requires application of statistical thermodynamic methods. The adsorption of ionic and nonionic surfactants will be treated separately. The surfaces (substrates) can also be hydrophobic or hydrophilic, and these may be treated separately.

The adsorption of ionic surfactants on hydrophobic surfaces such as agrochemical particles is governed by hydrophobic interaction between the alkyl chain of the surfactant and the hydrophobic surface. In this case, electrostatic interaction will play a relatively smaller role. However, if the surfactant head group is of the same sign of charge as that on the substrate surface, electrostatic repulsion may oppose adsorption. In contrast, if the head groups are of opposite sign to the surface, adsorption may be enhanced. Since the adsorption depends on the magnitude of the

hydrophobic bonding free energy, the amount of surfactant adsorbed increases directly with increase in the alkyl chain length in accordance with Traube's rule.

The adsorption of ionic surfactants on hydrophobic surfaces may be represented by the Stern-Langmuir isotherm (Hough and Randall 1983):

$$\frac{\theta}{1-\theta} = \frac{C}{55.5} \exp\left(-\frac{\Delta G_{\text{ads}}^{\circ}}{RT}\right) \quad (13)$$

where  $\theta$  is the fractional coverage,  $C$  is the surfactant concentration in  $\text{mol dm}^{-3}$ ,  $\Delta G_{\text{ads}}^{\circ}$  is the free energy of adsorption,  $R$  is the gas constant, and  $T$  is the absolute temperature. Equation 13 applies only at low surface coverage ( $\theta < 0.1$ ) where lateral interaction between the surfactant ions can be neglected. At high surface coverage ( $\theta > 0.1$ ), one should take the lateral interaction between the chains into account, by introducing a constant  $A$ , for example, using the Frumkin-Fowler-Guggenheim equation (Hough and Randall 1983):

$$\frac{\theta}{(1-\theta)} \exp(A\theta) = \frac{C}{55.5} \exp\left(-\frac{\Delta G_{\text{ads}}^{\circ}}{RT}\right) \quad (14)$$

Various authors (Fuerstenau and Healy 1972; Somasundaran and Goddard 1979) have used the Stern-Langmuir equation in a simple form to describe the adsorption of surfactant ions on mineral surfaces:

$$\Gamma = 2rC \exp\left(-\frac{\Delta G_{\text{ads}}^{\circ}}{RT}\right) \quad (15)$$

Various contributions to the adsorption free energy may be envisaged. To a first approximation, these contributions may be considered to be additive. In the first instance,  $\Delta G_{\text{ads}}$  may be taken to consist of two main contributions, that is,

$$\Delta G_{\text{ads}} = \Delta G_{\text{elec}} + \Delta G_{\text{spec}} \quad (16)$$

where  $\Delta G_{\text{elec}}$  accounts for any electrical interactions and  $\Delta G_{\text{spec}}$  is a specific adsorption term which contains all contributions to the adsorption free energy that are dependent on the "specific"

(nonelectrical) nature of the system (Fuerstenau and Healy 1972). Several authors subdivided  $\Delta G_{\text{spec}}$  into supposedly separate independent interactions (Somasundaran and Goddard 1979; Healy 1974), for example,

$$\Delta G_{\text{spec}} = \Delta G_{\text{cc}} + \Delta G_{\text{cs}} + \Delta G_{\text{hs}} + \dots \quad (17)$$

where  $\Delta G_{\text{cc}}$  is a term that accounts for the cohesive chain-chain interaction between the hydrophobic moieties of the adsorbed ions,  $\Delta G_{\text{cs}}$  is the term for chain/substrate interaction, whereas  $\Delta G_{\text{hs}}$  is a term for the head group/substrate interaction. Several other contributions to  $\Delta G_{\text{spec}}$  may be envisaged, for example, ion-dipole, ion-induced dipole, or dipole-induced dipole interactions. Since there is no rigorous theory that can predict adsorption isotherms, the most suitable method to investigate adsorption of surfactants is to determine the adsorption isotherm. Measurement of surfactant adsorption is fairly straightforward. A known mass  $m$  (g) of the particles (substrate) with known specific surface area  $A_s$  ( $\text{m}^2 \text{g}^{-1}$ ) is equilibrated at constant temperature with surfactant solution with initial concentration  $C_1$ . The suspension is kept stirred for sufficient time to reach equilibrium. The particles are then removed from the suspension by centrifugation, and the equilibrium concentration  $C_2$  is determined using a suitable analytical method. The amount of adsorption  $\Gamma$  ( $\text{mole m}^{-2}$ ) is calculated as follows:

$$\Gamma = \frac{(C_1 - C_2)}{m A_s} \quad (18)$$

The adsorption isotherm is represented by plotting  $\Gamma$  versus  $C_2$ . A range of surfactant concentrations should be used to cover the whole adsorption process, that is, from the initial values to the plateau values. To obtain accurate results, the solid should have a high surface area (usually  $> 1 \text{ m}^2$ ).

Several examples may be quoted from the literature to illustrate the adsorption of surfactant ions on solid surfaces. For a model hydrophobic surface, carbon black has been chosen (Somasundaran and Hannah 1979; Greenwood et al. 1968).

**Agrochemical Formulations,**

**Fig. 10** Adsorption isotherms for sodium dodecyl sulfate on carbon substrates

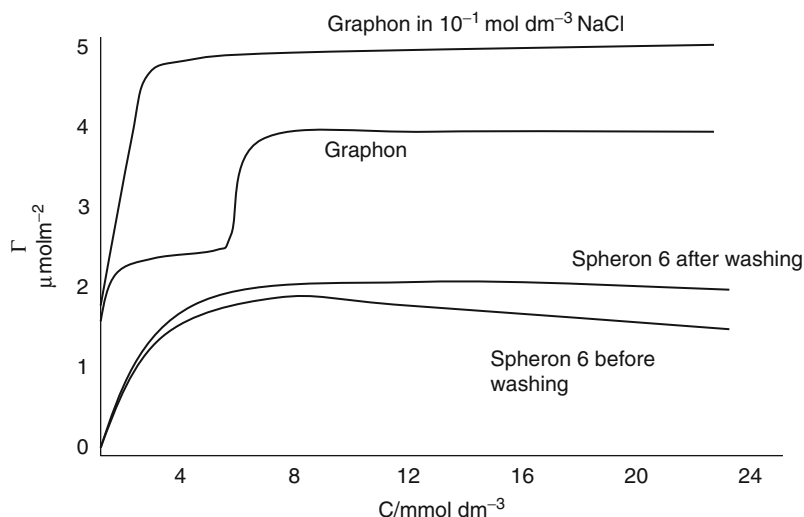
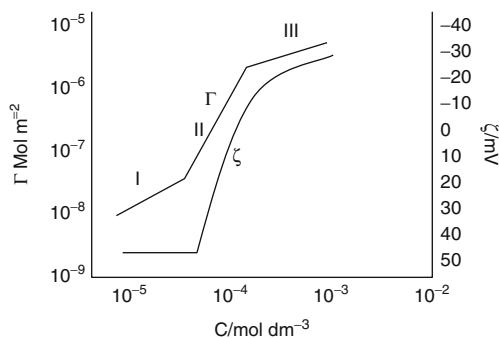


Figure 10 shows typical results for the adsorption of sodium dodecyl sulfate (SDS) on two carbon black surfaces, namely Spheron 6 (untreated) and Graphon (graphitized) which also describes the effect of surface treatment. The adsorption of SDS on untreated Spheron 6 tends to show a maximum that is removed on washing. This suggests the removal of impurities from the carbon black which becomes extractable at high surfactant concentration. The plateau adsorption value is  $\sim 2 \times 10^{-6} \text{ mol m}^{-2}$  ( $\sim 2 \mu \text{ mole m}^{-2}$ ). This plateau value is reached at  $\sim 8 \text{ m mole dm}^{-3}$  SDS, that is, close to the cmc of the surfactant in the bulk solution. The area per surfactant ion in this case is  $\sim 0.7 \text{ nm}^2$ . Graphitization (graphon) removes the hydrophilic ionizable groups (e.g.,  $-\text{C}=\text{O}$  or  $-\text{COOH}$ ), producing a surface that is more hydrophobic. The same occurs by heating Spheron 6 to  $2,700 \text{ }^\circ\text{C}$ . This leads to a different adsorption isotherm (Fig. 10) showing a step (inflection point) at a surfactant concentration in the region of  $\sim 6 \text{ m mole dm}^{-3}$ . The first plateau value is  $\sim 2.3 \mu \text{ mole m}^{-2}$ , whereas the second plateau value (that occurs at the cmc of the surfactant) is  $\sim 4 \mu \text{ mole m}^{-2}$ . It is likely in this case that the surfactant ions adopt different orientations at the first and second plateaus. In the first plateau region, a more “flat” orientation (alkyl chains adsorbing parallel to the surface) is obtained, whereas at

the second plateau, vertical orientation is more favorable, with the polar head groups being directed toward the solution phase. Addition of electrolyte ( $10^{-1} \text{ mole dm}^{-3} \text{ NaCl}$ ) enhances the surfactant adsorption. This increase is due to the reduction of lateral repulsion between the sulfate head groups and this enhances the adsorption. The adsorption of ionic surfactants on other hydrophobic surfaces resembles that for carbon black (Day et al. 1967; Saleeb and Kitchener 1965; Conner and Ottewill 1971). For example, Saleeb and Kitchener (Day et al. 1967) found similar limiting area for cetyltrimethyl ammonium bromide on graphon and polystyrene ( $\sim 0.4 \text{ nm}^2$ ). As with carbon black, the area per molecule depends on the nature and amount of added electrolyte. This can be accounted for in terms of reduction of head group repulsion and/or counter ion binding. Surfactant adsorption close to the cmc may appear Langmuirian, although this does not automatically imply a simple orientation. For example, rearrangement from horizontal to vertical orientation or electrostatic interaction and counter ion binding may be masked by simple adsorption isotherms. It is essential, therefore, to combine the adsorption isotherms with other techniques such as microcalorimetry and various spectroscopic methods to obtain a full picture on surfactant adsorption.



**Agrochemical Formulations, Fig. 11** Adsorption isotherm for sodium dodecyl sulfonate on alumina and corresponding zeta ( $\zeta$ ) potential

The adsorption of ionic surfactants on polar surfaces that contain ionizable groups may show characteristic features due to additional interaction between the head group and substrate and/or possible chain-chain interaction. This is best illustrated by the results of adsorption of sodium dodecyl sulfonate (SDSe) on alumina at pH = 7.2 obtained by Fuerstenau (1971) and shown in Fig. 11. At the pH value, the alumina is positively charged (the isoelectric point of alumina is at pH  $\sim$  9) and the counter ions are  $\text{Cl}^-$  from the added supporting electrolyte. In Fig. 11, the saturation adsorption  $\Gamma_1$  is plotted versus equilibrium surfactant concentration  $C_1$  in logarithmic scales. The figure also shows the results of zeta potential ( $\zeta$ ) measurements (which are a measure of the magnitude sign of charge on the surface). Both adsorption and zeta potential results show three distinct regions. The first region which shows a gradual increase of adsorption with increase in concentration, with virtually no change in the value of the zeta potential, corresponds to an ion-exchange process (Wakamatsu and Fuerstenau 1968). In other words, the surfactant ions simply exchange with the counter ions ( $\text{Cl}^-$ ) of the supporting electrolyte in the electrical double layer. At a critical surfactant concentration, the desorption increases dramatically with further increase in surfactant concentration (region II). In this region, the positive zeta potential gradually decrease, reaching a zero value (charge neutralization); after which, a negative value is obtained which increases rapidly with increase in

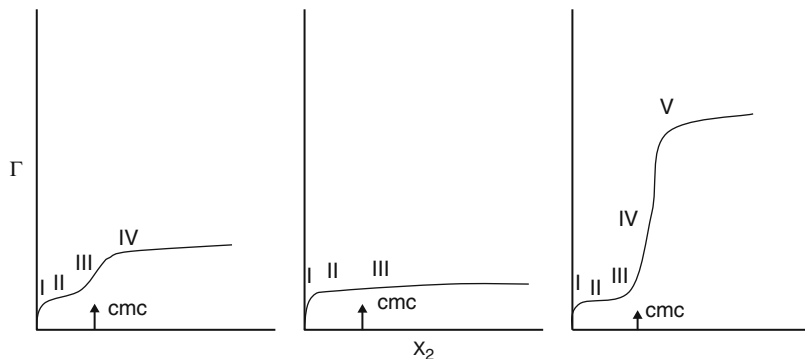
surfactant concentration. The rapid increase in region II was explained in terms of “hemi-micelle formation” that was originally postulated by Gaudin and Fuerstenau (1955). In other words, at a critical surfactant concentration (to be denoted the cmc of “hemi-micelle formation” or better the critical aggregation concentration CAC), the hydrophobic moieties of the adsorbed surfactant chains are “squeezed out” from the aqueous solution by forming two-dimensional aggregates on the adsorbent surface. This is analogous to the process of micellization in bulk solution. However, the CAC is lower than the cmc, indicating that the substrate promotes surfactant aggregation. At a certain surfactant concentration in the hemi-micellization process, the isoelectric point is exceeded and, thereafter, the adsorption is hindered by the electrostatic repulsion between the hem-micelles, and hence, the slope of the adsorption isotherm is reduced (region III).

Several types of nonionic surfactants exist, depending on the nature of the polar (hydrophilic) group. The most common type is that based on a poly(oxyethylene) glycol group, that is,  $(\text{CH}_2\text{CH}_2\text{O})_n\text{OH}$  (where  $n$  can vary from as little as 2 units to as high as 100 or more units) linked either to an alkyl ( $\text{C}_x\text{H}_{2x+1}$ ) or alkyl phenyl ( $\text{C}_x\text{H}_{2x+1}-\text{C}_6\text{H}_4-$ ) group. These surfactants may be abbreviated as  $\text{C}_xE_n$  or  $\text{C}_x\phi E_n$  (where  $C$  refers to the number of  $C$  atoms in the alkyl chain,  $\phi$  denotes  $\text{C}_6\text{H}_4$ , and  $E$  denotes ethylene oxide). These ethoxylated surfactants are characterized by a relatively large head group compared to the alkyl chain (when  $n > 4$ ). However, there are nonionic surfactants with small head group such as amine oxides ( $-\text{N} \rightarrow \text{O}$ ) head group, phosphate oxide ( $-\text{P} \rightarrow \text{O}$ ), or sulphinyl-alkanol ( $-\text{SO}-(\text{CH}_2)_n-\text{OH}$ ) (Eq. 23). Most adsorption isotherms in the literature are based on the ethoxylated type surfactants. The adsorption isotherm of nonionic surfactants are in many cases Langmuirian, like those of most other highly surface active solutes adsorbing from dilute solutions, and adsorption is generally reversible. However, several other adsorption types are produced (Clunie and Ingram 1983), and those are illustrated in Fig. 12. The steps in the isotherm



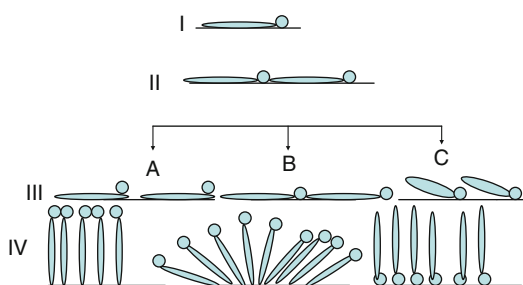
**Agrochemical Formulations,**

**Fig. 12** Adsorption isotherms corresponding to the three adsorption sequences shown in Fig. 14



may be explained in terms of the various adsorbate-adsorbate, adsorbate-adsorbent, and adsorbate-solvent interactions. These orientations are schematically illustrated in Fig. 14. In the first stage of adsorption (denoted by I in Figs. 12 and 13), surfactant-surfactant interaction is negligible (low coverage) and adsorption occurs mainly by van der Waals interaction. On a hydrophobic surface, the interaction is dominated by the hydrophobic portion of the surfactant molecule. This is mostly the case with agrochemicals which have hydrophobic surfaces. However, if the chemical is hydrophilic in nature, the interaction will be dominated by the EO chain. The approach to monolayer saturation with the molecules lying flat is accompanied by a gradual decrease in the slope of the adsorption isotherm (region II in Fig. 12). Increase in the size of the surfactant molecule, for example, increasing the length of the alkyl or EO chain, will decrease adsorption (when expressed in moles per unit area). On the other hand, increasing temperature will increase adsorption as a result of desolvation of the EO chains, thus reducing their size. Moreover, increasing temperature reduces the solubility of the nonionic surfactant, and this enhances adsorption.

The subsequent stages of adsorption (region III and IV) are determined by surfactant-surfactant interaction, although surfactant-surface interaction initially determines adsorption beyond stage II. This interaction depends on the nature of the surface and the hydrophilic-lipophilic balance of the surfactant molecule (HLB). For a hydrophobic surface, adsorption occurs via the alkyl group of the

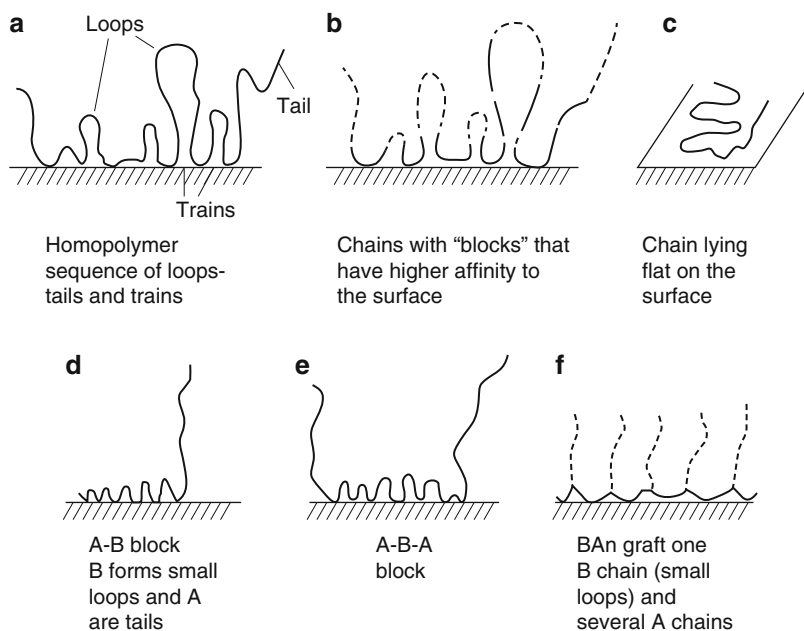


**Agrochemical Formulations, Fig. 13** Model for adsorption of nonionic surfactants

surfactant. For a given EO chain, the adsorption will increase with increase in the alkyl chain length. On the other hand, for a given alkyl chain length, adsorption increases with decrease of the PEO chain length. As the surfactant concentration approaches the cmc, there is a tendency for aggregation of the alkyl groups. This will cause vertical orientation of the surfactant molecules (stage IV), compress the head group, and, for an EO chain, result in a less coiled, more extended conformation. The larger the surfactant alkyl chain, the greater will be the cohesive forces and hence the smaller the cross-sectional area. This may explain why saturation adsorption increases with increasing alkyl chain length. The interaction occurring in the adsorption layer during the fourth and subsequent stages of adsorption is similar to those that occur in bulk solution. In this case, aggregate units, as shown in Fig. 13 V (hemi-micelles or micelles) may be formed.

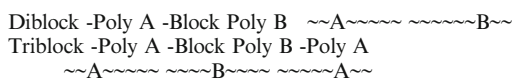
As mentioned above, the adsorption of polymeric surfactants is more complicated than that of monomeric surfactants. The simplest type of

**Agrochemical Formulations,**  
**Fig. 14** Various conformations of polymeric surfactants adsorbed on a plane surface

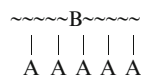


a polymeric surfactant is a homopolymer that is formed from the same repeating units (Piirma 1992): Poly(ethylene oxide) (PEO) and Poly(vinylpyrrolidone) (PVP). Homopolymers have little surface activity at the oil/water (O/W) interface. However, homopolymers may adsorb significantly at the solid/liquid (S/L) interface. Even if the adsorption energy per monomer segment is small (fraction of  $kT$ , where  $k$  is the Boltzmann constant and  $T$  is the absolute temperature), the total adsorption energy per molecule may be sufficient (several segments are adsorbed at the surface) to overcome the unfavorable entropy loss of the molecule at the S/L interface. Homopolymers may also adsorb at the solid surface by some specific interaction, for example, hydrogen bonding (e.g., adsorption of PEO or PVP on silica). In general, homopolymers are not the most suitable dispersants for suspension concentrates. A small variant is to use polymers that contain specific groups that have high affinity to the surface, for example, partially hydrolyzed poly(vinyl acetate) (PVAc), technically referred to as poly(vinyl alcohol) (PVA). Commercially available PVA molecules contain 4–12 % acetate groups. The acetate groups give the molecule its amphipathic character. On a hydrophobic surface (such as

agrochemical particles), the polymer adsorbs with preferential attachment of the acetate groups on the surface, leaving the more hydrophilic vinyl alcohol segments dangling in the aqueous medium. The most convenient polymeric surfactants are those of the block and graft copolymer type. A block copolymer is a linear arrangement of blocks of varying composition (Piirma 1992):



A graft copolymer is a non-linear array of one B block on which several A polymers are grafted



Most block and graft copolymers have low critical micelle concentrations (cmc), and in many cases, it is not easy to measure the cmc for these block and graft copolymers. The aggregation process is also affected by temperature and solvency of the medium for the A chains. One of the most useful methods to follow the aggregation of block and graft copolymers is to use time average light scattering. By measuring the

intensity as a function of concentration, one can extrapolate the results to zero concentration and obtain the molecular weight of the micelle – this allows one to obtain the aggregation number from a knowledge of the molecular weight of the monomer. Several examples of block and graft copolymers may be quoted, such as Triblock polymeric surfactants, referred to as “Pluronics” (BASF), with two poly A blocks of PEO and one block poly B of polypropylene oxide (PPO). Several chain lengths of PEO and PPO are available. Triblocks of PPO-PEO-PEO (inverse “Pluronics”) are also available. Polymeric triblock surfactants can be applied as dispersants. The hydrophobic PPO chain resides at the hydrophobic surface, leaving the two PEO chains dangling in aqueous solution (providing steric stabilization). These triblocks are not the most efficient dispersants; the PPO chain is not sufficiently hydrophobic to provide a strong “anchor” to a hydrophobic surface. Several other di- and triblock copolymers have been synthesized: Diblocks of polystyrene block-polyvinyl alcohol; triblocks of poly(methylmethacrylate)-block polyethylene oxide-poly(methyl methacrylate); diblocks of polystyrene-polyethylene oxide; and triblocks of polyethylene oxide-polystyrene-polyethylene oxide. An alternative (and perhaps more efficient) polymeric surfactant is the amphiphathic graft copolymer consisting of a polymeric backbone B (polystyrene or polymethylmethacrylate) and several A chains (“teeth”) such as polyethylene oxide. The graft copolymer is referred to as a “comb” stabilizer; the polymer forms a “brush” at the solid/liquid interface. The “grafting into” technique has also been used to synthesize polystyrene-polyethylene oxide graft copolymers. These molecules are not commercially available. Recently, a novel graft copolymer based on a naturally occurring polysaccharide, namely Inulin (polyfructose), has been synthesized (Stevens et al. 2001). Inulin is a polydisperse polysaccharide consisting mainly, if not exclusively, of  $\beta(2 \rightarrow 1)$  fructosyl fructose unite ( $F_m$ ) with normally, but not necessarily, one glucopyranose unit at the reducing end ( $GF_n$ ) (Hirst et al. 1950; Suzuki 1993). To produce the amphiphathic graft copolymer, the chains

were modified by introduction of alkyl groups ( $C_4$ – $C_{18}$ ) on the polyfructose backbone through isocyanates. The alkyl groups represent the B chains (that are randomly distributed on the sugar backbone on primary hydroxyl functions as well as on the secondary ones) which become strongly adsorbed on a hydrophobic solid such as an agrochemical particle. The sugar chain forms the stabilizing chain as this is highly water soluble. The graft copolymer will adsorb on hydrophobic surfaces with the alkyl groups strongly attached (multipoint anchoring) leaving the polyfructose chains dangling in solution and probably forming large loops. These graft copolymers can produce highly stable suspensions, in particular at high electrolyte concentrations (Tadros et al.).

Understanding the adsorption and conformation of polymeric surfactants at interfaces is key to knowing how these molecules act as stabilizers. Most basic ideas on adsorption and conformation of polymers have been developed for the solid/liquid interface (Tadros 1985). The process of polymer adsorption involves a number of various interactions that must be separately considered. Three main interactions must be taken into account, namely the interaction of the solvent molecules with the surface which needs to be displaced for the polymer segments to adsorb, the interaction between the chains and the solvent, and the interaction between the polymer and the surface. Apart from knowing these interactions, one of the most fundamental considerations is the conformation of the polymer molecule at the interface. These molecules adopt various conformations, depending on their structure. The simplest case to consider is that of a homopolymer that consists of identical segments (e.g., poly(ethylene oxide)), which shows a sequence of loops, trains, and tails, as is illustrated in Fig. 14a. It should be mentioned at this stage that for such a polymer to adsorb, the reduction in entropy of the chain as it approaches the interface must be compensated by an energy of adsorption between the segments and the surface. In other words, the chain segments must have a minimum adsorption energy,  $\chi^s$ , otherwise no adsorption occurs. With polymers that are highly

water soluble, such as poly(ethylene oxide) (PEO), the interaction energy with the surface may be too small for adsorption to occur, and if this takes place, the whole molecule may not be strongly adsorbed to the surface.

For this reason, many commercially available polymers that are described as homopolymers, such as poly(vinyl alcohol) (PVA), contain some hydrophobic groups or short blocks (vinyl acetate in the case of PVA) that ensured their adsorption to hydrophobic surfaces. This is illustrated in Fig. 14b. Clearly, if all the segments have a high affinity to the surface, the whole molecule may lie flat on the surface, as illustrated in Fig. 14c. This situation is rarely the case, since the molecule will have very low solubility in the continuous medium.

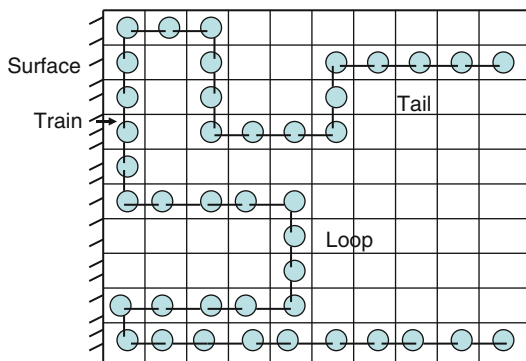
The most favorable structures for polymeric surfactants are those represented in Fig. 14d, e, and f referred to as block and graft copolymers. The molecule shown in Fig. 14d is an A-B block, consisting of a B chain that has a high affinity to the surface (or soluble in the oil phase), referred to as the “anchoring” chain, and an A chain that has very low affinity to the surface and strongly solvated by the medium. As will be discussed in the next section on stabilization, this is the most convenient structure, since the forces that ensure strong adsorption are opposite to those that ensure stability. A variance on the structure shown in Fig. 14e is the A-B-A block copolymer. In this case, the anchor chain B contains two stabilizing chains (tails). Another variance is that shown in Fig. 14f, described as graft copolymer (“comb” type structure) with one B chain and several A chains (tails or “teeth”).

It is clear from the above description of polymer configurations that for full characterization of the process of adsorption, it is necessary to know the following parameters, namely the amount of polymer adsorbed per unit area of the surface,  $\Gamma$  (mole  $\text{m}^{-2}$  or  $\text{mg m}^{-2}$ ), the fraction of segments in close contact with the surface,  $p$ , and the distribution of polymer segments,  $\rho(z)$ , from the surface toward the bulk solution. It is essential to know how far the segments extend into solution, that is, the adsorbed layer thickness  $\delta$ . It is important to know how these parameters change

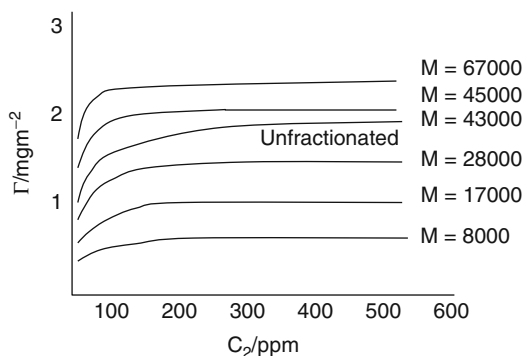
with polymer coverage (concentration), the structure of the polymer, and its molecular weight. It is also essential to know how these parameters change with the environment such as solvency of the medium fort, chains, and temperature. Several theories exist that describe the process of polymer adsorption, which have been developed either using statistical mechanical approach or quasi-lattice models. In the statistical mechanical approach, the polymer is considered to consist of three types of structures with different energy states, trains, loops, and tails (Silberberg 1968; Hoeve 1970). The structures close to the surface (trains) are adsorbed with an internal partition function determined by short range forces between the segment and surface (assigned an adsorption energy per segment  $\chi^s$ ). The segments in loops and tails are considered to have an internal partition function equivalent to that of segments in bulk solution, and these are assigned a segment-solvent interaction parameter  $\chi$  (Flory-Huggins interaction parameter). By equating the chemical potential of the macromolecule in the adsorbed state and in bulk solution, the adsorption isotherm can be determined. In the earlier theories, the case of an isolated chain on the surface (low coverage) was considered, but later, the theories were modified to take into account the lateral interaction between the chains, that is, at high coverage.

The quasi-lattice model was developed by Roe (1974) and by Scheutjens and Fleer (1979, 1980, 1982; Fleer et al. 1993). The basis procedure was to describe all chain conformations as step-weighted random walks on a quasi-crystalline lattice which extends in parallel layers away from the surface. This is illustrated in Fig. 15 which shows a possible conformation of a polymer molecule at a surface.

The amount of polymer adsorbed,  $\Gamma$ , can be directly determined in a similar way as described for surfactants, except in this case, one has to consider the relatively slow adsorption process which may take several hours or even days to reach equilibrium. In addition, one needs very sensitive analytical methods for determination of polymer concentration in the early stages of adsorption (which can be in the ppm range). As mentioned before, the amount of adsorption  $\Gamma$

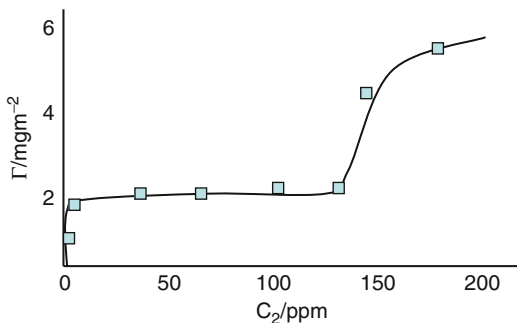


**Agrochemical Formulations, Fig. 15** Schematic representation of a polymer molecule adsorbing on a flat surface

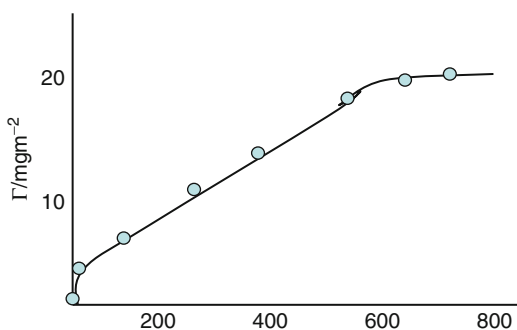


**Agrochemical Formulations, Fig. 16** Adsorption isotherms of polyvinyl alcohol on polystyrene latex at 25°C (groups) on polystyrene latex (Garvey et al. 1974)

can be calculated from a knowledge of the initial polymer concentration  $C_1$  and that after reaching equilibrium  $C_2$ , the mass of the solid  $m$  and the specific surface area  $A_s$  is given by Eq. 18. As an illustration, Fig. 16 shows the adsorption isotherms at 25 °C for poly(vinyl alcohol) (PVA) (containing 12 % acetate) on polystyrene latex (a model hydrophobic surface similar to most agrochemical particles) (Garvey et al. 1974; van den Boomgaard et al. 1978; Tadros and Vincent 1978). The polymer was fractionated using preparative gel permeation chromatography (Garvey et al. 1974) or by a sequential precipitation technique using acetone (van den Boomgaard et al. 1978). The fractions were characterized for



**Agrochemical Formulations, Fig. 17** Adsorption of PVA on ethirimol



**Agrochemical Formulations, Fig. 18** Adsorption of the “comb” graft copolymer on ethirimol obtained on the model particles of polystyrene. This could be due to the errors involved in surface area determination of such coarse particles using BET gas adsorption

their molecular weight using ultracentrifugation and later by intrinsic viscosity measurements. Fig. 16 shows the high affinity isotherms for the polymers and the increase in adsorption of the polymer with increase of the molecular weight.

Results for polymeric surfactant adsorption on agrochemical particles are scarce. However, Tadros et al. (1994) showed similar trends for polymer adsorption on agrochemical particles. This is illustrated in Figs. 17 and 18 which show the adsorption of PVA and a comb graft copolymer stabilizer (polymethylmethacrylate backbone with polyethylene oxide side chains) on ethirimol (a fungicide) at room temperature. The high affinity type isotherm is clearly demonstrated, and in both cases, adsorption was irreversible indicating the strong and irreversible adsorption. However, the amount of adsorption per unit area (using the

BET surface area of ethirimol of  $0.22 \text{ m}^2\text{g}^{-1}$  obtained by Kr adsorption) was significantly higher than the values.

The bound fraction  $p$  represents the ratio of the number of segments in close contact with the surface (i.e., in trains) to the total number of segments in the polymer chain. The polymer bound fraction,  $p$ , can be directly determined using spectroscopic methods such as infrared IR, electron spin resonance ESR, and nuclear magnetic resonance NMR. The IR method depends on measuring the shift in some absorption peak for a polymer and/or surface group (Killmann et al. 1977; Fontana and Thomas 1961; Robb and Smith 1974). The ESR and NMR methods depend on the reduction in the mobility of the segments that is in close contact with the surface (larger rotational correlation time for trains when compared to loops). By using a pulsed NMR technique, one can estimate  $p$  (Barnett et al. 1981; Cohen-Staury et al. 1982). An indirect method for estimation of  $p$  is to use microcalorimetry. Basically, one compares the enthalpy of adsorption per molecule with that per segment (Cohen-Staury et al. 1982). The latter may be obtained by using small molecules of similar structure to a polymer segment.

Three direct methods can be applied for determination of adsorbed layer thickness: ellipsometry, attenuated total reflection (ATR), and neutron scattering. Both ellipsometry and ATR (Abeles 1964) depend on the difference between refractive indices between the substrate, adsorbed layer, and bulk solution, and they require flat reflecting surface. Ellipsometry (Eq. 45) is based on the principle that light undergoes a change in polarizability when it is reflected at a flat surface (whether covered or uncovered with a polymer layer).

The above limitations when using ellipsometry or ATR are overcome by the application technique of neutron scattering, which can be applied to both flat surfaces as well as particulate dispersions. The basic principle of neutron scattering is to measure the scattering due to the adsorbed layer, when the scattering length density of the particle is matched to that of the

medium (the so-called “contrast-matching” method). Contrast matching of particles and medium can be achieved by changing the isotopic composition of the system (using deuterated particles and mixture of  $\text{D}_2\text{O}$  and  $\text{H}_2\text{O}$ ). It was also used for measurement of the adsorbed layer thickness of polymers, for example, PVA or poly(ethylene oxide) (PEO) on polystyrene latex (Cosgrove et al. 1987). Apart from obtaining  $\delta$ , one can also determine the segment density distribution  $\rho(z)$ .

The above technique of neutron scattering gives clearly a quantitative picture of the adsorbed polymer layer. However, its application in practice is limited since one needs to prepare deuterated particles or polymers for the contrast-matching procedure. The practical methods for determination of the adsorbed layer thickness are mostly based on hydrodynamic methods that are described below.

Several methods may be applied to determine the hydrodynamic thickness of adsorbed polymer layers of which viscosity, sedimentation coefficient (using an ultracentrifuge), and dynamic light scattering measurements are the most convenient. A less accurate method is from zeta potential measurements, although this does not require the use of model monodisperse particles, and hence, it can be used for agrochemical suspensions. The dynamic light scattering method (referred to as photon correlation spectroscopy, PCS) provides a rapid method for determination of the hydrodynamic thickness. This is followed by application of zeta potential measurements for measurement of hydrodynamic thickness that can be applied for agrochemical particles. PCS allows one to obtain the diffusion coefficient of the particles with and without the adsorbed layer ( $D_\delta$  and  $D$ , respectively). This is obtained from measurement of the intensity fluctuation of scattered light as the particles undergo Brownian diffusion (Garvey et al. 1976; Pusey 1973). From  $D$ , the particle radius  $R$  is calculated using the Stokes-Einstein equation:

$$D = \frac{kT}{6\pi\eta R} \quad (19)$$



where  $k$  is the Boltzmann constant and  $T$  is the absolute temperature. For a polymer, coated particle  $R$  is denoted  $R_\delta$  which is equal to  $R + \delta_h$ . Thus, by measuring  $D_\delta$  and  $D$ , one can obtain  $\delta_h$ . It should be mentioned that the accuracy of the PCS method depends on the ratio of  $\delta_\delta/R$ , since  $\delta_h$  is determined by difference. Since the accuracy of the measurement is  $\pm 1\%$ ,  $\delta_h$  should be at least  $10\%$  of the particle radius. This method can only be used with small particles and reasonably thick adsorbed layers.

Electrophoretic mobility,  $u$ , measurements can also be applied to measure  $\delta_h$  (Cohen-Stuart and Mulder 1985). From  $u$ , the zeta potential  $\zeta$ , that is, the potential at the slipping (shear) plane of the particles can be calculated. Adsorption of a polymer causes a shift in the shear plane from its value in the absence of a polymer layer (which is close to the Stern plane) to a value that depends on the thickness of the adsorbed layer. Thus, by measuring  $\zeta$  in the presence ( $\zeta_\delta$ ) and absence ( $\zeta$ ) of a polymer layer, one can estimate  $\delta_h$ . Assuming that the thickness of the Stern plane is  $\Delta$ , then  $\zeta_\delta$  may be related to the  $\zeta$  (which may be assumed to be equal to the Stern potential  $\psi_d$ ) by the equation:

$$\tanh\left(\frac{e\psi_\delta}{4kT}\right) = \tanh\left(\frac{e\zeta}{4kT}\right) \exp[-\kappa(\delta_h - \Delta)] \quad (20)$$

where  $\kappa$  is the Debye parameter that is related to electrolyte concentration and valency.

It should be mentioned that the value of  $\delta_h$  calculated using the above simple equation shows a dependence on electrolyte concentration, and hence the method cannot be used in a straightforward manner. Cohen-Stuart et al. (Eq. 48) showed that the measured electrophoretic thickness  $\delta_e$  approaches  $\delta_h$  only at low electrolyte concentrations. Thus, to obtain  $\delta_h$  from electrophoretic mobility measurements, results should be obtained at various electrolyte concentrations and  $\delta_e$  should be plotted versus the Debye length ( $1/\kappa$ ) to obtain the limiting value at high ( $1/\kappa$ ) (i.e., low electrolyte concentration) which now corresponds to  $\delta_h$ .

## Interaction Forces Between Particles or Droplets in Agrochemical Dispersions (Suspension Concentrates or Emulsions, EWs) and Their Role in Colloid Stability

The interaction forces between particles in a suspension or droplets in an emulsion determine the colloid stability of the agrochemical formulation. For example, in a suspension concentrate, one must ensure that the particles remain as individual units and any aggregation must be sufficiently weak so that the system can be easily redispersed on shaking and/or dilution in the spray tank. Strong aggregation must be avoided since the resulting large units can cause blockage of the spray nozzles, uneven distribution of the agrochemical particles on the target causing reduction in biological efficacy. With EWs, aggregation of droplets must also be avoided for the same reasons as for suspensions. In addition, aggregation of emulsion may result in their coalescence with ultimate oil separation. Maintenance of colloid stability is also essential with suspoemulsions (mixtures of suspensions and emulsions). Aggregation of particles and droplets (referred to as heteroflocculation) must be prevented, otherwise the formulation loses its physical stability on storage.

The stability/instability of any agrochemical dispersion is determined by the balance of three main forces: (1) van der Waals attraction that is universal for all disperse systems, and it results mainly from the London dispersion forces between the particles or droplets. (2) Double layer repulsion that arises when using ionic surfactants or polyelectrolytes. (3) Steric repulsion that arises when using adsorbed nonionic surfactants or polymers. A description of these three interaction forces is first given, and this is followed by combination of these forces and discussion of the theories of colloid stability. The latter can account for the stability/instability of the various dispersions.

As is well-known, atoms or molecules always attract each other at short distances of separation. The attractive forces are of three different types: Dipole-dipole interaction (Keesom), dipole-induced-dipole interaction (Debye), and London



dispersion force. The London dispersion force is the most important, since it occurs for polar and nonpolar molecules. It arises from fluctuations in the electron density distribution. At small distances of separation  $r$  in vacuum, the attractive energy between two atoms or molecules is given by

$$G_{aa} = -\frac{\beta_{11}}{r^6} \quad (21)$$

$\beta_{11}$  is the London dispersion constant.

For colloidal particles which are made of atom or molecular assemblies, the attractive energies may be added, and this results in the following expression for two spheres (at small  $h$ ) (Hamaker 1937):

$$G_A = -\frac{AR}{12h} \quad (22)$$

where  $A$  is the effective Hamaker constant:

$$A = (A_{11}^{1/2} - A_{22}^{1/2})^2 \quad (23)$$

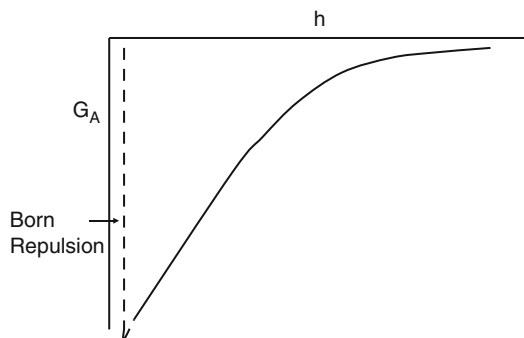
$A_{11}$  is the Hamaker constant between particles in vacuum and  $A_{22}$  Hamaker constant for equivalent volumes of the medium:

$$A = \pi q^2 \beta_{ii} \quad (24)$$

where  $q$  is the number of atoms or molecules per unit volume.

$G_A$  decreases with increase in  $h$  as schematically shown in Fig. 19.

Electrical double layers are produced when using ionic surfactants. On adsorption of these molecules on particles or droplets, a surface charge is produced from the head group of the ionic surfactant. This surface charge  $\sigma_o$  is compensated by unequal distribution of counter ions (opposite in charge to the surface) and co-ions (same sign as the surface) which extend to some distance from the surface. This forms the basis of the diffuse double layer proposed by Gouy and Chapman (Lyklema 1987). The double layer extension depends on electrolyte concentration and valency of the counter ions:



**Agrochemical Formulations, Fig. 19** Variation of the van der Waals attraction energy with separation distance

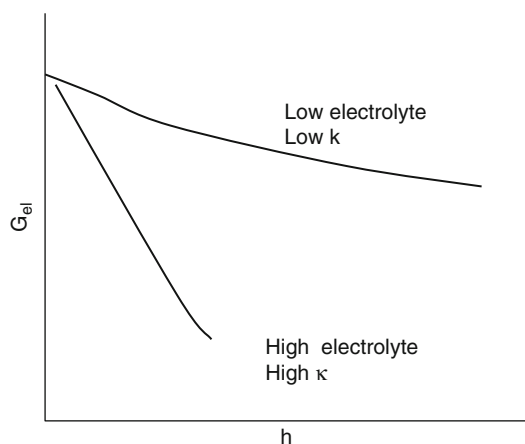
$$\left(\frac{1}{\kappa}\right) = \left(\frac{\epsilon_r \epsilon_o kT}{2 n_o Z_i^2 e^2}\right)^{1/2} \quad (25)$$

$\epsilon_r$  is the permittivity (dielectric constant); 78.6 for water at 25 °C.  $\epsilon_o$  is the permittivity of free space.  $k$  is the Boltzmann constant and  $T$  is the absolute temperature.  $n_o$  is the number of ions per unit volume of each type present in bulk solution and  $Z_i$  is the valency of the ions.  $e$  is the electronic charge. When charged colloidal particles in a dispersion approach each other such that the double layer begins to overlap (particle separation becomes less than twice the double layer extension), repulsion occurs. The individual double layers can no longer develop unrestrictedly, since the limited space does not allow complete potential decay (Bijesterbosch 1987). The potential  $\psi_{H/2}$  half way between the plates is no longer zero (as would be the case for isolated particles at  $x \rightarrow \infty$ ). For two spherical particles of radius  $R$  and surface potential  $\psi_o$  and condition  $\kappa R < 3$ , the expression for the electrical double layer repulsive interaction is given by

$$G_{el} = \frac{4\pi \epsilon_r \epsilon_o R^2 \psi_o^2 \exp(-\kappa h)}{2R + h} \quad (26)$$

where  $h$  is the closest distance of separation between the surfaces.

The above expression shows the exponential decay of  $G_{el}$  with  $h$ . The higher the value of  $\kappa$  (i.e., the higher the electrolyte concentration), the steeper the decay, as schematically shown in Fig. 20.



**Agrochemical Formulations, Fig. 20** Variation of  $G_{el}$  with  $h$  at different electrolyte concentrations

This means that at any given distance  $h$ , the double layer repulsion decreases with increase of electrolyte concentration.

Combination of  $G_{el}$  and  $G_A$  results in the well-known theory of stability of colloids (Deryaguin-Landau-Verwey-Overbeek, DLVO Theory) (Deryaguin and Landau 1941; Verwey and Overbeek 1948):

$$G_T = G_{el} + G_A \quad (27)$$

A plot of  $G_T$  versus  $h$  is shown in Fig. 21, which represents the case at low electrolyte concentrations, that is, strong electrostatic repulsion between the particles.  $G_{el}$  decays exponentially with  $h$ , that is,  $G_{el} \rightarrow 0$  as  $h$  becomes large.  $G_A$  is  $\propto 1/h$ , that is,  $G_A$  does not decay to 0 at large  $h$ . At long distances of separation,  $G_A > G_{el}$  resulting in a shallow minimum (secondary minimum). At very short distances,  $G_A \gg G_{el}$  resulting in a deep primary minimum. At intermediate distances,  $G_{el} > G_A$  resulting in energy maximum,  $G_{max}$ , whose height depends on  $\psi_o$  (or  $\psi_d$ ) and the electrolyte concentration and valency.

At low electrolyte concentrations ( $< 10^{-2} \text{ mol dm}^{-3}$  for a 1:1 electrolyte),  $G_{max}$  is high ( $> 25 \text{ kT}$ ), and this prevents particle aggregation into the primary minimum. The higher the electrolyte concentration (and the higher the valency of the ions), the lower

the energy maximum. Under some conditions (depending on electrolyte concentration and particle size), flocculation into the secondary minimum may occur. This flocculation is weak and reversible. By increasing the electrolyte concentration,  $G_{max}$  decreases until at a given concentration it vanishes and particle coagulation occurs. This is illustrated in Fig. 22 which shows the variation of  $G_T$  with  $h$  at various electrolyte concentrations.

Coagulation occurs at a critical electrolyte concentration, the critical coagulation concentration (c.c.c.) which depends on the electrolyte valency. At low surface potentials,  $c.c.c. \propto 1/Z^2$ . This is referred to as the Schulze-Hardy rule.

One can define a rate constant for flocculation:  $k_o$  = rapid rate of flocculation (in the absence of an energy barrier) (von Smoluchowski 1914) and  $k$  = slow rate of flocculation (in the presence of an energy barrier):

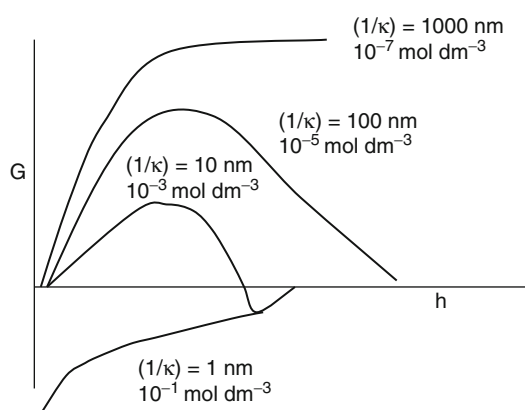
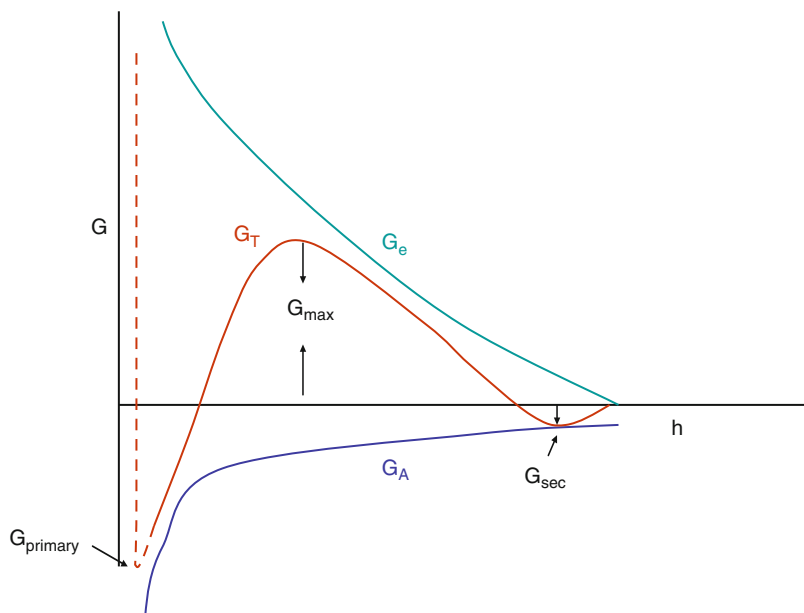
$$\frac{k_o}{k} = W \text{ (The Stability ratio)} \quad (28)$$

Note that  $W$  increases as  $G_{max}$  increases. The stability of colloidal dispersions can be quantitatively assessed from plots of  $\log W$  versus  $\log C$ , as illustrated in Fig. 23. The two main criteria for electrostatic stabilization can be considered: (1) High surface or Stern potential (zeta potential) (Hunter 1981) and high surface charge. (2) Low electrolyte concentration and low valency of counter- and co-ions. One should ensure that an energy maximum in excess of  $25 \text{ kT}$  should exist in the energy-distance curve. When  $G_{max} \gg \text{kT}$ , the particles in the dispersion cannot overcome the energy barrier, thus preventing coagulation. In some cases, particularly with large and asymmetric particles, flocculation into the secondary minimum may occur. This flocculation is usually weak and reversible and may be advantageous for preventing the formation of hard sediments.

Steric repulsion results from the presence of adsorbed layers of surfactants and/or polymers. The use of natural and synthetic polymers (referred to as polymeric surfactants) for stabilization of suspension concentrates and emulsions (EWs)

### Agrochemical Formulations,

**Fig. 21** Schematic representation of the variation of  $G_T$  with  $h$  according to the DLVO theory

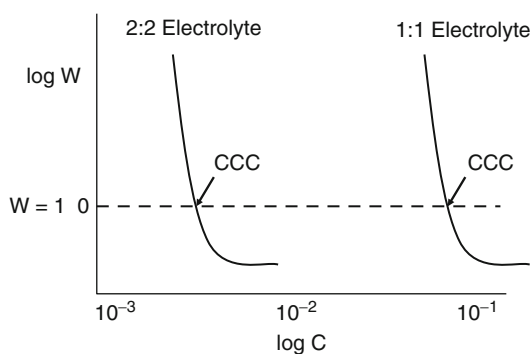


**Agrochemical Formulations, Fig. 22** Variation of  $G_T$  at various electrolyte concentrations

plays an important role in agrochemical formulations. Polymers are particularly important for preparation of concentrated dispersions, that is, at high volume fraction  $\phi$  of the disperse phase,

$$\phi = \frac{\text{(volume of all particles)}}{\text{(total volume of dispersion)}}.$$

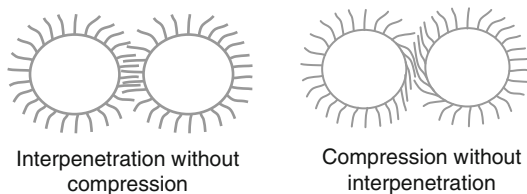
Polymers are also essential for stabilization of nonaqueous dispersions, since in this case,



**Agrochemical Formulations, Fig. 23** Log  $W$  - log  $C$  curves

electrostatic stabilization is not possible (due to the low dielectric constant of the medium). To understand the role of polymers in dispersion stability, it is essential to consider the adsorption and conformation of the macromolecule at the solid/liquid interface which was discussed before.

When two particles or droplets each with a radius  $R$  and containing an adsorbed polymer layer with a hydrodynamic thickness  $\delta_h$  approach each other to a surface-surface separation



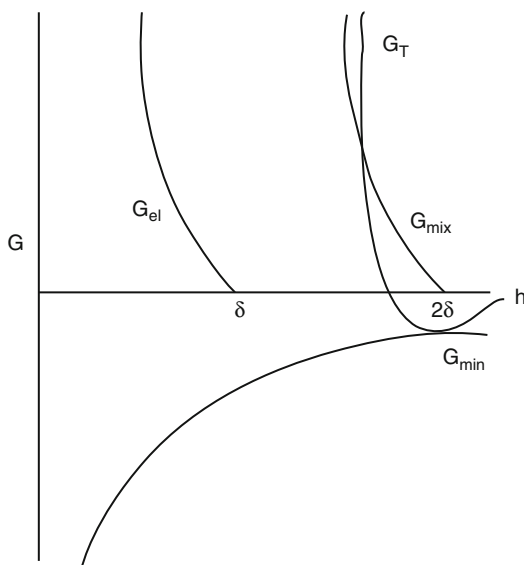
**Agrochemical Formulations, Fig. 24** Schematic representation of the interaction of two polymer layers

distance  $h$  that is smaller than  $2\delta_h$ , the polymer layers interact with each other resulting in two main situations (Tadros et al. 1981; Napper 1981). The polymer chains may overlap with each other, and the polymer layer may undergo some compression. In both cases, there will be an increase in the local segment density of the polymer chains in the interaction region. This is schematically illustrated in Fig. 24.

The real situation is perhaps in between the above two cases, that is, the polymer chains may undergo some interpenetration and some compression. Provided the dangling chains (the A chains in A-B, A-B-A block, or  $BA_n$  graft copolymers) are in a good solvent, this local increase in segment density in the interaction zone will result in strong repulsion as a result of two main effects: (1) Increase in the osmotic pressure in the overlap region as a result of the unfavorable mixing of the polymer chains, when these are in good solvent conditions (Flory and Krigbaum 1950; Fischer 1958). This is referred to as osmotic repulsion or mixing interaction, and it is described by a free energy of interaction  $G_{mix}$ . (2) Reduction of the configurational entropy of the chains in the interaction zone; this entropy reduction results from the decrease in the volume available for the chains when these are either overlapped or compressed (Mackor and van der Waals 1951). This is referred to as volume restriction interaction, entropic or elastic interaction, and it is described by a free energy of interaction  $G_{el}$ .

Combination of  $G_{mix}$  and  $G_{el}$  is usually referred to as the steric interaction (Hesselink et al. 1971) free energy,  $G_s$ , that is,

$$G_s = G_{mix} + G_{el} \quad (29)$$



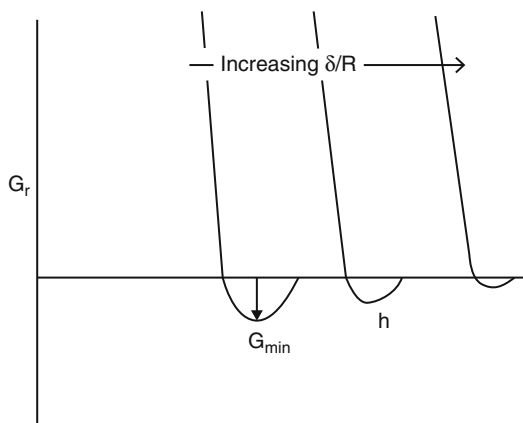
**Agrochemical Formulations, Fig. 25** Variation of  $G_{mix}$ ,  $G_{el}$ ,  $G_A$ , and  $G_T$  with surface-surface distance between the particles

The sign of  $G_{mix}$  depends on the solvency of the medium for the chains. If in a good solvent, that is, the Flory-Huggins interaction parameter  $\chi$  is less than 0.5, then  $G_{mix}$  is positive and the mixing interaction leads to repulsion (see below). In contrast, if  $\chi > 0.5$  (i.e., the chains are in a poor solvent condition),  $G_{mix}$  is negative and the mixing interaction becomes attractive.  $G_{el}$  is always positive, and hence, in some cases, one can produce stable dispersions in a relatively poor solvent (enhanced steric stabilization). Combination of  $G_{mix}$  and  $G_{el}$  with  $G_A$  gives the total free energy of interaction  $G_T$  (assuming there is no contribution from any residual electrostatic interaction) (Hesselink et al. 1971), that is,

$$G_T = G_{mix} + G_{el} + G_A \quad (30)$$

A schematic representation of the variation of  $G_{mix}$ ,  $G_{el}$ ,  $G_A$ , and  $G_T$  with surface-surface separation distance  $h$  is shown in Fig. 25.

$G_{mix}$  increases very sharply with decrease of  $h$ , when  $h < 2\delta$ .  $G_{el}$  increases very sharply with decrease of  $h$ , when  $h < \delta$ .  $G_T$  versus  $h$  shows a minimum,  $G_{min}$ , at separation distances comparable to  $2\delta$ ; when  $h < 2\delta$ ,  $G_T$  shows a rapid



**Agrochemical Formulations, Fig. 26** Variation of  $G_{\min}$  with  $\delta/R$

increase with further decrease in  $h$  (Eqs. 6, 7). Unlike the  $G_T-h$  curve predicted by the DLVO theory (which shows two minima and one energy maximum), the  $G_T-h$  for systems that are sterically stabilized show only one minimum,  $G_{\min}$ , followed by sharp increase in  $G_T$  with decrease of  $h$  (when  $h, 2\delta$ ). The depth of the minimum depends on the Hamaker constant  $A$ , particle radius  $R$ , and adsorbed layer thickness  $\delta-G_{\min}$  increases with increase of  $A$  and  $R$ . At a given  $A$  and  $R$ ,  $G_{\min}$  increases with decrease in  $\delta$  (i.e., with decrease of the molecular weight,  $M_w$ , of the stabilizer). This is illustrated in Fig. 26 which shows the energy-distance curves at various  $\delta/R$  ratios. As the latter increases,  $G_{\min}$  decreases and at sufficiently high value of  $\delta/R$   $G_{\min}$  becomes smaller than  $kT$  and the dispersion approaches thermodynamic stability. This explains the very high stability of nanosuspensions and nanoemulsions.

Several criteria must be considered for effective steric stabilization: (1) The particles should be completely covered by the polymer (the amount of polymer should correspond to the plateau value). Any bare patches may cause flocculation either by van der Waals attraction (between the bare patches) or by bridging flocculation (whereby a polymer molecule will become simultaneously adsorbed on two or more particles). (2) The polymer should be strongly “anchored” to the particle surfaces, to prevent any displacement during particle approach.

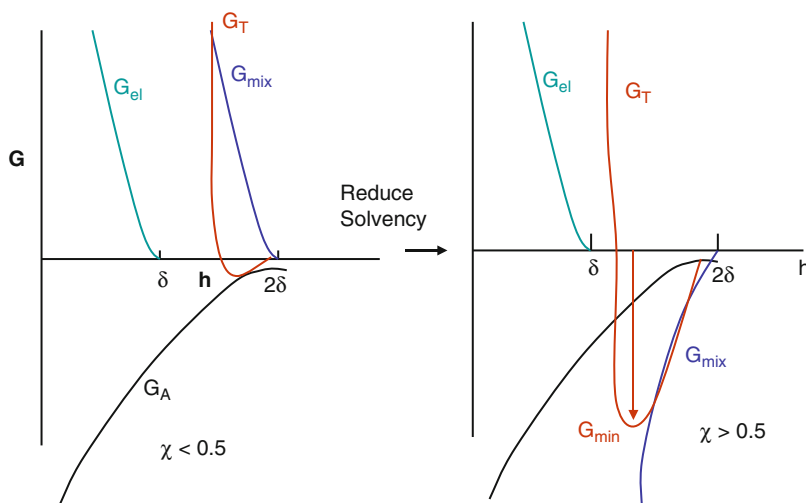
This is particularly important for concentrated suspensions and emulsions. For this purpose, A-B, A-B-A block, and  $BA_n$  graft copolymers are the most suitable where the chain B is chosen to be highly insoluble in the medium and has a strong affinity to the surface. Examples of B groups for hydrophobic particles in aqueous media are polystyrene and polymethylmethacrylate. (3) The stabilizing chain A should be highly soluble in the medium and strongly solvated by its molecules. Examples of A chains in aqueous media are poly(ethylene oxide) and poly(vinyl alcohol) and polysaccharides. (4)  $\delta$  should be sufficiently large ( $> 5$  nm) to prevent weak flocculation.

Two main types of flocculation may be distinguished for sterically stabilized dispersions: (1) Weak flocculation: This occurs when the thickness of the adsorbed layer is small (usually  $< 5$  nm), particularly when the particle radius and Hamaker constant are large. (2) Incipient flocculation: This occurs when the solvency of the medium is reduced to become worse than  $\theta$ -solvent (i.e.,  $\chi > 0.5$ ). This is illustrated in Fig. 27 where  $\chi$  was increased from  $< 0.5$  (good solvent) to  $> 0.5$  (poor solvent).

When  $\chi > 0.5$ ,  $G_{\text{mix}}$  becomes negative (attractive) which when combined with the van der Waals attraction at this separation distance gives a deep minimum causing flocculation. In most cases, there is a correlation between the critical flocculation point and the  $\theta$  condition of the medium. Good correlation is found in many cases between the critical flocculation temperature (CFT) and  $\theta$ -temperature of the polymer in solution (with block and graft copolymers one should consider the  $\theta$ -temperature of the stabilizing chains A) (Tadros et al. 1981; Napper 1981). Good correlation is also found between the critical volume fraction (CFV) of a non-solvent for the polymer chains and their  $\theta$ -point under these conditions. However, in some cases, such correlation may break down, particularly the case for polymers which adsorb by multipoint attachment. This situation has been described by Napper (1981) who referred to it as “enhanced” steric stabilization. Thus, by measuring the  $\theta$ -point (CFT or CFV) for the polymer chains

**Agrochemical Formulations,**

**Fig. 27** Influence of reduction in solvency on the energy-distance curves for sterically stabilized dispersions



(A) in the medium under investigation (which could be obtained from viscosity measurements), one can establish the stability conditions for a dispersion, before its preparation. This procedure helps also in designing effective steric stabilizers such as block and graft copolymers.

**Emulsion Concentrates (EWs)**

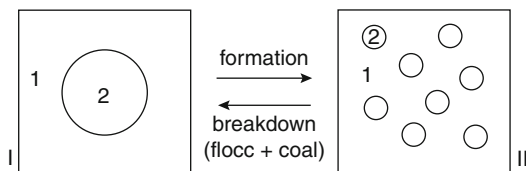
Recently, many agrochemicals have been formulated as oil-in-water (O/W) emulsion concentrates (EWs). These systems offer many advantages over the more traditionally used emulsifiable concentrates (ECs). By using an O/W system, one can reduce the amount of oil in the formulation, since in most cases, a small proportion of oil is added to the agrochemical oil (if this has a high viscosity) before emulsification. In some cases, if the agrochemical oil has a low to medium viscosity, one can emulsify the active ingredient directly into water. With many agrochemicals with low melting point, which is not suitable for the preparation of a suspension concentrate, one can dissolve the active ingredient in a suitable oil and the oil solution is then emulsified into water. EWs which are aqueous based produce less hazard to the operator reducing any skin irritation. In addition, in most cases, EWs are less phytotoxic to plants when compared with ECs. The O/W emulsion is convenient for

incorporation of water soluble adjuvants (mostly surfactants). EWs can also be less expensive when compared to ECs since a lower surfactant concentration is used to produce the emulsion and also one replaces a great proportion of oil by water. The only drawback of EWs when compared to ECs is the need of using high-speed stirrers and/or homogenizers to obtain the required droplet size distribution. In addition, EWs require control and maintenance of its physical stability. As will be discussed later, EWs are only kinetically stable, and one has to control the breakdown process that occur on storage such as creaming or sedimentation, flocculation, Ostwald ripening, coalescence, and phase inversion.

In this section, I will start with the principles of formation of emulsions and the role of the surfactants. This is followed by a section on the procedures that can be applied to select the emulsifiers. The third section will deal to the breakdown processes that may occur on storage and methods of their prevention. The last section will deal with the assessment and prediction of the long-term physical stability of EWs.

**Formation of Emulsions**

Consider a system in which an oil is represented by a large drop 2 of area  $A_1$  immersed in a liquid 2, which is now subdivided into a large number of smaller droplets (Eq. 1) with total area  $A_2$  ( $A_2 \gg A_1$ ) as shown in Fig. 28 The interfacial



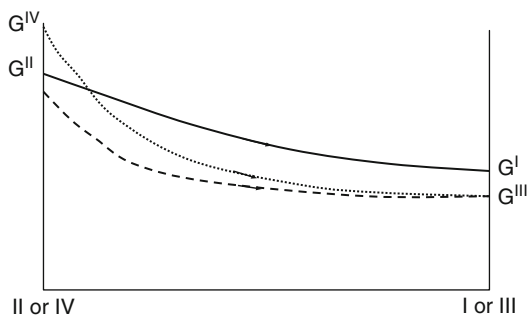
**Agrochemical Formulations, Fig. 28** Schematic representation of emulsion formation and breakdown

tension  $\gamma_{12}$  is the same for the large and smaller droplets since the latter are generally in the region of 0.1 to few  $\mu\text{m}$ . The change in free energy in going from state I to state II is made from two contributions: a surface energy term (i.e., positive) that is equal to  $\Delta A \gamma_{12}$  (where  $\Delta A = A_2 - A_1$ ) and an entropy of dispersion term which is also positive (since producing a large number of droplets is accompanied by an increase in configurational entropy) which is equal to  $T \Delta S^{\text{conf}}$ . From the second law of thermodynamics,

$$\Delta G^{\text{form}} = \Delta A \gamma_{12} - T \Delta S^{\text{conf}} \quad (31)$$

In most cases,  $\Delta A \gamma_{12} \gg T \Delta S^{\text{conf}}$ , which means that  $\Delta G^{\text{form}}$  is positive, that is, the formation of emulsions is non-spontaneous and the system is thermodynamically unstable. In the absence of any stabilization mechanism, the emulsion will break by flocculation, coalescence, Ostwald ripening, or combination of all these processes. This is illustrated in Fig. 29 which shows several paths for emulsion breakdown processes. In the presence of a stabilizer (surfactant and/or polymer), an energy barrier is created between the droplets and, therefore, the reversal from state II to state I becomes noncontinuous as a result of the presence of these energy barriers; this is illustrated in Fig. 30. In the presence of the above energy barriers, the system becomes kinetically stable (Tadros and Vincent 1983). As discussed before, the energy barrier can be created by electrostatic and/or steric repulsion which will overcome the everlasting van der Waals attraction.

To prepare an emulsion, oil, water, surfactant, and energy are needed (Tadros and Vincent 1983; Walstra 1983). This can be considered from



**Agrochemical Formulations, Fig. 29** Free energy path in emulsion breakdown - —, Floc. + coal., ---, Floc. + coal. + Sed., ..... Floc. + coal. + sed. + Ostwald ripening

a consideration of the energy required to expand the interface,  $\Delta A \gamma$  (where  $\Delta A$  is the increase in interfacial area when the bulk oil with area  $A_1$  produces a large number of droplets with area  $A_2$ ;  $A_2 \gg A_1$ ,  $\gamma$  is the interfacial tension). Since  $\gamma$  is positive, the energy to expand the interface is large and positive. This energy term cannot be compensated by the small entropy of dispersion  $T \Delta S$  (which is also positive), and as discussed before, the total free energy of formation of an emulsion,  $\Delta G$  is positive. Thus, emulsion formation is non-spontaneous and energy is required to produce the droplets. The formation of large droplets (few  $\mu\text{m}$ ) as is the case for macroemulsions is fairly easy, and hence high-speed stirrers such as the Ultraturrax or the Silverson mixer are sufficient to produce the emulsion. In contrast, the formation of small drops (submicron as is the case with nanoemulsions) is difficult, and this requires a large amount of surfactant and/or energy. The high energy required for formation of nanoemulsions can be understood from a consideration of the Laplace pressure  $p$  (the difference in pressure between inside and outside the droplet) (Tadros and Vincent 1983; Walstra 1983):

$$\Delta p = \gamma \left( \frac{1}{R_1} + \frac{1}{R_2} \right) \quad (32)$$

where  $R_1$  and  $R_2$  are the principal radii of curvature of the drop.

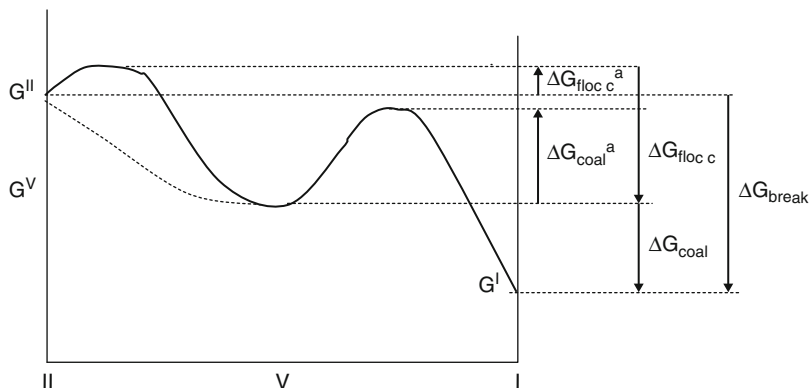
For a spherical drop,  $R_1 = R_2 = R$  and

$$\Delta p = \frac{\gamma}{2R} \quad (33)$$



**Agrochemical Formulations,**

**Fig. 30** Schematic representation of free energy path for breakdown (flocculation and coalescence) for systems containing an energy barrier



To break up a drop into smaller ones, it must be strongly deformed, and this deformation increases  $p$  (Walstra and Smolders 1998). Surfactants play major roles in the formation of emulsions: By lowering the interfacial tension,  $p$  is reduced, and hence the stress needed to break up a drop is reduced (Eqs. 2, 3). Surfactants prevent coalescence of newly formed drops. To describe emulsion formation, one has to consider two main factors: Hydrodynamics and interfacial science. To assess emulsion formation, one usually measures the droplet size distribution using, for example, laser diffraction techniques. A useful average diameter  $d$  is

$$d_{nm} = \left( \frac{S_m}{S_n} \right)^{1/(n-m)} \quad (34)$$

In most cases,  $d_{32}$  (the volume/surface average or Sauter mean) is used. The width of the size distribution can be given as the variation coefficient  $c_m$  which is the standard deviation of the distribution weighted with  $d^m$  divided by the corresponding average  $d$ . Generally,  $C_2$  will be used which corresponds to  $d_{32}$ .

An alternative way to describe the emulsion quality is to use the specific surface area  $A$  (surface area of all emulsion droplets per unit volume of emulsion):

$$A = \pi s^2 = \frac{6\phi}{d_{32}} \quad (35)$$

where  $\phi$  is the volume fraction of the emulsion.

Surfactants lower the interfacial tension  $\gamma$ , and this causes a reduction in droplet size. The latter decrease with decrease in  $\gamma$ . For turbulent regime, the droplet diameter is proportional to  $\gamma^{3/5}$ . The amount of surfactant required to produce the smallest drop size will depend on its activity (concentration) in the bulk which determines the reduction in  $\gamma$ , as given by the Gibbs adsorption equation:

$$-d\gamma = RT\Gamma d\ln a \quad (36)$$

where  $R$  is the gas constant,  $T$  is the absolute temperature, and  $\Gamma$  is the surface excess (number of moles adsorbed per unit area of the interface).  $\Gamma$  increases with increase in surfactant concentration and eventually reaches a plateau value (saturation adsorption).

The value of  $\gamma$  obtained depends on the nature of the oil and surfactant used. Small molecules such as nonionic surfactants lower  $\gamma$  more than polymeric surfactants such as PVA. Another important role of the surfactant is its effect on the interfacial dilational modulus  $\varepsilon$  (Reynders 1996):

$$\varepsilon = \frac{d\gamma}{d\ln A} \quad (37)$$

During emulsification, an increase in the interfacial area  $A$  takes place, and this causes a reduction in  $\Gamma$ . The equilibrium is restored by adsorption of surfactant from the bulk, but this takes time (shorter times occur at higher surfactant activity). Thus,  $\varepsilon$  is small at small  $a$  and also

at large  $a$ . Because of the lack or slowness of equilibrium with polymeric surfactants,  $\varepsilon$  will not be the same for expansion and compression of the interface. In practice, surfactant mixtures are used, and these have pronounced effects on  $\gamma$  and  $\varepsilon$ . Some specific surfactant mixtures give lower  $\gamma$  values than either of the two individual components (Reynders 1996; Lucasses-Reynders 1994). The presence of more than one surfactant molecule at the interface tends to increase  $\varepsilon$  at high surfactant concentrations. The various components vary in surface activity. Those with the lowest  $\gamma$  tend to predominate at the interface, but if present at low concentrations, it may take long time before reaching the lowest value. Polymer-surfactant mixtures may show some synergetic surface activity.

Apart for their effect on reducing  $\gamma$ , surfactants play major roles in deformation and breakup of droplets (Walstra and Smolders 1998; Reynders 1996; Lucasses-Reynders 1994). This is summarized as follows. Surfactants allow the existence of interfacial tension gradients which is crucial for formation of stable droplets. In the absence of surfactants (clean interface), the interface cannot withstand a tangential stress; the liquid motion will be continuous. If a liquid flows along the interface with surfactants, the latter will be swept downstream causing an interfacial tension gradient. The interface will then drag some of the bordering liquid with it (the Marangoni effect). Interfacial tension gradients (Reynders 1996; Lucasses-Reynders 1994; van den Tempel 1960) are very important in stabilizing the thin liquid film between the droplets which is very important during the beginning of emulsification (films of the continuous phase may be drawn through the disperse phase, and collision is very large). The magnitude of the  $\gamma$ -gradients and of the Marangoni effect depends on the surface dilational modulus  $\varepsilon$ . Another important role of the emulsifier is to prevent coalescence during emulsification. This is certainly not due to the strong repulsion between the droplets, since the pressure at which two drops are pressed together is much greater than the repulsive stresses. The counteracting stress must be due to the formation of  $\gamma$ -gradients. Closely related to this mechanism

is the Gibbs-Marangoni effect. The depletion of surfactant in the thin film between approaching drops results in  $\gamma$ -gradient without liquid flow being involved. This results in an inward flow of liquid that tends to drive the drops apart (Reynders 1996; Lucasses-Reynders 1994; van den Tempel 1960). The Gibbs-Marangoni effect also explains the Bancroft rule which states that the phase in which the surfactant is most soluble form the continuous phase. If the surfactant is in the droplets, a  $\gamma$ -gradient cannot develop and the drops would be prone to coalescence. Thus, surfactants with  $HLB > 7$  tend to form O/W emulsions and  $HLB < 7$  tend to form W/O emulsions. The Gibbs-Marangoni effect also explains the difference between surfactants and polymers for emulsification. Polymers give larger drops when compared with surfactants. Polymers give a smaller value of  $\varepsilon$  at small concentrations when compared to surfactants. Various other factors should also be considered for emulsification: The disperse phase volume fraction  $\phi$ . Increase in  $\phi$  leads to increase in droplet collision and hence coalescence during emulsification. With increase in  $\phi$ , the viscosity of the emulsion increases and could change the flow from being turbulent to being laminar. The presence of many particles results in a local increase in velocity gradients. This means that  $G$  increases. In turbulent flow, increase in  $\phi$  will induce turbulence depression. This will result in larger droplets. Turbulence depression by added polymers tend to remove the small eddies, resulting in the formation of larger droplets. If the mass ratio of surfactant to continuous phase is kept constant, increase in  $\phi$  results in decrease in surfactant concentration and hence an increase in  $\gamma_{eq}$ . This results in larger droplets. If the mass ratio of surfactant to disperse phase is kept constant, the above changes are reversed.

### Selection of Emulsifiers

The selection of different surfactants in the preparation of either O/W or W/O emulsions is often still made on an empirical basis. A semiempirical scale for selecting surfactants is the Hydrophilic-Lipophilic balance (HLB number) developed by Griffin (1949; Becher 1987). This scale is based

on the relative percentage of hydrophilic to lipophilic (hydrophobic) groups in the surfactant molecule(s). For an O/W emulsion droplet, the hydrophobic chain resides in the oil phase, whereas the hydrophilic head group resides in the aqueous phase. For a W/O emulsion droplet, the hydrophilic group(s) reside in the water droplet, whereas the lipophilic groups reside in the hydrocarbon phase. A summary of HLB ranges and their application is given in Table 1.

The above table gives a guide to the selection of surfactants for a particular application. The HLB number depends on the nature of the oil (Griffin 1949; Becher 1987). As an illustration Table 2 gives the required HLB numbers to emulsify various oils.

The relative importance of the hydrophilic and lipophilic groups was first recognized when using mixtures of surfactants containing varying proportions of a low and high HLB number (Griffin 1949; Becher 1987). The efficiency of any combination (as judged by phase separation) was found to pass a maximum when the blend contained a particular proportion of the surfactant with the higher HLB number. This is illustrated in Fig. 31 which shows the variation of emulsion stability, droplet size, and interfacial tension as a function of % surfactant with high HLB number.

The average HLB number may be calculated from additivity:

$$HLB = x_1 HLB_1 + x_2 HLB_2 \quad (38)$$

$x_1$  and  $x_2$  are the weigh fractions of the two surfactants with HLB<sub>1</sub> and HLB<sub>2</sub>.

Griffin (1949; Becher 1987) developed simple equations for calculation of the HLB number of relatively simple nonionic surfactants. For a polyhydroxy fatty acid ester,

$$HLB = 20 \left( 1 - \frac{S}{A} \right) \quad (39)$$

S is the saponification number of the ester and A is the acid number.

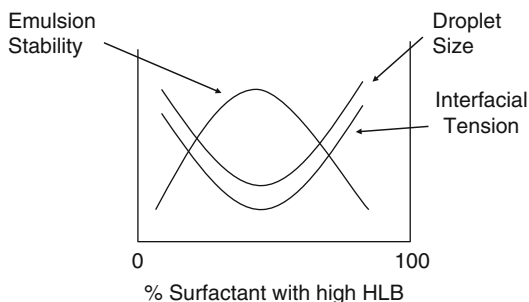
For a glyceryl monostearate, S = 161 and A = 198 – The HLB is 3.8 (suitable for w/o

**Agrochemical Formulations, Table 1** Summary of HLB ranges and their applications

HLB Range	Application
3–6	W/O emulsifier
7–9	Wetting agent
8–18	O/W emulsifier
13–15	Detergent
15–18	Solubilize

**Agrochemical Formulations, Table 2** Required HLB numbers to emulsify various oils

Oil	W/O emulsion	O/W emulsion
Paraffin oil	4	10
Beeswax	5	9
Linolin, anhydrous	8	12
Cyclohexane	–	15
Toluene	–	15



**Agrochemical Formulations, Fig. 31** Arianation of emulsion stability, droplet size, and interfacial tension with % surfactant with high HLB number

emulsion). For a simple alcohol ethoxylate, the HLB number can be calculated from the weight percent of ethylene oxide (E) and polyhydric alcohol (P),

$$HLB = \frac{E + P}{5} \quad (40)$$

If the surfactant contains PEO as the only hydrophilic group contribution from one OH group neglected,

**Agrochemical Formulations, Table 3** HLB group numbers

<i>Hydrophilic</i>	
-SO <sub>4</sub> Na <sup>+</sup>	38.7
-COO <sup>-</sup>	21.2
-COONa	19.1
N(tertiary amine)	9.4
Ester (sorbitan ring)	6.8
-O-	1.3
CH-(sorbitan ring)	0.5
<i>Lipophilic</i>	
(-CH-), (-CH <sub>2</sub> -), CH <sub>3</sub>	0.475
<i>Derived</i>	
-CH <sub>2</sub> -CH <sub>2</sub> -O	0.33
-CH <sub>2</sub> -CH <sub>2</sub> -CH <sub>2</sub> -O-	-0.15

$$HLB = \frac{E}{5} \quad (41)$$

For a nonionic surfactant C<sub>12</sub>H<sub>25</sub>-O-(CH<sub>2</sub>-CH<sub>2</sub>-O)<sub>6</sub>, the HLB is 12 (suitable for O/W emulsion).

The above simple equations cannot be used for surfactants containing propylene oxide or butylene oxide. They cannot be also applied for ionic surfactants. Davies (1959) devised a method for calculating the HLB number for surfactants from their chemical formulae, using empirically determined group numbers. A group number is assigned to various component groups. A summary of the group numbers for some surfactants is given in Table 3.

The HLB is given by the following empirical equation:

$$HLB = 7 + \sum(\text{hydrophilic group Nos}) - \sum(\text{lipophilic group Nos}) \quad (42)$$

Davies (1959) has shown that the agreement between HLB numbers calculated from the above equation and those determined experimentally is quite satisfactory. Various other procedures were developed to obtain a rough estimate of the HLB number. Griffin found good correlation between the cloud point of 5 % solution of various ethoxylated surfactants and their HLB number.

Davies (1959) attempted to relate the HLB values to the selective coalescence rates of emulsions. Such correlations were not realized since it was found that the emulsion stability and even its type depends to a large extent on the method of dispersing the oil into the water and vice versa. At best, the HLB number can only be used as a guide for selecting optimum compositions of emulsifying agents. One may take any pair of emulsifying agents, which fall at opposite ends of the HLB scale, for example, Tween 80 (sorbitan monooleate with 20 moles EO, HLB = 15) and Span 80 (sorbitan monooleate, HLB = 5), using them in various proportions to cover a wide range of HLB numbers. The emulsions should be prepared in the same way, with a few percent of the emulsifying blend. The stability of the emulsions is then assessed at each HLB number from the rate of coalescence or qualitatively by measuring the rate of oil separation. In this way, one may be able to find the optimum HLB number for a given oil. Having found the most effective HLB value, various other surfactant pairs are compared at this HLB value, to find the most effective pair.

The phase inversion temperature (PIT) concept which has been developed by Shinoda (1967; Shinoda and Saito 1969) is closely related to the HLB balance concept described above. Shinoda and coworkers found that many O/W emulsions stabilized with nonionic surfactants undergo a process of inversion at a critical temperature (PIT). The PIT can be determined by following the emulsion conductivity (small amount of electrolyte is added to increase the sensitivity) as function of temperature. The conductivity of the O/W emulsion increases with increase of temperature till the PIT is reached, above which there will be a rapid reduction in conductivity (w/o emulsion is formed).

Shinoda and coworkers (1967; Shinoda and Saito 1969) found that the PIT is influenced by the HLB number of the surfactant. The size of the emulsion droplets was found to depend on the temperature and HLB number of the emulsifiers. The droplets are less stable toward coalescence close to the PIT. However, by rapid cooling of the emulsion, a stable system may be produced.

Relatively stable o/w emulsions were obtained when the PIT of the system was 20–65 °C higher than the storage temperature. Emulsions prepared at a temperature just below the PIT followed by rapid cooling generally have smaller droplet sizes. This can be understood if one considers the change of interfacial tension with temperature. The interfacial tension decreases with increase of temperature reaching a minimum close to the PIT, after which it increases. Thus, the droplets prepared close to the PIT are smaller than those prepared at lower temperatures. These droplets are relatively unstable toward coalescence near the PIT, but by rapid cooling of the emulsion, one can retain the smaller size. This procedure may be applied to prepare mini (nano) emulsions. The optimum stability of the emulsion was found to be relatively insensitive to changes in the HLB value or the PIT of the emulsifier, but instability was very sensitive to the PIT of the system. It is essential, therefore, to measure the PIT of the emulsion as a whole (with all other ingredients). At a given HLB value, stability of the emulsions against coalescence increases markedly as the molar mass of both the hydrophilic and lipophilic components increases. The enhanced stability using high molecular weight surfactants (polymeric surfactants) can be understood from a consideration of the steric repulsion which produces more stable films. Films produced using macromolecular surfactants resist thinning and disruption thus reducing the possibility of coalescence. The emulsions showed maximum stability when the distribution of the PEO chains was broad. The cloud point is lower but the PIT is higher than in the corresponding case for narrow-size distributions. The PIT and HLB number are directly related parameters. Addition of electrolytes reduces the PIT and, hence, an emulsifier with a higher PIT value is required when preparing emulsions in the presence of electrolytes. Electrolytes cause dehydration of the PEO chains, and, in effect, this reduces the cloud point of the nonionic surfactant. One needs to compensate for this effect by using a surfactant with higher HLB. The optimum PIT of the emulsifier is fixed if the storage temperature is fixed.

### Emulsion Stability

Several breakdown processes may occur on storage depending on: (1) Particle size distribution and density difference between the droplets and the medium. (2) Magnitude of the attractive versus repulsive forces which determines flocculation. (3) Solubility of the disperse droplets and the particle size distribution which determines Ostwald ripening. (4) Stability of the liquid film between the droplets that determines coalescence. (5) Phase Inversion. The various breakdown processes are illustrated in the Fig. 32. This is followed by description of each of the breakdown processes and methods that can be applied to prevent such instability.

Emulsion creaming or sedimentation is the result of gravity, when the density of the droplets and the medium are not equal. For small droplets ( $< 0.1 \mu$ , i.e., nanoemulsions), the Brownian diffusion  $kT$  (where  $k$  is the Boltzmann constant and  $T$  is the absolute temperature) exceeds the force of gravity (mass  $\times$  acceleration due to gravity  $g$ ):

$$kT \ll \frac{4}{3}\pi R^3 \Delta\rho g L \quad (43)$$

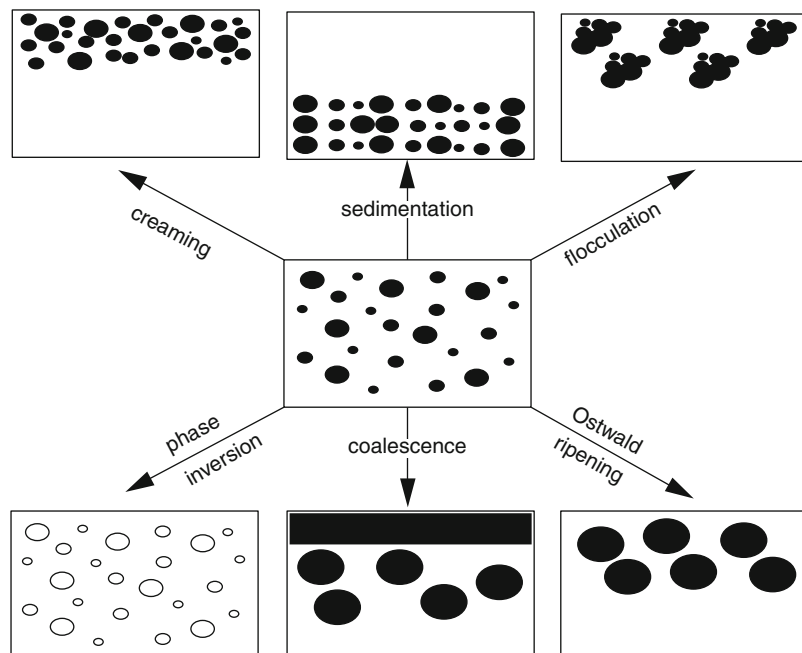
where  $R$  is the droplet radius,  $\Delta\rho$  is the density difference between the droplets and the medium, and  $L$  is the height of the container. In this case, no creaming or sedimentation occurs.

For emulsions consisting of “monodisperse” droplets with radius  $> 1 \mu\text{m}$ , the emulsion separates into two distinct layers with the droplets forming a cream or sediment leaving the clear supernatant liquid. This situation is seldom observed in practice. For a polydisperse (practical) emulsion, the droplets will cream or sediment at various rates. In the last case, a concentration gradient builds up with the larger droplets staying at the top of the cream layer or the bottom:

$$C(h) = C_0 \exp\left(-\frac{mgh}{kT}\right) \quad (44)$$

$$m = \frac{4}{3}\pi R^3 \Delta\rho g \quad (45)$$

**Agrochemical Formulations,**  
**Fig. 32** Schematic representation of the various breakdown processes in emulsions



$C(h)$  is the concentration (or volume fraction  $\phi$ ) of droplets at height  $h$ , whereas  $C_0$  is the concentration at zero time which is the same at all heights.

For very dilute emulsions ( $\phi < 0.01$ ), the rate  $v_0$  can be calculated using Stokes' law which balances the hydrodynamic force with gravity force:

$$v_0 = \frac{2}{9} \frac{\Delta\rho g R^2}{\eta_0} \quad (46)$$

$v_0$  is the Stokes' velocity and  $\eta_0$  is the viscosity of the medium. For an O/W emulsion with  $\Delta\rho = 0.2$  in water ( $\eta_0 \sim 10^{-3}$  Pa s), the rate of creaming or sedimentation is  $\sim 4.4 \times 10^{-5} \text{ ms}^{-1}$  for 10  $\mu\text{m}$  droplets and  $\sim 4.4 \times 10^{-7} \text{ ms}^{-1}$  for 1  $\mu\text{m}$  droplets. This means that in a 0.1-m container, creaming or sedimentation of the 10- $\mu\text{m}$  droplets is complete in  $\sim 0.6$  h, and for the 1- $\mu\text{m}$  droplet, this takes  $\sim 60$  h. For moderately concentrated emulsions ( $0.2 < \phi < 0.1$ ), one has to take into account the hydrodynamic interaction between the droplets, which reduces the Stokes velocity to a value  $v$  given by the following expression (96):

$$v = v_0 (1 - k\phi) \quad (47)$$

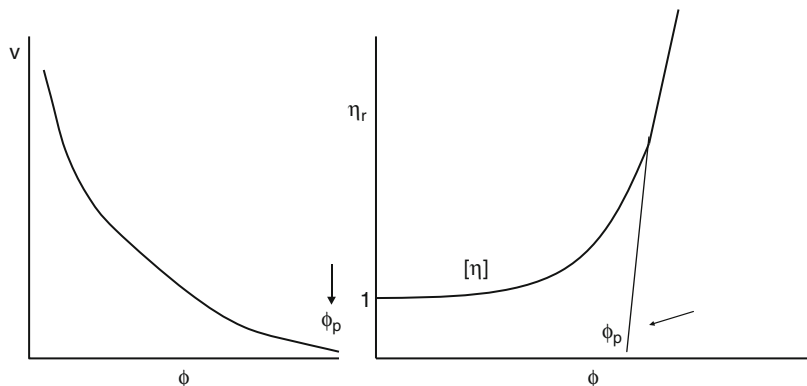
where  $k$  is a constant that accounts for hydrodynamic interaction.  $k$  is of the order of 6.5, which means that the rate of creaming or sedimentation is reduced by about 65 %. For concentrated emulsions ( $\phi > 0.2$ ), the rate of creaming or sedimentation becomes a complex function of  $\phi$  as is illustrated in Fig. 33 which also shows the change of relative viscosity  $\eta_r$  with  $\phi$ . As can be seen from Fig. 34,  $v$  decreases with increase in  $\phi$ , and ultimately, it approaches zero when  $\phi$  exceeds a critical value,  $\phi_p$ , which is the so-called maximum packing fraction.

The value of  $\phi_p$  for monodisperse "hard-spheres" ranges from 0.64 (for random packing) to 0.74 for hexagonal packing. The value of  $\phi_p$  exceeds 0.74 for polydisperse systems. Also, for emulsions which are deformable,  $\phi_p$  can be much larger than 0.74. Figure 34 also shows that when  $\phi$  approaches  $\phi_p$ ,  $\eta_r$  approaches  $\infty$ . In practice, most emulsions are prepared at  $\phi$  values well below  $\phi_p$ , usually in the range 0.2–0.5, and under these conditions, creaming or sedimentation is the rule rather than the exception. Several procedures may be applied to reduce or eliminate



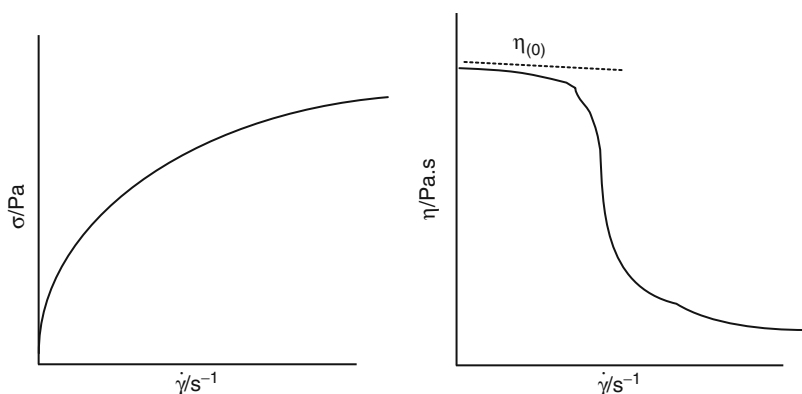
**Agrochemical Formulations,**

**Fig. 33** Variation of  $v$  and  $\eta_r$  with  $\phi$



**Agrochemical Formulations,**

**Fig. 34** Variation of (stress)  $\sigma$  and viscosity  $\eta$  with shear rate  $\dot{\gamma}$



creaming or sedimentation: (1) Matching density of oil and aqueous phases. Clearly, if  $\Delta\rho = 0$ ,  $v = 0$ ; however, this method is seldom practical. Density matching, if possible, only occurs at one temperature. (2) Reduction of droplet size; since the gravity force is proportional to  $R^3$ , then if  $R$  is reduced by a factor of 10, the gravity force is reduced by 1,000. Below a certain droplet size (which also depends on the density difference between oil and water), the Brownian diffusion may exceed gravity and creaming or sedimentation is prevented. This is the principle of formulation of nanoemulsions (with size range 50–200 nm) which may show very little or no creaming or sedimentation. The same applies for microemulsions (size range 5–50 nm). (3) Use of “thickeners,” that is, high molecular weight polymers, natural or synthetic such as Xanthan gum, hydroxyethyl cellulose, alginates, carragenans, etc. To understand the role of these “thickeners,”

let us consider the gravitational stresses exerted during creaming or sedimentation:

$$\begin{aligned} \text{Stress} &= \text{mass of drop} \times \text{acceleration of gravity} \\ &= \frac{4}{3} \pi R^3 \Delta\rho g \end{aligned} \tag{48}$$

To overcome such stress, one needs a restoring force:

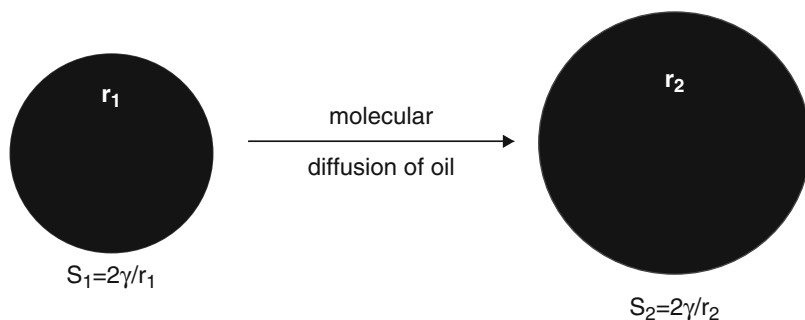
$$\begin{aligned} \text{Restoring Force} &= \text{Area of drop} \times \text{stress of drop} \\ &= 4\pi R^2 \sigma_p \end{aligned} \tag{49}$$

Thus, the stress exerted by the droplet  $\sigma_p$  is given by

$$\sigma_p = \frac{\Delta\rho Rg}{3} \tag{50}$$

### Agrochemical Formulations,

**Fig. 35** Schematic representation of Ostwald ripening



Simple calculation shows that  $\sigma_p$  is in the range  $10^{-3}$  to  $10^{-1}$  Pa, which implies that for prediction of creaming or sedimentation, one needs to measure the viscosity at such low stresses. This can be obtained by using constant stress or creep measurements. These above “thickeners” satisfy the criteria for obtaining very high viscosities at low stresses or shear rates. This can be illustrated from plots of shear stress  $\tau$  and viscosity  $\eta$  versus shear rate (or shear stress) as shown in Fig. 34. These systems are described as “pseudoplastic” or shear thinning. The low-shear (residual or zero shear rate) viscosity  $\eta(0)$  can reach several thousand Pas, and such high values prevent creaming or sedimentation. This behavior is obtained above a critical polymer concentration ( $C^*$ ) which can be located from plots of  $\log \eta$  versus  $\log C$ ; above  $C^*$ , the viscosity increases very sharply with further increase in polymer concentration.

Flocculation of emulsions is the result of van der Waals attraction that is universal for all disperse systems. The van der Waals attraction  $G_A$  was described before. It showed that  $G_A$  is inversely proportional to the droplet-droplet distance of separation  $h$ , and it depends on the effective Hamaker constant  $A$  of the emulsion system. One way to overcome the van der Waals attraction is by electrostatic stabilization using ionic surfactants which results in the formation of electrical double layers that introduce a repulsive energy that overcomes the attractive energy. Emulsions stabilized by electrostatic repulsion become flocculated at intermediate electrolyte concentrations. The second and most effective method of overcoming flocculation is by “steric stabilization” using nonionic surfactants or

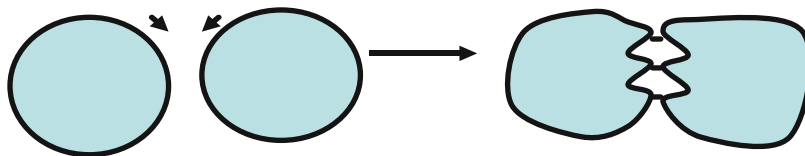
polymers. Stability may be maintained in electrolyte solutions (as high as  $1 \text{ mol dm}^{-3}$  depending on the nature of the electrolyte) and up to high temperatures (in excess of  $50^\circ\text{C}$ ) provided the stabilizing chains (e.g., PEO) are still in better than  $\theta$ -conditions ( $\chi < 0.5$ ). The main criteria that are required to reduce (eliminate) flocculation are: (1) For electrostatically stabilized emulsions, high surface or zeta potential, low electrolyte concentration, and low valency of ions. (2) For sterically stabilized emulsions, complete coverage of the droplets by the stabilizing chains, firm attachment (strong anchoring) of the chains to the droplets, good solvency of the stabilizing chain by the molecules of the medium, and reasonably thick adsorbed layers.

The driving force for Ostwald ripening is the difference in solubility between the small and large droplets (the smaller droplets have higher Laplace pressure and higher solubility than the larger ones). This is illustrated in Fig. 35 where  $r_1$  decreases and  $r_2$  increases as a result of diffusion of molecules from the smaller to the larger droplets.

The difference in chemical potential between different-sized droplets was given by Lord Kelvin (Thompson (Lord Kelvin) 1871):

$$S(r) = S(\infty) \exp\left(\frac{2\gamma V_m}{rRT}\right) \quad (51)$$

where  $S(r)$  is the solubility surrounding a particle of radius  $r$ ,  $S(\infty)$  is the bulk solubility,  $V_m$  is the molar volume of the dispersed phase,  $R$  is the gas constant, and  $T$  is the absolute temperature. The quantity  $(2\gamma V_m/RT)$  is termed the characteristic length. It has an order of  $\sim 1 \text{ nm}$  or less,

**Agrochemical Formulations,****Fig. 36** Schematic representation of surface fluctuations

indicating that the difference in solubility of a 1- $\mu$ m droplet is of the order of 0.1 % or less. Theoretically, Ostwald ripening should lead to condensation of all droplets into a single drop (Thompson (Lord Kelvin) 1871). This does not occur in practice since the rate of growth decreases with increase of droplet size.

For two droplets with radii  $r_1$  and  $r_2$  ( $r_1 < r_2$ ),

$$\frac{RT}{V_m} \ln \left[ \frac{S(r_1)}{S(r_2)} \right] = 2\gamma \left[ \frac{1}{r_1} - \frac{1}{r_2} \right] \quad (52)$$

Equation 52 shows that the larger the difference between  $r_1$  and  $r_2$ , the higher the rate of Ostwald ripening. The latter can be quantitatively assessed from plots of the cube of the radius versus time  $t$  (Kabalanov and Shchukin 1992; Lifshitz and Slesov 1959; Wagner 1961):

$$r^3 = \frac{8}{9} \left[ \frac{S(\infty)\gamma V_m D}{\rho RT} \right] t \quad (53)$$

$D$  is the diffusion coefficient of the disperse phase in the continuous phase.

Several methods may be applied to reduce Ostwald ripening: (1) Addition of a second disperse phase component which is insoluble in the continuous medium (e.g., squalane) (Higuchi and Misra 1962). In this case, partitioning between different droplet sizes occurs, with the component having low solubility expected to be concentrated in the smaller droplets. During Ostwald ripening in a two-component system, equilibrium is established when the difference in chemical potential between different size droplets (which results from curvature effects) is balanced by the difference in chemical potential resulting from partitioning of the two components – this effect reduces further growth of droplets. (2) Modification of the interfacial film at the O/W interface. According to Eq. 53, reduction in  $\gamma$  results in

reduction of Ostwald ripening rate. By using surfactants that are strongly adsorbed at the O/W interface (i.e., polymeric surfactants) and which do not desorb during ripening (by choosing a molecule that is insoluble in the continuous phase), the rate could be significantly reduced (Walstra 1996). An increase in the surface dilational modulus  $\varepsilon$  ( $= d\gamma/d\ln A$ ) and decrease in  $\gamma$  would be observed for the shrinking drop, and this tends to reduce further growth. A-B-A block copolymers such as PHS-PEO-PHS (which is soluble in the oil droplets but insoluble in water) can be used to achieve the above effect. This polymeric emulsifier enhances the Gibbs elasticity and causes reduction of  $\gamma$  to very low values.

Emulsion coalescence may occur when the droplets approach each other below a critical distance  $h$ . When two emulsion droplets come in close contact in a floc or creamed layer or during Brownian diffusion, thinning and disruption of the liquid film may occur resulting in eventual rupture. On close approach of the droplets, film thickness fluctuations may occur. Alternatively, the liquid surfaces undergo some fluctuations forming surface waves, as illustrated in Fig. 36. The surface waves may grow in amplitude and the apices may join as a result of the strong van der Waals attraction (at the apex, the film thickness is the smallest). The same applies if the film thins to a small value (critical thickness for coalescence). A very useful concept was introduced by Deryaguin (Deryaguin and Scherbaker 1961) who suggested that a “disjoining pressure”  $\pi(h)$  is produced in the film which balances the excess normal pressure:

$$\pi(h) = P(h) - P_o \quad (54)$$

where  $P(h)$  is the pressure of a film with thickness  $h$  and  $P_o$  is the pressure of a sufficiently thick film such that the net interaction-free energy is zero.

$\pi(h)$  may be equated to the net force (or energy) per unit area acting across the film:

$$\pi(h) = -\frac{dG_T}{dh} \quad (55)$$

where  $G_T$  is the total interaction energy in the film.

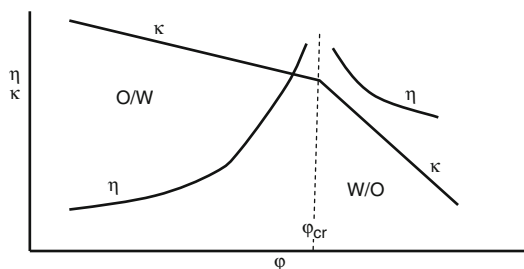
$\pi(h)$  is made of three contributions due to electrostatic repulsion ( $\pi_E$ ), steric repulsion ( $\pi_S$ ), and van der Waals attraction ( $\pi_A$ ):

$$\pi(h) = \pi_E + \pi_S + \pi_A \quad (56)$$

To produce a stable film,  $\pi_E + \pi_S > \pi_A$ , and this is the driving force for prevention of coalescence which can be achieved by two mechanisms and their combination: (1) Increased repulsion both electrostatic and steric. (2) Dampening of the fluctuation by enhancing the Gibbs elasticity. In general, smaller droplets are less susceptible to surface fluctuations, and hence coalescence is reduced. This explains the high stability of nanoemulsions.

Several methods may be applied to achieve the above effects: (1) Use of mixed surfactant films. In many cases, using mixed surfactants, say anionic and nonionic, or long-chain alcohols can reduce coalescence as a result of several effects: High Gibbs elasticity, high surface viscosity, and hindered diffusion of surfactant molecules from the film. (2) Formation of lamellar liquid crystalline phases at the O/W interface. This mechanism was suggested by Friberg and coworkers (Friberg et al. 1976), who suggested that surfactant or mixed surfactant film can produce several bilayers that “wrap” the droplets. As a result of these multilayer structures, the potential drop is shifted to longer distances thus reducing the van der Waals attraction. For coalescence to occur, these multilayers have to be removed “two-by-two,” and this forms an energy barrier preventing coalescence.

Since film drainage and rupture is a kinetic process, coalescence is also a kinetic process. If one measures the number of particles  $n$  (floculated or not) at time  $t$ ,



**Agrochemical Formulations, Fig. 37** Variation of viscosity ( $\eta$ ) and conductivity ( $\kappa$ ) with oil volume fraction

$$n = n_t + n_v m \quad (57)$$

where  $n_t$  is the number of primary particles remaining and  $n$  is the number of aggregates consisting of  $m$  separate particles.

For studying emulsion coalescence, one should consider the rate constant of flocculation and coalescence. If coalescence is the dominant factor, then the rate  $K$  follows a first-order kinetics:

$$n = \frac{n_0}{Kt} [1 + \exp -(Kt)] \quad (58)$$

which shows that a plot of  $\log n$  versus  $t$  should give a straight line from which  $K$  can be calculated.

Phase inversion of emulsions can be one of two types: Transitional inversion induced by changing facers which affect the HLB of the system, for example, temperature and/or electrolyte concentration and catastrophic inversion which is induced by increasing the volume fraction of the disperse phase. Catastrophic inversion is illustrated in Fig. 37 which shows the variation of viscosity and conductivity with the oil volume fraction  $\phi$ . As can be seen, inversion occurs at a critical  $\phi$ , which may be identified with the maximum packing fraction. At  $\phi_{cr}$ ,  $\eta$  suddenly decreases; the inverted W/O emulsion has a much lower volume fraction.  $\kappa$  also decreases sharply at the inversion point since the continuous phase is now oil, which has very low conductivity. Earlier theories of phase inversion were based on packing parameters. When  $\phi$  exceeds the maximum packing ( $\sim 0.64$  for random packing

and  $\sim 0.74$  for hexagonal packing of monodisperse spheres; for polydisperse systems, the maximum packing exceeds 0.74), inversion occurs. However, these theories are not adequate, since many emulsions invert at  $\phi$  values well below the maximum packing as a result of the change in surfactant characteristics with variation of conditions. For example, when using a nonionic surfactant based on PEO, the latter chain changes its solvation by increase of temperature and/or addition of electrolyte. Many emulsions show phase inversion at a critical temperature (the phase inversion temperature) that depends on the HLB number of the surfactant as well as the presence of electrolytes. By increasing temperature and/or addition of electrolyte, the PEO chains become dehydrated, and finally they become more soluble in the oil phase. Under these conditions, the O/W emulsion will invert to a W/O emulsion. This dehydration effect amounts to a decrease in the HLB number, and when the latter reaches a value that is more suitable for W/O emulsion, inversion will occur. At present, there is no quantitative theory that accounts for phase inversion of emulsions.

### Experimental Methods for Assessment of Emulsion Stability

Understanding the emulsion breakdown processes at a molecular level is far from being achieved at present. It is, thus, necessary to develop methods of assessment of each process and attempt to predict the long-term physical stability of emulsions. Several methods may be applied to assess the creaming or sedimentation of emulsion: (1) Measurement of the rate by direct observation of emulsion separation using graduated cylinders that are placed at constant temperature. This method allows one to obtain the rate as well as the equilibrium cream or sediment volume. (2) Turbidity measurements as a function of height at various times, using, for example, the Turboscan (that measures turbidity from the back scattering of near IR light). (3) Ultrasonic velocity and absorption at various heights in the cream or sedimentation tubes.

Centrifugation may be applied to accelerate the rate of creaming or sedimentation, and this method is sometimes used for prediction of emulsion stability. The assumption is made that by increasing the  $g$  force, the rate of sedimentation or creaming is significantly increased, and this could be applied to predict the process from measurement at short time periods. In a centrifuge, the gravity force is given by

$$g = \omega^2 x \quad (59)$$

where  $x$  is the mean distance of the centrifuge tube from the axis of rotation and  $\omega$  is the angular velocity ( $\omega = 2\pi\nu$ , where  $\nu$  is the number of revolutions per second). Note that if the centrifuge tube is not small compared to  $x$ , then the applied centrifugal field cannot be considered to be uniform over the length of the tube.

Modern analytical ultracentrifuges allow one to follow the separation of emulsions in a quantitative manner. With typical O/W emulsions, three layers are generally observed: A clear aqueous phase, an opaque phase consisting of distorted polyhedral oil droplets, and a clear separated oil phase, resulting from coalescence of the polyhedra. The degree of emulsion stability may be taken as the volume of the opaque phase remaining after time  $t$ . Alternatively, one may use the volume of oil separated at infinite time as an index for stability.

A simple expression may be used to treat the data in a quantitative manner:

$$\frac{t}{V} = \frac{1}{bV_\infty} + \frac{t}{V_\infty} \quad (60)$$

where  $V$  is the volume of oil separated at time  $t$ ,  $V_\infty$  is the extrapolated volume at infinite time and  $b$  is a constant. A plot of  $t/V$  versus  $t$  should give a straight line from which  $b$  and  $V_\infty$  may be calculated. These two parameters may be taken as indices for emulsion stability. A more rigorous procedure to study emulsion stability using the ultracentrifuge is to observe the system at various speeds of rotation. At relatively low centrifuge speeds, one may observe the expected opaque cream layer. At sufficiently high centrifuge

speeds, one may observe a coalesced oil layer and a cream layer which are separated by an extra layer of deformed oil droplets. This deformed layer looks like a “foam,” that is, it consists of oil droplets separated by thin aqueous films. For certain emulsions, one may find that by increasing the centrifuge speed, the “foam”/cream layer boundary does not move. Under conditions where there is an equilibrium between the “foam”/cream layer, one may conclude that there is no barrier to be overcome in forming the foam layer from the cream layer. This implies that in the foam layer, the aqueous film separating two oil droplets thins to a “black” film under the action of van der Waals forces. The boundary between the foam layer and the coalesced layer is associated with a force (or pressure) barrier. One may observe the minimum centrifuge speed that is necessary to produce a visible amount of coalesced oil after say 30 min of centrifugation. This centrifuge speed may be used to calculate the “critical pressure” that needs to be applied to induce coalescence.

The flocculation of emulsions can be assessed using turbidity measurements. For dilute emulsions (which may be obtained by carefully diluting the concentrate in the supernatant liquid), the rate of flocculation can be determined by measuring turbidity,  $\tau$ , as a function of time:

$$\tau = A n_o V_1^2 (1 + n_o kt) \quad (61)$$

where  $A$  is an optical constant,  $n_o$  is the number of droplets at time  $t = \text{zero}$ ,  $V_1$  is the volume of the droplets, and  $k$  is the rate constant of flocculation. Thus, a plot of  $\tau$  versus  $t$  gives a straight line, in the initial time of flocculation, and  $k$  can be calculated from the slope of the line. Flocculation of emulsions can also be assessed by direct droplet counting using optical microscopy (with image analysis), using the Coulter counter and light diffraction techniques (e.g., using the Master sizer, Malvern, UK). The flocculation of emulsion concentrate can be followed using rheological methods. In the absence of any Ostwald ripening and/or coalescence, flocculation of the emulsion concentrates is accompanied by

increase in its viscosity, yield value, or elastic modulus. These rheological parameters can be easily measured using rotational viscometers. Clearly, if Ostwald ripening and/or coalescence occur at the same time as emulsion flocculation, the viscosity, yield value, or elastic modulus will show a complex dependence of these parameters on time, and this makes the analysis of the rheological results very difficult.

As mentioned above, the best procedure to follow Ostwald ripening is to plot  $r^3$  versus time, following Eq. 53. This gives a straight line from which the rate of Ostwald ripening can be calculated. In this way, one can assess the effect of the various additives that may reduce Ostwald ripening, for example, addition of highly insoluble oil and/or an oil soluble polymeric surfactant.

The rate of coalescence is measured by following the droplet number  $n$  or average droplet size  $d$  (diameter) as a function of time. Plots of log droplet number or average diameter versus time give straight lines (at least in the initial stages of coalescence) from which the rate of coalescence  $K$  can be estimated using Eq. 58. In this way, one can compare the different stabilizers, for example, mixed surfactant films, liquid crystalline phase, and macromolecular surfactants.

The most common procedure to assess phase inversion is to measure the conductivity or the viscosity of the emulsion as a function of  $\phi$ , increase of temperature, and/or addition of electrolyte. For example, for an O/W emulsion, phase inversion to W/O is accompanied by a rapid decrease in conductivity and viscosity.

## Suspension Concentrates

The formulation of agrochemicals as dispersions of solids in aqueous solution (to be referred to as suspension concentrates or SCs) has attracted considerable attention in recent years. Several advantages may be quoted for SCs. Firstly, one may control the particle size by controlling the milling conditions and proper choice of the dispersing agent. Secondly, it is possible to



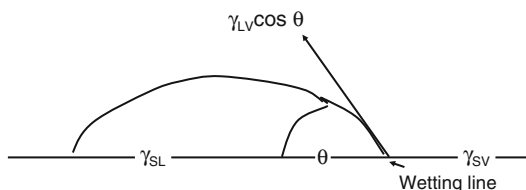
incorporate high concentrations of surfactants in the formulation which is sometimes essential for enhancing wetting, spreading, and penetration. Stickers may also be added to enhance adhesion and in some cases to provide slow release. In recent years, there has been considerable research into the factors that govern the stability of suspension concentrates (Ottewill 1987; Tadros 1980, 1983). The theories of colloid stability could be applied to predict the physical states of these systems on storage. In addition, analysis of the problem of sedimentation of SCs at a fundamental level has been undertaken (Parfitt 1977). Since the density of the particles is usually larger than that of the medium (water), SCs tend to separate as a result of sedimentation. The sedimented particles tend to form a compact layer at the bottom of the container (sometimes referred to as clay or cake), which is very difficult to redisperse. It is, therefore, essential to reduce sedimentation and formation of clays by incorporation of an antisetling agent.

In this section, I will attempt to address the above-mentioned phenomena at a fundamental level. It will start with a section on the preparation of suspension concentrates and the role of surfactants (dispersing agents). This is followed by a section on the control of the physical stability of suspensions. The problem of Ostwald ripening (crystal growth) will also be briefly described, and particular attention will be paid to the role of surfactants. The next part will deal with the problem of sedimentation and prevention of claying. The various methods that may be applied to reduce sedimentation and prevention of the formation of hard clays will be summarized. The last part in this section will deal with the methods that may be applied for the assessment of the physical stability of SCs. For the assessment of flocculation and crystal growth, particle size analysis techniques are commonly applied. The bulk properties of the suspension, such as sedimentation and separation, and redispersion on dilution may be assessed using rheological techniques. The latter will be summarized with particular emphasis on their application in prediction of the long-term physical stability of suspension concentrates.

## Preparation of Suspension Concentrates and the Role of Surfactants/Dispersing Agents

Suspension concentrates are usually formulated using a wet milling process which requires the addition of a surfactant/dispersing agent. The latter should satisfy the following criteria: (1) A good wetting agent for the agrochemical powder (both external and internal surfaces of the powder aggregates or agglomerates must be spontaneously wetted). (2) A good dispersing agent to break such aggregates or agglomerates into smaller units and subsequently help in the milling process (one usually aims at a dispersion with a volume mean diameter of 1–2  $\mu\text{m}$ ). (3) It should provide good stability in the colloid sense (this is essential for maintaining the particles as individual units once formed). Powerful dispersing agents are particularly important for the preparation of highly concentrated suspensions (sometimes required for seed dressing). Any flocculation will cause a rapid increase in the viscosity of the suspension, and this makes the wet milling of the agrochemical a difficult process.

Dry powders of organic compounds usually consist of particles of various degrees of complexity, depending on the isolation stages and the drying process. Generally, the particles in a dry powder form aggregates (in which the particles are joined together with their crystal faces) or agglomerates (in which the particles touch at edges or corners) forming a looser more open structure. It is essential in the dispersion process to wet the external as well as the internal surfaces and displace the air entrapped between the particles. This is usually achieved by the use of surface active agents of the ionic or nonionic type. In some cases, macromolecules or polyelectrolytes may be efficient in this wetting process. This may be the case since these polymers contain a very wide distribution of molecular weights and the low molecular weight fractions may act as efficient wetting agents. For efficient wetting, the molecules should lower the surface tension of water (see below) and they should diffuse fast in solution and become quickly adsorbed at the solid/solution interface.



**Agrochemical Formulations, Fig. 38** Schematic representation of the contact angle and wetting line

Wetting of a solid is usually described in terms of the equilibrium contact angle  $\theta$  and the appropriate interfacial tensions. This is illustrated in Fig. 38.

Using the classical Young's equation,

$$\gamma_{SV} - \gamma_{SL} = \gamma_{LV} \cos \theta \quad (62)$$

or

$$\cos \theta = \frac{(\gamma_{SV} - \gamma_{SL})}{\gamma_{LV}} \quad (63)$$

where  $\gamma$  represents the interfacial tension and the symbols S, L, and V refer to solid, liquid, and vapor, respectively. It is clear from Eq. 2 that if  $\theta < 90^\circ$ , a reduction in  $\gamma_{LV}$  improves wetting. Hence, the use of surfactants which reduce both  $\gamma_{LV}$  and  $\gamma_{SL}$  to aid wetting is clear. However, the process of wetting of particulate solids is more complex, and it involves at least three distinct types of wetting (Tadros 1987), namely, adhesional wetting, spreading wetting, and immersional wetting. All these processes are determined by the liquid surface tension and the contact angle. The difference between  $\gamma_{SV}$  and  $\gamma_{SL}$  or  $\gamma_{LV} \cos \theta$  is referred to as the adhesion or wetting tension.

Let us consider an agrochemical powder with surface area  $A$ . Before the powder is dispersed in the liquid, it has a surface tension  $\gamma_{SV}$ , and after immersion in the liquid, it has a surface tension  $\gamma_{SL}$ . The work of dispersion  $W_d$  is simply given by the difference in adhesion or wetting tension of the SL and SV:

$$W_d = A(\gamma_{SL} - \gamma_{SV}) = -A\gamma_{LV} \cos \theta \quad (64)$$

It is clear from Eq. 64 that if  $\theta < 90^\circ$   $\cos \theta$  is positive and  $W_d$  is negative, that is, wetting of the powder is spontaneous. Since surfactants are added in sufficient amounts ( $\gamma_{dynamic}$  is lowered sufficiently), spontaneous dispersion is the rule rather than the exception.

Wetting of the internal surface requires penetration of the liquid into channels between and inside the agglomerates. The process is similar to forcing a liquid through fine capillaries. To force a liquid through a capillary with radius  $r$ , a pressure  $p$  is required that is given by

$$p = -\frac{2\gamma_{LV} \cos \theta}{r} = \left[ \frac{-2(\gamma_{SV} - \gamma_{SL})}{r\gamma_{LV}} \right] \quad (65)$$

$\gamma_{SL}$  has to be made as small as possible and rapid surfactant adsorption to the solid surface, low  $\theta$ . When  $\theta = 0$ ,  $p \propto \gamma_{LV}$ . Thus, for penetration into pores, one requires a high  $\gamma_{LV}$ . Thus, wetting of the external surface requires low contact angle  $\theta$  and low surface tension  $\gamma_{LV}$ . Wetting of the internal surface (i.e., penetration through pores) requires low  $\theta$  but high  $\gamma_{LV}$ . These two conditions are incompatible, and a compromise has to be made:  $\gamma_{SV} - \gamma_{SL}$  must be kept at a maximum, and  $\gamma_{LV}$  should be kept as low as possible but not too low.

The above conclusions illustrate the problem of choosing the best dispersing agent for a particular powder. This requires measurement of the above parameters as well as testing the efficiency of the dispersion process.

The next stage to be considered is the wetting of the internal surface, which implies penetration of the liquid into channels between and inside the agglomerates. This is more difficult to define precisely. However, one may make use of the equation derived for capillary phenomena as discussed by Rideal and Washburn (Rideal 1922; Washburn 1921) who considered the penetration of liquids in capillaries.

For horizontal capillaries (gravity neglected), the depth of penetration  $l$  in time  $t$  is given by the Rideal-Washburn equation (Rideal 1922; Washburn 1921):

$$l = \left[ \frac{rt\gamma_{LV} \cos \theta}{2\eta} \right]^{1/2} \quad (66)$$

To enhance the rate of penetration,  $\gamma_{LV}$  has to be made as high as possible,  $\theta$  as low as possible, and  $\eta$  as low as possible. For dispersion of powders into liquids, one should use surfactants that are lower  $\theta$  while not reducing  $\gamma_{LV}$  too much. The viscosity of the liquid should also be kept at a minimum. Thickening agents (such as polymers) should not be added during the dispersion process. It is also necessary to avoid foam formation during the dispersion process. For a packed bed of particles,  $r$  may be replaced by  $k$ , which contains the effective radius of the bed and a tortuosity factor, which takes into account the complex path formed by the channels between the particles, that is,

$$l^2 = \left( \frac{kt\gamma_{LV} \cos \theta}{2\eta} \right) t \quad (67)$$

Thus, a plot of  $l^2$  versus  $t$  gives a straight line, and from the slope of the line, one can obtain  $\theta$ . The Rideal-Washburn equation can be applied to obtain the contact angle of liquids (and surfactant solutions) in powder beds.  $k$  should first be obtained using a liquid that produces zero contact angle. A packed bed of powder is prepared say in a tube fitted with a sintered glass at the end (to retain the powder particles). It is essential to pack the powder uniformly in the tube (a plunger may be used in this case). The tube containing the bed is immersed in a liquid that gives spontaneous wetting (e.g., a lower alkane), that is, the liquid gives a zero contact angle and  $\cos \theta = 1$ . By measuring the rate of penetration of the liquid (this can be carried out gravimetrically using, for example, a microbalance or a Kruss instrument), one can obtain  $k$ . The tube is then removed from the lower alkane liquid and left to stand for evaporation of the liquid. It is then immersed in the liquid in question and the rate of penetration is measured again as a function of time. Using Eq. 67, one can calculate  $\cos \theta$  and hence  $\theta$ .

Thus, in summary, the dispersion of a powder in a liquid depends on three main factors, namely the energy of wetting of the external surface, the pressure involved in the liquid penetrating inside and between the agglomerates, and the rate of penetration of the liquid into the powder.

All these factors are related to two main parameters, namely  $\gamma_{LV}$  and  $\theta$ . In general, the process is likely to be more spontaneous the lower the  $\theta$  and the higher  $\gamma_{LV}$ . Since these two factors tend to operate in opposite senses, the choice of the proper surfactant (dispersing agent) can be a difficult task.

For the dispersion of aggregates and agglomerates into smaller units, one requires high-speed mixing, for example, a Silverson mixer. In some cases, the dispersion process is easy and the capillary pressure may be sufficient to break up the aggregates and agglomerates into primary units. The process is aided by the surfactant which becomes adsorbed on the particle surface. However, one should be careful during the mixing process not to entrap air (foam) which causes an increase in the viscosity of the suspension and prevents easy dispersion and subsequent grinding. If foam formation becomes a problem, one should add antifoaming agents such as polysiloxane antifoaming agents.

After completion of the dispersion process, the suspension is transferred to a ball or bead mill for size reduction. Milling or comminution (the generic term for size reduction) is a complex process, and there is little fundamental information on its mechanism. For the breakdown of single crystals into smaller units, mechanical energy is required. This energy in a bead mill, for example, is supplied by impaction of the glass beads with the particles. As a result, permanent deformation of the crystals and crack initiation result. This will eventually lead to the fracture of the crystals into smaller units. However, since the milling conditions are random, it is inevitable that some particles receive impacts that are far in excess of those required for fracture, whereas others receive impacts that are insufficient to fracture them. This makes the milling operation grossly inefficient, and only a small fraction of the applied energy is actually used in comminution. The rest of the energy is dissipated as heat, vibration, sound, interparticulate friction, friction between the particles and beads, and elastic deformation of unfractured particles. For these reasons, milling conditions are usually established by a trial-and-error procedure.

Of particular importance is the effect of various surface active agents and macromolecules on the grinding efficiency. The role played by these agents in the comminution process is far from being understood. As a result of adsorption of surfactants at the solid/liquid interface, the surface energy at the boundary is reduced, and this facilitates the process of deformation or destruction. The adsorption of the surfactant at the solid/solution interface in cracks facilitates their propagation. The surface energy manifests itself in destructive processes on solids, since the generation and growth of cracks and separation of one part of a body from another is directly connected with the development of new free surface. Thus, as a result of adsorption of surface active agents at structural defects in the surface of the crystals, fine grinding is facilitated. In the extreme case where there is a very great reduction in surface energy at the solid/liquid boundary, spontaneous dispersion may take place with the result of the formation of colloidal particles ( $< 1 \mu\text{m}$ ).

Surfactants lower the surface tension of water,  $\gamma$ , and they adsorb at the solid/liquid interface. A plot of  $\gamma_{LV}$  versus  $\log C$  (where  $C$  is the surfactant concentration) results in a gradual reduction in  $\gamma_{LV}$  followed by a linear decrease of  $\gamma_{LV}$  with  $\log C$  (just below the critical micelle concentration, cmc), and when the cmc is reached,  $\gamma_{LV}$  remains virtually constant. This was discussed before.

From the slope of the linear portion of the  $\gamma - \log C$  curve (just below the cmc), one can obtain the surface excess (number of moles of surfactant per unit area at the L/A interface). Using the Gibbs adsorption isotherm,

$$\frac{d\gamma}{d\log C} = -2.303RT\Gamma \quad (68)$$

$\Gamma$  = surface excess (moles  $\text{m}^{-2}$ ),  $R$  = gas constant, and  $T$  = absolute temperature.

From  $\Gamma$ , one can obtain the area per molecule,

$$\text{Area per molecule} = \frac{1}{\Gamma N_{av}} (\text{m}^2) = \frac{10^{18}}{\Gamma N_{av}} (\text{nm}^2) \quad (69)$$

Most surfactants produce a vertically oriented monolayer just below the cmc. The area/molecule is usually determined by the cross-sectional area of the head group. For ionic surfactants containing, say,  $-\text{OSO}_3^-$  or  $-\text{SO}_3^-$  head group, the area per molecule is in the region of  $0.4 \text{ nm}^2$ . For nonionic surfactants containing several moles of ethylene oxide (Eqs. 12–14), the area per molecule can be much larger ( $1\text{--}2 \text{ nm}^2$ ). Surfactants will also adsorb at the solid/liquid interface. For hydrophobic surfaces, the main driving force for adsorption is by hydrophobic bonding. This results in lowering of the contact angle of water on the solid surface. For hydrophilic surfaces, adsorption occurs via the hydrophilic group, for example, cationic surfactants on silica. Initially, the surface becomes more hydrophobic and the contact angle  $\theta$  increases with increase in surfactant concentration. However, at higher cationic surfactant concentration, a bilayer is formed by hydrophobic interaction between the alkyl groups and the surface becomes more and more hydrophilic and eventually the contact angle reaches zero at high surfactant concentrations.

Smolders (Smolders 1960) suggested the following relationship for change of  $\theta$  with  $C$ :

$$\frac{d\gamma_{LV} \cos\theta}{d\ln C} = \frac{d\gamma_{SV}}{d\ln C} - \frac{d\gamma_{SL}}{d\ln C} \quad (70)$$

Using the Gibbs equation,

$$\sin\theta \left( \frac{d\gamma}{d\ln C} \right) = RT(\Gamma_{SV} - \Gamma_{SL} - \gamma_{LV} \cos\theta) \quad (71)$$

since  $\gamma_{LV} \sin\theta$  is always positive, then  $(d\theta/d\ln C)$  will always have the same sign as the RHS of Eq. 33. Three cases may be distinguished:  $(d\theta/d\ln C) < 0$ ;  $\Gamma_{SV} < \Gamma_{SL} + \Gamma_{LV} \cos\theta$ ; addition of surfactant improves wetting.  $(d\theta/d\ln C) = 0$ ;  $\Gamma_{SV} = \Gamma_{SL} + \Gamma_{LV} \cos\theta$ ; surfactant has no effect on wetting.  $(d\theta/d\ln C) > 0$ ;  $\Gamma_{SV} > \Gamma_{SL} + \Gamma_{LV} \cos\theta$ ; surfactant causes dewetting.

### Control of the Physical Stability of Suspension Concentrates

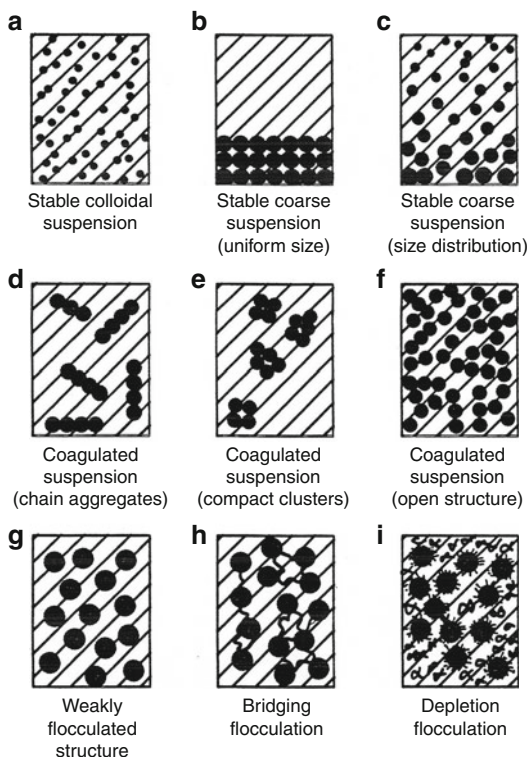
When considering the stability of suspension concentrates, one must distinguish between the colloid stability and the overall physical stability. Colloid stability implies absent of an aggregation between the particles which requires the presence of an energy barrier that is produced by electrostatic, steric repulsion, or combination of the two (electrosteric). Physical stability implies absence of a sedimentation and/or separation, ease of dispersion on shaking, and/or dilution in the spray tanks. As will be discussed later, to achieve the overall physical stability, one may apply control and reversible flocculation methods and/or using a rheology modifier.

To distinguish between colloid stability/instability and physical stability, one must consider the state of the suspension on standing as schematically illustrated in Fig. 39. These states are determined by: (1) Magnitude and balance of the various interaction forces, electrostatic repulsion, steric repulsion, and van der Waals attraction; (2) particle size and shape distribution; (2) density difference between disperse phase and medium which determines the sedimentation characteristics; (4) conditions and prehistory of the suspension, for example, agitation which determines the structure of the flocs formed (chain aggregates, compact clusters, etc.); and (5) presence of additives, for example, high molecular weight polymers that may cause bridging or depletion flocculation.

These states may be described in terms of three different energy-distance curves: (a) Electrostatic, produced, for example, by the presence of ionogenic groups on the surface of the particles or adsorption of ionic surfactants. (b) Steric, produced, for example, by adsorption of nonionic surfactants or polymers. (c) Electrostatic + Steric (Electrosteric) as, for example, produced by polyelectrolytes. These are illustrated below in Fig. 40.

A brief description of the various states shown in Fig. 39 is given below:

States (a)–(c) correspond to a suspension that is stable in the colloid sense. The stability is



Agrochemical Formulations, Fig. 39 States of the suspension

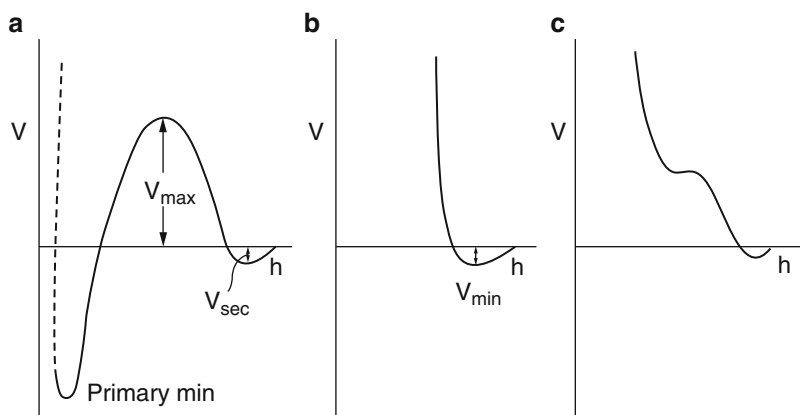
obtained as a result of net repulsion due to the presence of extended double layers (i.e., at low electrolyte concentration), the result of steric repulsion produced adsorption of nonionic surfactants or polymers or the result of combination of double layer and steric repulsion (electrosteric). State (a) represents the case of a suspension with small-particle size (submicron) whereby the Brownian diffusion overcomes the gravity force producing uniform distribution of the particles in the suspension, that is,

$$kT > (4/3)\pi R^3 \Delta\rho gh \quad (72)$$

where  $k$  is the Boltzmann constant,  $T$  is the absolute temperature,  $R$  is the particle radius,  $\Delta\rho$  is the buoyancy (difference in density between the particles and the medium),  $g$  is the acceleration due to gravity, and  $h$  is the height of the container. A good example of this case is a nano suspension with particle size well below 1  $\mu\text{m}$  that is

### Agrochemical Formulations,

**Fig. 40** Energy-distance curves for three stabilization mechanisms



stabilized by an ionic surfactant or nonionic surfactant or polymer. This suspension will show no separation on storage for long periods of time.

States (b) and (c) represent the case of suspensions, whereby the particle size range is outside the colloid range ( $> 1 \mu\text{m}$ ). In this case, the gravity force exceeds the Brownian diffusion. With state (b), the particles are uniform and they will settle under gravity forming a hard sediment (technically referred to “clay” or “cake”). The repulsive forces between the particles allow them to move past each other till they reach small distances of separation (that are determined by the location of the repulsive barrier). Due to the small distances between the particles in the sediment, it is very difficult to redisperse the suspension by simple shaking. With case (c) consisting of a wide distribution of particle sizes, the sediment may contain larger proportions of the larger size particles, but still a hard “clay” is produced. These “clays” are dilatant (i.e., shear thickening), and they can be easily detected by inserting a glass rod in the suspension. Penetration of the glass rod into these hard sediments is very difficult.

States (d)–(f) represent the case for coagulated suspensions which either have a small repulsive energy barrier or its complete absence. State (d) represents the case of coagulation under no stirring conditions in which case chain aggregates are produced that will settle under gravity forming a relatively open structure. State (e) represents the case of coagulation under stirring conditions whereby compact aggregates are

produced that will settle faster than the chain aggregates and the sediment produced is more compact. State (f) represents the case of coagulation at high volume fraction of the particles,  $\phi$ . In this case, the whole particles will form a “one-floc” structure that is formed from chains and cross chains that extend from one wall to the other in the container. Such coagulated structure may undergo some compression (consolidation) under gravity leaving a clear supernatant liquid layer at the top of the container. This phenomenon is referred to as syneresis.

State (g) represents the case of weak and reversible flocculation. This occurs when the secondary minimum in the energy-distance curve (Fig. 40a) is deep enough to cause flocculation. This can occur at moderate electrolyte concentrations, in particular with larger particles. The same occurs with sterically and electrosterically stabilized suspensions (Fig. 40b and c). This occurs when the adsorbed layer thickness is not very large, particularly with large particles. The minimum depth required for causing weak flocculation depends on the volume fraction of the suspension. The higher the volume fraction, the lower the minimum depth required for weak flocculation. This flocculation is weak and reversible, that is, on shaking the container, redispersion of the suspension occurs. On standing, the dispersed particles aggregate to form a weak “gel.” This process (referred to as sol  $\leftrightarrow$  gel transformation) leads to reversible time dependence of viscosity (thixotropy). On shearing the suspension, the viscosity decreases, and



when the shear is removed, the viscosity is recovered.

State (h) represents the case whereby the particles are not completely covered by the polymer chains. In this case, simultaneous adsorption of one polymer chain on more than one particle occurs, leading to bridging flocculation. If the polymer adsorption is weak (low adsorption energy per polymer segment), the flocculation could be weak and reversible. In contrast, if the adsorption of the polymer is strong, tough flocs are produced and the flocculation is irreversible. The last phenomenon is used for solid/liquid separation, for example, in water and effluent treatment.

Case (i) represents a phenomenon, referred to as depletion flocculation, produced by addition of “free” non-adsorbing polymer (Asakura and Oosawa 1954). In this case, the polymer coils cannot approach the particles to a distance  $\Delta$  (that is determined by the radius of gyration of free polymer  $R_G$ ), since the reduction of entropy on close approach of the polymer coils is not compensated by an adsorption energy. The suspension particles will be surrounded by a depletion zone with thickness  $\Delta$ . Above a critical volume fraction of the free polymer,  $\phi_p^+$ , the polymer coils are “squeezed out” from between the particles and the depletion zones begin to interact. The interstices between the particles are now free from polymer coils, and hence an osmotic pressure is exerted outside the particle surface (the osmotic pressure outside is higher than in between the particles) resulting in weak flocculation (Asakura and Oosawa 1954). A schematic representation of depletion flocculation is shown in Fig. 41.

The magnitude of the depletion attraction free energy,  $G_{\text{dep}}$ , is proportional to the osmotic pressure of the polymer solution, which in turn is determined by  $\phi_p$  and molecular weight  $M$ . The range of depletion attraction is proportional to the thickness of the depletion zone,  $\Delta$ , which is roughly equal to the radius of gyration,  $R_G$ , of the free polymer. A simple expression for  $G_{\text{dep}}$  is (Asakura and Oosawa 1954)

$$G_{\text{dep}} = \frac{2\pi R \Delta^2}{V_1} (\mu_1 - \mu_1^0) \left( 1 + \frac{2\Delta}{R} \right) \quad (73)$$

where  $V_1$  is the molar volume of the solvent,  $\mu_1$  is the chemical potential of the solvent in the presence of free polymer with volume fraction  $\phi_p$ , and  $\mu_1^0$  is the chemical potential of the solvent in the absence of free polymer.  $(\mu_1 - \mu_1^0)$  is proportional to the osmotic pressure of the polymer solution.

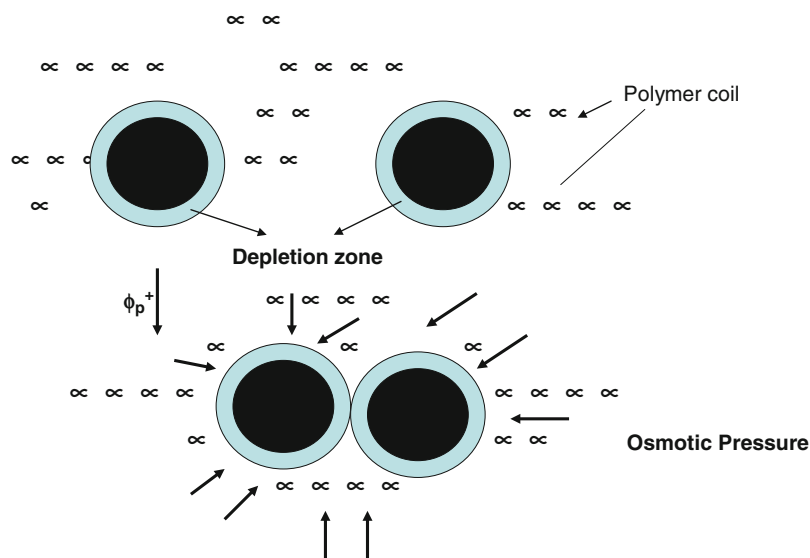
The control of stability against irreversible flocculation (where the particles are held together into aggregates that cannot be redispersed by shaking or on dilution) is achieved by the use of powerful dispersing agents, for example, surfactants of the ionic or nonionic type, nonionic polymers, or polyelectrolytes. These dispersing agents must be strongly adsorbed onto the particle surfaces and fully cover them. With ionic surfactants, irreversible flocculation is prevented by the repulsive force generated from the presence of an electrical double layer at the particle solution interface as discussed before. Depending on the conditions, this repulsive force can be made sufficiently large to overcome the ubiquitous van der Waals attraction between the particles, at intermediate distances of separation. With nonionic surfactants and macromolecules, repulsion between the particles is ensured by the steric interaction of the adsorbed layers on the particle surfaces. With polyelectrolytes, both electrostatic and steric repulsion exist. Below, a summary of the role of surfactants in stabilization of particles against flocculation is described.

Ionic surfactants such as sodium dodecyl benzene sulfonate (NaDBS) or cetyl trimethyl ammonium chloride (CTACl) adsorb on hydrophobic particles of agrochemicals, as a result of the hydrophobic interaction between the alkyl group of the surfactant and the particle surface. As a result, the particle surface will acquire a charge that is compensated by counter ions ( $\text{Na}^+$  in the case of NaDBS and  $\text{Cl}^-$  in the case of CTACl) forming an electrical double layer.

The adsorption of ionic surfactants at the solid/solution interface is of vital importance in determining the stability of suspension concentrates. As discussed before, the adsorption of ionic surfactants on solid surfaces can be directly measured by equilibrating a known amount of solid (with known surface area) with surfactant

### Agrochemical Formulations,

**Fig. 41** Schematic representation of depletion flocculation



solutions of various concentrations. After reaching equilibrium, the solid particles are removed (e.g., by centrifugation) and the concentration of surfactant in the supernatant liquid is analytically determined. From the difference between the initial and final surfactant concentrations ( $C_1$  and  $C_2$ , respectively), the number of moles of surfactant adsorbed,  $\Gamma$ , per unit area of solid is determined and the results may be fitted to a Langmuir isotherm:

$$\Gamma = \frac{\Delta C}{mA} = \frac{abC_2}{1 + bC_2} \quad (74)$$

where  $\Delta C = C_1 - C_2$ ,  $m$  is the mass of the solid with surface area  $A$ ,  $a$  is the saturation adsorption, and  $b$  is a constant that is related to the free energy of adsorption,  $\Delta G$  ( $b \propto \exp \Delta G/RT$ ). From  $a$ , the area per surfactant ion on the surface can be calculated (area per surfactant ion =  $1/a N_{av}$ ).

Results on the adsorption of ionic surfactants on pesticides are scarce. However, Tadros (Eq. 17) obtained some results on the adsorption of NaDBS and CTABr on a fungicide, namely ethirimol. For NaDBS, the shape of the isotherm was of a Langmuir type, giving an area/DBS<sup>-</sup> at saturation of  $\sim 0.14 \text{ nm}^2$ . The adsorption of CTA<sup>+</sup> showed a two-step isotherm with areas/CTA<sup>+</sup> of 0.27 and  $0.14 \text{ nm}^2$ , respectively. These

results suggest full saturation of the surface with surfactant ions which are vertically oriented.

The above discussion shows that ionic surfactants can be used to stabilize agrochemical suspensions by producing sufficient electrostatic repulsion. When two particles with adsorbed surfactant layers approach each other to a distance where the electrical double layers begin to overlap, strong repulsion occurs preventing any particle aggregation. The energy-distance curve for such electrostatically stabilized dispersions is schematically shown in Fig. 41a. This shows an energy maximum, which if high enough ( $> 25 \text{ kT}$ ), prevents particle aggregation into the primary minimum. However, ionic surfactants are the least attractive dispersing agents for the following reasons. Adsorption of ionic surfactants is seldom strong enough to prevent some desorption with the result of production of "bare" patches which may induce particle aggregation. The system is also sensitive to ionic impurities which are present in the water used for suspension preparation. In particular, the system will be sensitive to bivalent ions ( $\text{Ca}^{+2}$  or  $\text{Mg}^{+2}$ ) which produce flocculation at relatively low concentrations.

Nonionic surfactants of the ethoxylate type, for example,  $\text{R}(\text{CH}_2\text{CH}_2\text{O})_n\text{OH}$  or  $\text{RC}_6\text{H}_5(\text{CH}_2\text{CH}_2\text{O})_2\text{OH}$ , provide a better

alternative provided the molecule contains sufficient hydrophobic groups to ensure their adsorption and enough ethylene oxide units to provide an adequate energy barrier. As discussed before, the origin of steric repulsion arises from two main effects. The first effect arises from the unfavorable mixing of the poly(ethylene oxide) chains which are in good solvent conditions (water as the medium). This effect is referred to as the mixing or osmotic repulsion. The second effect arises from the loss in configurational entropy of the chains when these are forced to overlap on approach of the particles. This is referred to as the elastic or volume restriction effect. The energy-distance curve for such systems (Fig. 41b) clearly demonstrates the attraction of steric stabilization. Apart from a small attractive energy minimum (which can be reasonably shallow with sufficiently long poly(ethylene oxide) chains), strong repulsion occurs, and there is no barrier to overcome. A better option is to use block and graft copolymers (polymeric surfactants) consisting of A and B units combined together in A-B, A-B-A or BA<sub>n</sub> fashion. B represents units with high affinity for the particle surface and basically insoluble in the continuous medium, thus providing strong adsorption (“anchoring units”). A, on the other hand, represents units with high affinity to the medium (high chain-solvent interaction) and little or no affinity to the particle surface. An example of such powerful dispersant is a graft copolymer of polymethyl methacrylate-methacrylic acid (the anchoring portion) and methoxy polyethylene oxide (the stabilizing chain) methacrylate (Eq. 18). Adsorption measurements of such a polymer on a pesticide, namely ethirimol (a fungicide), showed a high affinity isotherm with no desorption. Using such macromolecular surfactant, a suspension of high volume fractions could be prepared.

The third class of dispersing agents which is commonly used in SC formulations is that of polyelectrolytes. Of these, sulfonated naphthalene-formaldehyde condensates and lignosulfonates are the most commonly used in agrochemical formulations. These systems show a combined electrostatic and steric repulsion, and

the energy-distance curve is schematically illustrated in Fig. 40c. It shows a shallow minimum and maximum at intermediate distances (characteristic of electrostatic repulsion) as well as strong repulsion at relatively short distances (characteristic of steric repulsion). The stabilization mechanism of polyelectrolytes is sometimes referred to as electrosteric. These polyelectrolytes offer some versatility in SC formulations. Since the interaction is fairly long range in nature (due to the double layer effect), one does not obtain the “hard-sphere” type behavior which may lead to the formation of hard sediments. The steric repulsion ensures the colloid stability and prevention of any aggregation on storage.

The second instability problem in SCs is that of Ostwald ripening (crystal growth). There are several ways in which crystals can grow in an aqueous suspension. One of the most familiar is the phenomenon of “Ostwald ripening,” which occurs as a result of the difference in solubility between the small and large crystals (Thompson (Lord Kelvin) 1871)”:

$$\frac{RT}{M} \ln \frac{S_1}{S_2} = \frac{2\sigma}{\rho} \left( \frac{1}{r_1} - \frac{1}{r_2} \right) \quad (75)$$

where  $S_1$  and  $S_2$  are the solubilities of crystals of radii  $r_1$  and  $r_2$ , respectively,  $\sigma$  is the specific surface energy,  $\rho$  is the density and  $M$  is the molecular weight of the solute molecules,  $R$  is the gas constant, and  $T$  the absolute temperature. Since  $r_1$  is smaller than  $r_2$ ,  $S_1$  is larger than  $S_2$ . Another mechanism for crystal growth is related to polymorphic changes in solutions, and again, the driving force is the difference in solubility between the two polymorphs. In other words, the less soluble form grows at the expense of the more soluble phase. This is sometimes also accompanied by changes in the crystal habit. Different faces of the crystal may have different surface energies, and deposition may preferentially take place on one of the crystal faces modifying its shape. Other important factors are the presence of crystal dislocations, kinks, surface impurities, etc.

The growth of crystals in suspension concentrates may create undesirable changes. As a result

of the drastic change in particle size distribution, the settling of the particles may be accelerated leading to caking and cementing together of some particles in the sediment. Moreover, increase in particle size may lead to a reduction in biological efficiency. Thus, prevention of crystal growth or at least reducing it to an acceptable level is essential in most suspension concentrates. Surfactants affect crystal growth in a number of ways. The surfactant may affect the rate of dissolution by affecting the rate of transport away from the boundary layer at the crystal solution interface. On the other hand, if the surfactant forms micelles that can solubilize the solute, crystal growth may be enhanced as a result of increasing the concentration gradient. Thus, by proper choice of dispersing agent, one may reduce crystal growth of suspension concentrates. This has been demonstrated by Tadros (1973) for terbacil suspensions. When using Pluronic P75 (polyethylene oxide-polypropylene oxide block copolymer), crystal growth was significant. By replacing the Pluronic surfactant with polyvinyl alcohol, the rate of crystal growth was greatly reduced and the suspension concentrate was acceptable.

It should be mentioned that many surfactants and polymers may act as crystal growth inhibitors if they adsorb strongly on the crystal faces, thus preventing solute deposition. However, the choice of an inhibitor is still an art, and there are not many rules that can be used for selection of crystal growth inhibitors.

The third instability problem with SCs is claying or caking which results from gravity effect. Once a dispersion that is stable in the colloid sense has been prepared, the next task is to eliminate claying or caking. This is the consequence of settling of the colloidally stable suspension particles. The repulsive forces necessary to ensure this colloid stability allow the particles to move past each other forming a dense sediment which is very difficult to redisperse. Such sediments are dilatant (shear thickening, see section on "Rheology"), and hence the SC becomes unusable. Before describing the methods used for controlling settling and prevention of formation of dilatant clays, an account is given on the

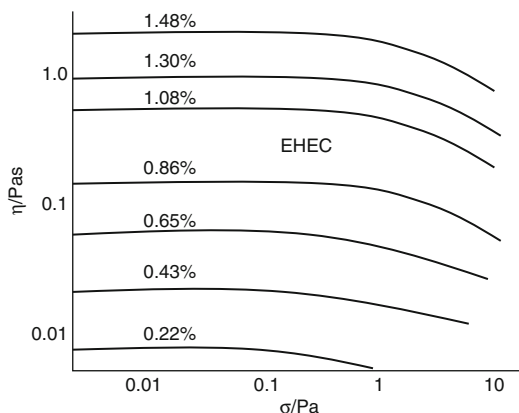
settling of suspensions and the effect of increasing the volume fraction of the suspension on the settling rate.

The sedimentation velocity  $v_o$  of a very dilute suspension of rigid noninteracting particles with radius  $a$  can be determined by equating the gravitational force with the opposing hydrodynamic force as given by Stokes' law, as given by Eq. 46. Equation 46 predicts a sedimentation rate for particles with radius  $1\ \mu\text{m}$  in a medium with a density difference of  $0.2\ \text{g cm}^{-3}$  and a viscosity of  $1\ \text{mPa s}$  (i.e., water at  $20\ ^\circ\text{C}$ ) of  $4.4 \times 10^{-7}\ \text{m s}^{-1}$ . Such particles will sediment to the bottom of  $0.1\text{-m}$  container in about 60 h. For  $10\text{-}\mu\text{m}$  particles, the sedimentation velocity is  $4.4 \times 10^{-5}\ \text{m s}^{-1}$ , and such particles will sediment to the bottom of  $0.1\text{-m}$  container in about 40 min.

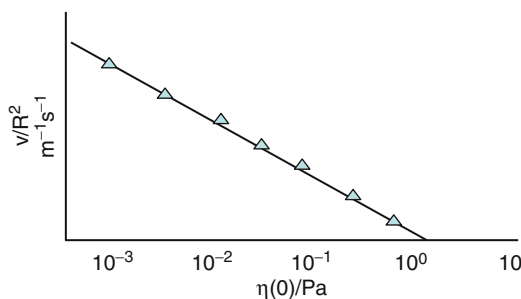
The above treatment using Stokes' law applied only to very dilute suspensions (volume fraction  $\phi < 0.01$ ). For more concentrated suspensions, the particles no longer sediment independent of each other, and one has to take into account both the hydrodynamic interaction between the particles (which applies for moderately concentrated suspensions) and other higher order interactions at relatively high volume fractions. As mentioned in the section on EWs, a theoretical relationship between the sedimentation velocity  $v$  of non-flocculated suspensions and particle volume fraction has been derived by Batchelor (1972). Such theories apply to relatively low volume fractions ( $< 0.1$ ), and they show that the sedimentation velocity  $v$  at a volume fraction  $\phi$  is related to that at infinite dilution  $v_o$  (the Stokes' velocity) by Eq. 47.

At higher volume fractions, the sedimentation velocity becomes a complex function of  $\phi$ , and only empirical equations are available to describe the variation of  $v$  with  $\phi$ . It seems that there is a correlation between the reduction in sedimentation rate and the increase in relative viscosity of the suspension as the volume fraction of the suspension is increased. This was schematically shown in Fig. 34 which shows that  $v \rightarrow 0$  and  $\eta_r \rightarrow \infty$  as  $\phi \rightarrow \phi_p$ . This implies that suspension concentrates with volume fractions approaching the maximum packing do not show any appreciable settling. However, such dense suspensions

have extremely high viscosities and are not a practical solution for reduction of settling. In most cases, one prepares a suspension concentrate at practical volume fractions (0.2–0.4) and then uses an antissettling agent to reduce settling. As we will discuss in the next section, most of the antissettling agents used in practice are high molecular weight polymers. These materials show an increase in the viscosity of the medium with increase in their concentration. However, at a critical polymer concentration (which depends on the nature of the polymer and its molecular weight), they show a very rapid increase in viscosity with further increase in their concentration. This critical concentration (sometimes denoted by  $C^*$ ) represents the situation where the polymer coils or rods begin to overlap. Under these conditions, the solutions become significantly non-Newtonian (viscoelastic), and they produce stresses that are sufficient to overcome the stress exerted by the particles. The settling of suspensions in these non-Newtonian fluids is not simple since one has to consider the non-Newtonian behavior of these polymer solutions. This problem has been addressed by Buscall et al. (1982). In order to adequately describe the settling of particles in non-Newtonian fluids, one needs to know how the viscosity of the medium changes with shear rate or shear stress. Most of these viscoelastic fluids show a gradual increase of viscosity with decrease of shear rate or shear stress, but below a critical stress or shear rate, they show a Newtonian region with a limiting high viscosity that is denoted as the residual (or zero shear) viscosity. This is illustrated in Fig. 42 which shows the variation of the viscosity with shear stress for a number of solutions of ethyl hydroxyethyl cellulose at various concentrations. It can be seen that the viscosity increases with decrease of stress and the limiting value, that is, the residual viscosity  $\eta(o)$ , increases rapidly with increase in polymer concentration. The shear thinning behavior of these polymer solutions is clearly shown, since above a critical stress value the viscosity decreases rapidly with increase in shear stress. The limiting value of the viscosity is reached at low stresses ( $< 0.2$  Pa). It is now



**Agrochemical Formulations, Fig. 42** Constant stress (creep) measurements for PS latex dispersions as a function of EHEC concentration



**Agrochemical Formulations, Fig. 43** Sedimentation rate versus  $\eta(0)$

important to calculate the stress exerted by the particles. This stress is equal to  $a\Delta\rho g/3$ . For polystyrene latex particles with radius  $1.55 \mu\text{m}$  and density  $1.05 \text{ g cm}^{-3}$ , this stress is equal to  $1.6 \times 10^{-4} \text{ Pa}$ . Such stress is lower than the critical stress for most EHEC solutions. In this case, one would expect a correlation between the settling velocity and the zero shear viscosity. This is illustrated in Fig. 43 whereby  $v/a^2$  is plotted versus  $\eta(o)$ . As is clear, a linear relationship between  $\log (v/a^2)$  and  $\log \eta(o)$  is obtained, with a slope of  $-1$ , over three decades of viscosity. This indicates that the settling rate is proportional to  $[\eta(o)]^{-1}$ . Thus, the settling rate of isolated spheres in non-Newtonian (pseudoplastic) polymer solutions is determined by the zero shear viscosity in which the particles are suspended.

The above correlation applies to the simple case of relatively dilute suspensions. For more concentrated suspensions, other parameters should be taken into consideration, such as the bulk (elastic) modulus. It is also clear that the stress exerted by the particles depends not only on the particle size but the density difference between the particle and the medium. Many SCs have particles with radii up to  $10\ \mu\text{m}$  and density difference of more than  $1\ \text{g cm}^{-3}$ . However, the stress exerted by such particles will seldom exceed  $10^{-2}\ \text{Pa}$ , and most polymer solutions will reach their limiting viscosity value at higher stresses than this value. Thus, in most cases, the correlation between settling velocity and zero shear viscosity is justified, at least for relatively dilute systems. For more concentrated suspensions, an elastic network is produced in the system which encompasses the suspension particles as well as the polymer chains. In this case, settling of individual particles may be prevented. However, in this case, the elastic network may collapse under its own weight and some liquid is squeezed out from between the particles. This is manifested in a clear liquid layer at the top of the suspension, a phenomenon usually referred to as syneresis. If such separation is not significant, it may not cause any problem on application since by shaking the container, the whole system redisperses. However, significant separation is not acceptable since it becomes difficult to homogenize the system. In addition, such extensive separation is cosmetically unacceptable and the formulation rheology should be controlled to reduce such separation to a minimum.

Several methods are applied in practice to control the settling and prevent the formation of dilatant clays: (1) Balance of the density of disperse phase and medium. This is obviously the simplest method for retarding settling, since as clear from Eq. 46 that if  $\rho = \rho_0$ , then  $v_0 = 0$ . However, this method is of limited application and can only be applied to systems where the difference in density between the particle and the medium is not too large. For example, with many organic solids with densities between  $1.1$  and  $1.3\ \text{g cm}^{-3}$  suspended in water, some soluble substances such as sugar or electrolytes may be

added to the continuous phase to increase the density of the medium to a level that is equal to that of the particles. However, one should be careful that the added substance does not cause any flocculation for the particles. This is particularly the case when using electrolytes, whereby one should avoid any "salting out" materials which cause the medium to be a poor solvent for the stabilizing chains. It should also be mentioned that density matching can only be achieved at one temperature. Liquids usually have larger thermal expansion coefficients than solids, and if say, the density is matched at room temperature, settling may occur at higher temperatures. Thus, one has to be careful when applying the density matching method, particularly if the formulation is subjected to large temperature changes. (2) Use of high molecular weight polymers ("thickeners"). High molecular weight materials such as natural gums, hydroxyethyl cellulose, or synthetic polymers such as poly(ethylene oxide) may be used to reduce settling of suspension concentrates. The most commonly used material in agrochemical formulations is Xanthan gum (produced by converting waste sugar into a high molecular weight material using a microorganism and sold under the trade names Kelzan or Rhodopol) which is effective at relatively low concentrations (of the order of  $0.1$ – $0.2\ \%$  depending on the formulation). As mentioned above, these high molecular weight materials produce viscoelastic solutions above a critical concentration. This viscoelasticity produces sufficient residual viscosity to stop the settling of individual particles. The solutions also give enough elasticity to overcome separation of the suspension. However, one cannot rule out the interaction of these polymers with the suspension particles which may result in "bridging," and hence the role by which such molecules reduce settling and prevent the formation of clays may be complex. To arrive at the optimum concentration and molecular weight of the polymer necessary for prevention of settling and claying, one should study the rheological characteristics of the formulation as a function of the variables of the system such as its volume fraction, concentration, and molecular weight of the polymer and



temperature. (3) Use of “inert” fine particles. It has long been known that fine inorganic materials such as swellable clays and finely divided oxides (silica or alumina), when added to the dispersion medium of coarser suspensions, can eliminate claying or caking. These fine inorganic materials form a “three-dimensional” network in the continuous medium which by virtue of its elasticity prevents sedimentation and claying. With swellable clays such as sodium montmorillonite, the gel arises from the interaction of the platelike particles in the medium. The platelike particles of sodium montmorillonite consist of an octahedral alumina sheet sandwiched between two tetrahedral silica sheets. In the tetrahedral sheets, tetravalent Si may be replaced by trivalent Al, whereas in the octahedral sheet, there may be replacement of trivalent Al with divalent Mg, Fe, Cr, or Zn. This replacement is usually referred to as isomorphic substitution (Eq. 28), that is, an atom of higher valency is replaced by one of lower valency. This results in deficit of positive charges or excess of negative charges. Thus, the faces of the clay platelets become negatively charged, and these negative charges are compensated by counter ions such as  $\text{Na}^+$  or  $\text{Ca}^{+2}$ . As a result, a double layer is produced with a constant charge (that is independent of the pH of the solution). However, at the edges of the platelets, some disruption of the bonds occurs resulting in the formation of an oxide-like layer, for example,  $-\text{Al}-\text{OH}$ , which undergoes dissociation giving a negative ( $-\text{Al}-\text{O}^-$ ) or positive ( $-\text{Al}-\text{OH}_2^+$ ) depending on the pH of the solution. An isoelectric point may be identified for the edges (usually between pH 7 and 9). This means that the double layer at the edges is different from that at the faces and the surface charges can be positive or negative depending on the pH of the solution. For that reason, van Olphen (1963) suggested an edge-to-face association of clay platelets (which he termed the “house of card” structure), and this was assumed to be the driving force for gelation of swellable clays. However, Norrish (1954) suggested that clay gelation is caused simply by the interaction of the expanded double layers. This is particularly the case in dilute electrolyte solutions whereby the double

layer thickness can be several orders of magnitude higher than the particle dimensions.

With oxides, such as finely divided silica, gel formation is caused by formation of chain aggregates, which interact forming a three-dimensional network that is elastic in nature. Clearly, the formation of such networks depends on the nature and particle size of the silica particles. For effective gelation, one should choose silicas with very small particles and highly solvated surfaces. (4) Use of mixtures of polymers and finely divided solids. Mixtures of polymers such as hydroxyethyl cellulose or Xanthan gum with finely divided solids such as sodium montmorillonite or silica offer one of the most robust antisetling systems. By optimizing the ratio of the polymer to the solid particles, one can arrive at the right viscosity and elasticity to reduce settling and separation. Such system is more shear thinning than the polymer solutions, and hence, they are more easily dispersed in water on application. The most likely mechanism by which these mixtures produce viscoelastic network is probably through bridging or depletion flocculation. The polymer-particulate mixtures also show less temperature dependence of viscosity and elasticity than the polymer solutions, and hence, they ensure the long-term physical stability at high temperatures.

### **Characterization of Suspension Concentrates and Assessment of Their Long-Term Physical Stability**

For the full assessment of the properties of suspension concentrates, three main types of investigations are needed: (1) Fundamental investigation of the system at a molecular level. (2) Investigations into the state of the suspension on standing. (3) Bulk properties of the suspension. All these investigations require a number of sophisticated techniques such as zeta potential measurements, surfactant and polymer adsorption and their conformation at the solid/liquid interface, measurement of the rate of flocculation and crystal growth, and several rheological measurements. Apart from these practical



methods which are present in most industrial laboratories, more fundamental information can be obtained using modern sophisticated techniques such as small angle x-ray and neutron scattering measurements, ultrasonic absorption techniques, etc. Several other modern techniques are also now available for investigation of the state of the suspension: Freeze fracture and electron microscopy, atomic force microscopy, scanning tunneling microscopy, and confocal laser microscopy.

In all the above methods, care should be taken in sampling the suspension, which should cause as little disturbance as possible for the "structure" to be investigated. For example, when one investigates the flocculation of a concentrated suspension, dilution of the system for microscopic investigation may lead to breakdown of the flocs and a false assessment is obtained. The same applies when one investigates the rheology of a concentrated suspension, since transfer of the system from its container to the rheometer may lead to breakdown of the structure. For these reasons, one must establish well-defined procedures for every technique, and this requires a great deal of skill and experience. It is advisable in all cases to develop standard operation procedures for the above investigations.

Two general techniques may be applied for measuring the rate of flocculation of suspensions, both of which can only be applied for dilute systems. The first method is based on measuring the scattering of light by the particles. For monodisperse particles with a radius that is less than  $\lambda/20$  (where  $\lambda$  is the wave length of light), one can apply the Rayleigh equation, whereby the turbidity  $\tau_o$  is given by

$$\tau_o = A' n_o V_1^2 \quad (76)$$

where  $A'$  is an optical constant (which is related to the refractive index of the particle and medium and the wave length of light) and  $n_o$  is the number of particles, each with a volume  $V_1$ .

By combining the Rayleigh theory with the Smoluchowski-Fuchs theory of flocculation kinetics (Eq. 31), one can obtain the following expression for the variation of turbidity with time:

$$\tau = A' n_o V_1^2 (1 + 2 n_o kt) \quad (77)$$

where  $k$  is the rate constant of flocculation.

The second method for obtaining the rate constant of flocculation is by direct particle counting as a function of time. For this purpose, optical microscopy or image analysis may be used, provided the particle size is within the resolution limit of the microscope. Alternatively, the particle number may be determined using electronic devices such as the Coulter counter or the flow ultramicroscope. The rate constant of flocculation is determined by plotting  $1/n$  versus  $t$ , where  $n$  is the number of particles after time  $t$ , that is,

$$\left(\frac{1}{n}\right) = \left(\frac{1}{n_o}\right) + kt \quad (78)$$

The rate constant  $k$  of slow flocculation is usually related to the rapid rate constant  $k_o$  (the Smoluchowski rate) by the stability ratio  $W$ :

$$W = \left(\frac{k}{k_o}\right) \quad (79)$$

One usually plots  $\log W$  versus  $\log C$  (where  $C$  is the electrolyte concentration) to obtain the critical coagulation concentration (c.c.c.), which is the point at which  $\log W = 0$ .

For sterically stabilized suspensions, one can measure the incipient flocculation when the medium for the chains becomes a  $\theta$ -solvent. This occurs, for example, on heating an aqueous suspension stabilized with poly(ethylene oxide) (PEO) or pol(vinyl alcohol) chains. Above a certain temperature (the  $\theta$ -temperature) that depends on electrolyte concentration, flocculation of the suspension occurs. The temperature at which this occurs is defined as the critical flocculation temperature (CFT). This process of incipient flocculation can be followed by measuring the turbidity of the suspension as a function of temperature. Above the CFT, the turbidity of the suspension rises very sharply. For this purpose, the cell in the spectrophotometer that is used to measure the turbidity is placed in a metal block

that is connected to a temperature programming unit (which allows one to increase the temperature rise at a controlled rate).

To obtain a measure of the rate of crystal growth, the particle size distribution of the suspension is followed as a function of time, using either a Coulter counter, a Master sizer, or an optical disc centrifuge. One usually plots the cube of the average radius versus time which gives a straight line from which the rate of crystal growth can be determined (the slope of the linear curve).

The bulk properties of suspension concentrates can be investigated by measuring the sediment volume (height) as well as its rheological properties. For a “structured” suspension, obtained by “controlled” flocculation or addition of “thickeners” (such polysaccharides, clays, or oxides), the “flocs” sediment at a rate depending on their size and porosity of the aggregated mass. After this initial sedimentation, compaction and rearrangement of the floc structure occurs, a phenomenon referred to as consolidation. Normally, in sediment volume measurements, one compares the initial volume  $V_o$  (or height  $H_o$ ) with the ultimately reached value  $V$  (or  $H$ ). A colloiddally stable suspension gives a “close-packed” structure with relatively small sediment volume (dilatant sediment referred to as clay). A weakly “floculated” or “structured” suspension gives a more open sediment and hence a higher sediment volume. Thus, by comparing the relative sediment volume  $V/V_o$  or height  $H/H_o$ , one can distinguish between a clayed and floculated suspension.

Three different rheological measurements may be applied to study the bulk properties of suspension concentrates (Whorlow 1980; Goodwin and Hughes 2000; Tadros 2010): (1) Steady-state shear stress-shear rate measurements (using a controlled shear rate instrument). (2) Constant stress (creep) measurements (carried out using a constant stress instrument). (3) Dynamic (oscillatory) measurements (preferably carried out using a constant strain instrument). These rheological techniques can be used to assess sedimentation and flocculation of suspensions. This will be discussed in detail below.

As discussed before, the rate of sedimentation decreases with increase of the volume fraction of the disperse phase,  $\phi$ , and ultimately, it approaches zero at a critical volume fraction  $\phi_p$  (the maximum packing fraction). However, at  $\phi \sim \phi_p$ , the viscosity of the system approaches  $\infty$ . Thus, for most practical emulsions, the system is prepared at  $\phi$  values below  $\phi_p$  and then add “thickeners” to reduce sedimentation. These “thickeners” are usually high molecular weight polymers (such as Xanthan gum, hydroxyethyl cellulose, or associative thickeners), finely divided inert solids (such as silica or swelling clays), or a combination of the two.

In all cases, a “gel” network is produced in the continuous phase which is shear thinning (i.e., its viscosity decreases with increase of shear rate) and viscoelastic (i.e., it has a viscous and elastic components of the modulus). If the viscosity of the elastic network, at shear stresses (or shear rates) comparable to those exerted by the particles, exceeds a certain value, then sedimentation is completely eliminated.

The shear stress,  $\sigma_p$ , exerted by a particle (force/area) can be simply calculated:

$$\sigma_p = \frac{(4/3)\pi R^3 \Delta\rho g}{4\pi R^2} = \frac{\Delta\rho R g}{3} \quad (80)$$

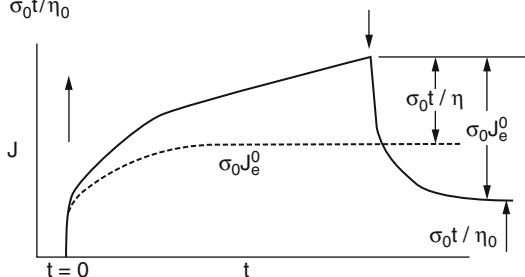
For a 10- $\mu\text{m}$  radius particle with density difference  $\Delta\rho = 0.2$ ,  $\sigma_p$  is equal to

$$\sigma_p = \frac{0.2 \times 10^3 \times 10 \times 10^{-6} \times 9.8}{3} \approx 6 \times 10^{-3} \quad (81)$$

For smaller particles, smaller stresses are exerted.

Thus, to predict sedimentation, one has to measure the viscosity at very low stresses (or shear rates). These measurements can be carried out using a constant stress rheometer (Carrimed, Bohlin, Rheometrics, or Physica). A constant stress  $\sigma$  (using, e.g., a drag cup motor that can apply very small torques and using an air bearing system to reduce the frictional torque) is applied on the system (which may be placed in the gap between two concentric cylinders or a cone-plate geometry), and the deformation (strain  $\gamma$  or

Creep is the sum of a constant value  $J_e \sigma_0$  (elastic part) and a viscous contribution  $\sigma_0 t / \eta_0$



**Agrochemical Formulations, Fig. 44** Creep curve for a viscoelastic liquid

compliance  $J = \gamma/\sigma = \text{Pa}^{-1}$ ) is followed as a function of time (Whorlow 1980; Goodwin and Hughes 2000; Tadros 2010).

For a viscoelastic system, the compliance shows a rapid elastic response  $J_0$  at  $t \rightarrow 0$  (instantaneous compliance  $J_0 = 1/G_0$ , where  $G_0$  is the instantaneous modulus that is a measure of the elastic (i.e., “solid-like”) component). At  $t > 0$ ,  $J$  increases slowly with time, and this corresponds to the retarded response (“bonds” are broken and reformed but not at the same rate). Above a certain time period (that depends on the system), the compliance shows a linear increase with time (i.e., the system reaches a steady state with constant shear rate). If after the steady state is reached, the stress is removed, elastic recovery occurs, and the strain changes sign.

The above behavior (usually referred to as “creep”) is schematically represented in Fig. 44.

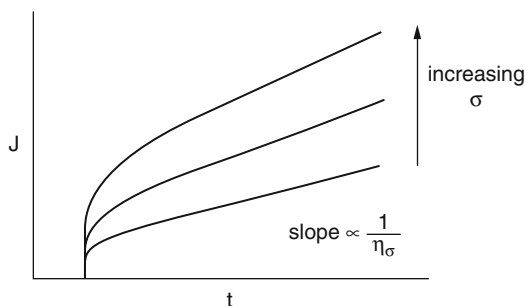
The slope of the linear part of the creep curve gives the value of the viscosity at the applied stress,  $\eta_\sigma$ :

$$\frac{J}{t} = \frac{\text{Pa}^{-1}}{\text{s}} = \frac{1}{\text{Pa s}} = \eta_\sigma \quad (82)$$

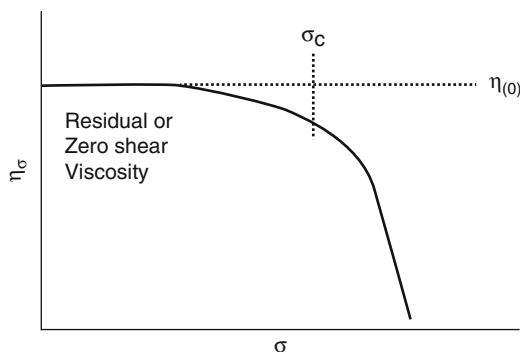
The recovery curve will only give the elastic component, which if superimposed on the ascending part of the curve will give the viscous component.

Thus, one measures creep curves as a function of the applied stress (starting from a very small stress of the order of 0.01 Pa). This is illustrated in Fig. 45. The viscosity  $\eta_\sigma$  (which is equal to the

Creep measurements (Constant stress) can be used to obtain the residual or zero shear viscosity



**Agrochemical Formulations, Fig. 45** Creep curves at increasing applied stress



Critical stress is a useful parameter (related to yield stress) as denotes the stress at which structure “breaks down”.

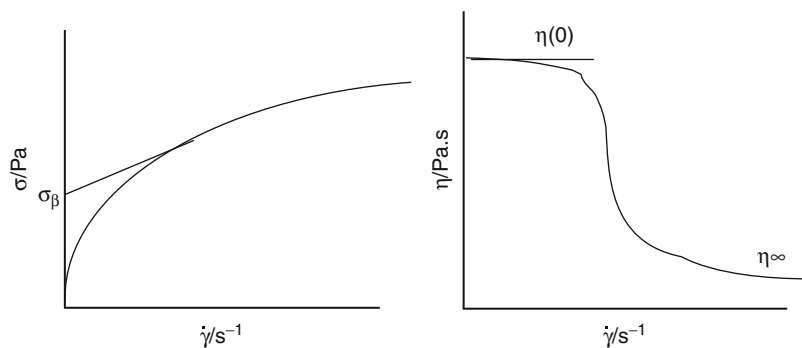
**Agrochemical Formulations, Fig. 46** Variation of viscosity with applied stress

reciprocal of the slope of the straight portion of the creep curve) is plotted as a function of the applied stress. This is schematically shown in Fig. 46. Below a critical stress  $\sigma_{cr}$ , the viscosity reaches a limiting value,  $\eta_{(0)}$ , namely the residual (or zero shear) viscosity. Above  $\sigma_{cr}$ ,  $\eta_\sigma$  decreases rapidly with further increase of the shear stress (the shear thinning regime). It reaches another Newtonian value  $\eta_\infty$ , which is the high shear limiting viscosity.  $\sigma_{cr}$  may be identified as the critical stress above which the structure of the suspension is “broken down.”  $\sigma_{cr}$  is denoted as the “true yield stress” of the suspension.

$\eta_{(0)}$  could be several orders of magnitudes ( $10^4$ – $10^8$ ) higher than  $\eta_\infty$ . Usually, one obtains

### Agrochemical Formulations,

**Fig. 47** Shear stress and viscosity versus shear rate for a pseudoplastic system



good correlation between the rate of sedimentation  $v$  and the residual viscosity  $\eta_{(0)}$  (Buscall et al. 1982). This was illustrated in Fig. 43. Above a certain value of  $\eta_{(0)}$ ,  $v$  becomes equal to 0. Clearly, to minimize sedimentation, one has to increase  $\eta_{(0)}$ ; an acceptable level for the high shear viscosity  $\eta_{\infty}$  must be achieved, depending on the application. In some cases, a high  $\eta_{(0)}$  may be accompanied by a high  $\eta_{\infty}$  (which may not be acceptable for application, e.g., if spontaneous dispersion on dilution is required). If this is the case, the formulation chemist should look for an alternative thickener.

Another problem encountered with many suspensions is that of “syneresis,” that is, the appearance of a clear liquid film at the top of the suspension. “Syneresis” occurs with most “flocculated” and/or “structured” (i.e., those containing a thickener in the continuous phase) suspensions. “Syneresis” may be predicted from measurement of the yield value (using steady-state measurements of shear stress as a function of shear rate) as a function of time or using oscillatory techniques (whereby the storage and loss modulus are measured as a function of strain amplitude and frequency of oscillation). It is sufficient to state in this section that when a network of the suspension particles (either alone or combined with the thickener) is produced, the gravity force will cause some contraction of the network (which behaves as a porous plug) thus causing some separation of the continuous phase which is entrapped between the droplets in the network.

Rheological techniques are most convenient to assess suspension flocculation without the need of any dilution (which in most cases result

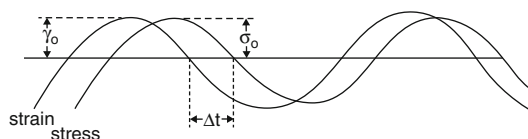
in breakdown of the floc structure). In steady-state measurements, the suspension is carefully placed in the gap between concentric cylinder or cone-and-plate platens. For the concentric cylinder geometry, the gap width should be at least 10X larger than the largest particle size (a gap width that is greater than 1 mm is usually used). For the cone-and-plate geometry, a cone angle of  $4^{\circ}$  or smaller is usually used. A controlled rate instrument is usually used for the above measurements; the inner (or outer) cylinder of the cone (or the plate) is rotated at various angular velocities (which allows one to obtain the shear rate  $\dot{\gamma}$ ), and the torque is measured on the other element (this allows one to obtain the stress  $\sigma$ ).

For most practical suspensions (with  $\phi > 0.1$  and containing thickeners to reduce sedimentation), a plot of  $\sigma$  versus  $\dot{\gamma}$  is not linear (i.e., the viscosity depends on the applied shear rate). The most common flow curve is shown in Fig. 47 (usually described as a pseudoplastic or shear thinning system). In this case, the viscosity decreases with increase in shear rate, reaching a Newtonian value above a critical shear rate.

Several models may be applied to analyze the results of Fig. 47: (a) Power law model:

$$\sigma = k \dot{\gamma}^n \quad (83)$$

where  $k$  is the consistency index of the suspension and  $n$  is the power (shear thinning) index ( $n < 1$ ); the lower the value of  $n$  the more shear thinning the suspension is. This is usually the case with weakly flocculated suspensions or those to which a “thickener” is added.



$\Delta t$  = time shift for sine waves of stresses and strain

$\Delta t \omega = \delta$  phase angle shift

$\omega$  = frequency in radian  $s^{-1}$

$\omega = 2 \pi \nu$

Perfectly elastic solid  $\delta = 0$

Perfectly viscous liquid  $\delta = 90^\circ$

Viscoelastic system  $0 < \delta < 90^\circ$

**Agrochemical Formulations, Fig. 48** Stress-strain relationship for a viscoelastic system

By fitting the results of Fig. 48 to Eq. 34 (this is usually in the software of the computer connected to the rheometer), one can obtain the viscosity of the suspension at a given shear rate:

$$\eta(\text{at a given shear rate}) = \frac{\sigma}{\dot{\gamma}} = k \dot{\gamma}^{n-1} \quad (84)$$

(b) Bingham model:

$$\sigma = \sigma_\beta + \eta_{pl} \dot{\gamma} \quad (85)$$

where  $\sigma_\beta$  is the extrapolated yield value (obtained by extrapolation of the shear stress-shear rate curve to  $\dot{\gamma} = 0$ ). Again, this is provided in the software of the rheometer.  $\eta_{pl}$  is the slope of the linear portion of the  $\sigma$ - $\dot{\gamma}$  curve (usually referred to as the plastic viscosity).

Both  $\sigma_\beta$  and  $\eta_{pl}$  may be related to the flocculation of the suspension. At any given volume fraction of the emulsion and at a given particle size distribution, the higher the value of  $\sigma_\beta$  and  $\eta_{pl}$ , the more the flocculated the suspension is. Thus, if one stores a suspension at any given temperature and makes sure that the particle size distribution remains constant (i.e., no Ostwald ripening occurred), an increase in the above parameters indicate flocculation of the suspension on storage. Clearly, if Ostwald ripening occurs simultaneously,  $\sigma_\beta$  and  $\eta_{pl}$  may change in a complex manner with storage time. Ostwald ripening result in a shift of the particle size

distribution to higher diameters; this has the effect of reducing  $\sigma_\beta$  and  $\eta_{pl}$ . If flocculation occurs simultaneously (having the effect of increasing these rheological parameters), the net effect may be an increase or decrease of the rheological parameters.

The above trend depends on the extent of flocculation relative to Ostwald ripening. Therefore, following  $\sigma_\beta$  and  $\eta_{pl}$  with storage time requires knowledge of Ostwald ripening and/or coalescence. Only in the absence of this latter breakdown process, one can use rheological measurements as a guide of assessment of flocculation.

(c) Herschel-Buckley model (Tadros 2010)

In many cases, the shear stress-shear rate curve may not show a linear portion at high shear rates. In this case, the data may be fitted with a Herschel-Buckley model:

$$\sigma = \sigma_\beta + k \dot{\gamma}^n \quad (86)$$

(d) Casson's model (Tadros 2010)

This is another semiempirical model that may be used to fit the data of Fig. 48:

$$\sigma^{1/2} = \sigma_C^{1/2} + \eta_C^{1/2} \dot{\gamma}^{1/2} \quad (87)$$

Note that  $\sigma_\beta$  is not equal to  $\sigma_C$ . Equation 87 shows that a plot of  $\sigma^{1/2}$  versus  $\dot{\gamma}^{1/2}$  gives a straight line from which  $\sigma_C$  and  $\eta_C$  can be evaluated.

In all the above analyses, the assumption was made that a steady state was reached. In other words, no time effects occurred during the duration of the flow experiment. Many suspensions (particularly those that are weakly flocculated or "structured" to reduce sedimentation) show time effects during flow. At any given shear rate, the viscosity of the suspension continues to decrease with increasing the time of shear; on stopping the shear, the viscosity recovers to its initial value. This reversible decrease of viscosity is referred to as thixotropy.

The most common procedure of studying thixotropy is to apply a sequence of shear stress = shear rate regimes within controlled periods. If the flow curve is carried out within

a very short time (say increasing the rate from 0 to say  $500 \text{ s}^{-1}$  in 30 s and then reducing it again from 500 to  $0 \text{ s}^{-1}$  within the same period), one finds that the descending curve is below the ascending one.

The above behavior can be explained from consideration of the structure of the system. If, for example, the suspension is weakly flocculated, then on applying a shear force on the system, this flocculated structure is broken down (and this is the cause of the shear thinning behavior). On reducing the shear rate back to zero, the structure builds up only in part within the duration of the experiment (30 s).

The ascending and descending flow curves show hysteresis that is usually referred to as “thixotropic loop.” If now, the same experiment is repeated within a longer time (say 120 s for the ascending and 120 s for the descending curves), the hysteresis decreases, that is, the “thixotropic loop” becomes smaller.

The above study may be used to investigate the state of flocculation of a suspension. Weakly flocculated suspensions usually show thixotropy, and the change of thixotropy with applied time may be used as an indication of the strength of this weak flocculation.

The above analysis is only qualitative and one cannot use the results in a quantitative manner. This is due to the possible breakdown of the structure on transferring the suspension to the rheometer and also during the uncontrolled shear experiment.

A very important point that must be considered during rheological measurements is the possibility of “slip” during the measurements. This is particularly the case with highly concentrated suspensions, whereby the flocculated system may form a “plug” in the gap of the platens leaving a thin liquid film at the walls of the concentric cylinder or cone-and-plate geometry. To reduce “slip,” one should use roughened walls for the platens. Strongly flocculated suspensions usually show much less thixotropy than weakly flocculated systems. Again, one must be careful in drawing definite conclusions without other independent techniques (e.g., microscopy).

Another method for studying flocculation is that of constant stress (creep) measurements that was described before. This allows one to obtain the residual viscosity  $\eta_{(o)}$  and critical stress  $\sigma_{cr}$ . The values of  $\eta_{(o)}$  and  $\sigma_{cr}$  may be used to assess the flocculation of the suspension on storage. If flocculation occurs on storage (without any Ostwald ripening), the values of  $\eta_{(o)}$  and  $\sigma_{cr}$  may show a gradual increase with increase of storage time. As discussed in the previous section (on steady-state measurements), the trend becomes complicated if Ostwald ripening occurs simultaneously (both have the effect of reducing  $\eta_{(o)}$  and  $\sigma_{cr}$ ). These measurements should be supplemented by particle size distribution measurements of the diluted suspension (making sure that no flocs are present after dilution) to assess the extent of Ostwald ripening. Another complication may arise from the nature of the flocculation. If the latter occurs in an irregular way (producing strong and tight flocs),  $\eta_{(o)}$  may increase, while  $\sigma_{cr}$  may show some decrease and this complicates the analysis of the results. In spite of these complications, constant stress measurements may provide valuable information on the state of the suspension on storage. Carrying out creep experiments and ensuring that a steady state is reached can be time-consuming. One usually carries out a stress sweep experiment, whereby the stress is gradually increased (within a predetermined time period to ensure that one is not too far from reaching the steady state) and plots of  $\eta_{\sigma}$  versus  $\sigma$  are established. These experiments are carried out at various storage times (say every 2 weeks) and temperatures. From the change of  $\eta_{(o)}$  and  $\sigma_{cr}$  with storage time and temperature, one may obtain information on the degree and the rate of flocculation of the system.

Another rheological technique for investigation of flocculation of SCs is the dynamic (oscillatory) method. These are by far the most commonly used method to obtain information on the flocculation of a suspension. A strain is applied in a sinusoidal manner, with an amplitude  $\gamma_o$  and a frequency  $\nu$  (cycles/s or Hz) or  $\omega$  ( $\text{rad s}^{-1}$ ). In a viscoelastic system (such as the case with a flocculated suspension), the stress



oscillates with the same frequency but out of phase from the strain. From measurement of the time shift between strain and stress amplitudes ( $\Delta t$ ), one can obtain the phase angle shift  $\delta$ :

$$\delta = \Delta t \omega \quad (88)$$

A schematic representation of the variation of strain and stress with  $\epsilon t$  is shown in Fig. 48.

From the amplitudes of stress and strain and the phase angle shift, one can obtain the various viscoelastic parameters: The complex modulus  $G^*$ , the storage modulus (the elastic component of the complex modulus)  $G'$ , the loss modulus (the viscous component of the complex modulus)  $G'' \tan \delta$ , and the dynamic viscosity  $\eta'$ :

$$\text{Complex Modulus } |G^*| = \frac{\sigma_0}{\gamma_0} \quad (89)$$

$$\text{Storage Modulus } G' = |G^*| \cos \delta \quad (90)$$

$$\text{Loss Modulus } G'' = |G^*| \sin \delta \quad (91)$$

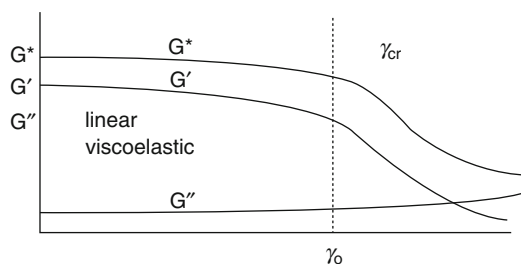
$$\tan \delta = \frac{G''}{G'} \quad (92)$$

$$\text{Dynamic Viscosity } \eta' = \frac{G''}{\omega} \quad (93)$$

$G'$  is a measure of the energy stored in a cycle of oscillation.  $G''$  is a measure of the energy dissipated as viscous flow in a cycle of oscillation.  $\tan \delta$  is a measure of the relative magnitudes of the viscous and elastic components. Clearly, the smaller the value of  $\tan \delta$ , the more elastic the system is and vice versa.  $\eta'$ , the dynamic viscosity, shows a decrease with increase of frequency  $\omega$ .  $\eta'$  reaches a limiting value as  $\omega \rightarrow 0$ . The value of  $\eta'$  in this limit is identical to the residual (or zero shear) viscosity  $\eta_{(0)}$ . This is referred to as the Cox-Mertz rule.

In oscillatory measurements, one carries out two sets of experiments: (a) Strain sweep measurements. In this case, the oscillation is fixed (say at 1 Hz) and the viscoelastic parameters are measured as a function of strain amplitude. This allows one to obtain the linear viscoelastic

Fixed frequency (0.1 or 1 Hz) and follow  $G^*$ ,  $G'$  and  $G''$  with strain amplitude  $\gamma_0$

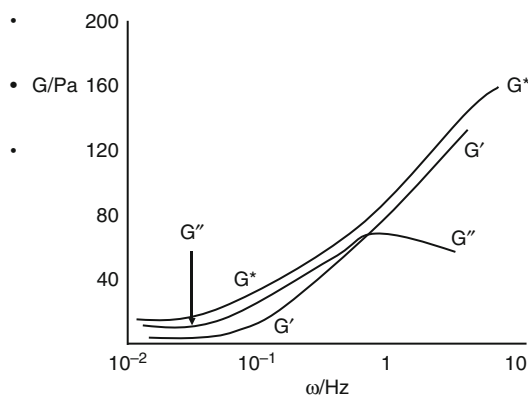


Linear viscoelastic region

$G^*$ ,  $G'$  and  $G''$  are independent of strain amplitude

$\gamma_{cr}$  is the critical strain above which system shows non-linear response (break down of structure)

**Agrochemical Formulations, Fig. 49** Strain sweep results



**Agrochemical Formulations, Fig. 50** Schematic representation of oscillatory measurements for a viscoelastic liquid

region. In this region, all moduli are independent of the applied strain amplitude and become only a function of time or frequency. This is illustrated in Fig. 50, which shows a schematic representation of the variation of  $G^*$ ,  $G'$ , and  $G''$  with strain amplitude (at a fixed frequency). It can be seen from Fig. 49 that  $G^*$ ,  $G'$ , and  $G''$  remain virtually constant up to a critical strain value,  $\gamma_{cr}$ . This region is the linear viscoelastic region. Above  $\gamma_{cr}$ ,  $G^*$  and  $G'$  starts to fall, whereas  $G''$  starts to increase. This is the nonlinear region. The value of  $\gamma_{cr}$  may be identified with the minimum strain above which the “structure” of the suspension

starts to breakdown (e.g., breakdown of flocs into smaller units and/or breakdown of a “structuring” agent).

From  $\gamma_{cr}$  and  $G'$ , one can obtain the cohesive energy  $E_c$  ( $Jm^{-3}$ ) of the flocculated structure (Tadros 2010):

$$E_c = \int_0^{\gamma_{cr}} \sigma d\gamma = \int_0^{\gamma_{cr}} G' \gamma d\gamma = \frac{1}{2} G' \gamma_{cr}^2 \quad (94)$$

$E_c$  may be used in a quantitative manner as a measure of the extent and strength of the flocculated structure in a suspension. The higher the value of  $E_c$ , the more flocculated the structure is. Clearly,  $E_c$  depends on the volume fraction of the suspension as well as the particle size distribution (which determines the number of contact points in a floc). Therefore, for quantitative comparison between various systems, one has to make sure that the volume fraction of the disperse particles is the same and the suspensions have very similar particle size distribution.  $E_c$  also depends on the strength of the flocculated structure, that is, the energy of attraction between the particles. This depends on whether the flocculation is in the primary or secondary minimum. Flocculation in the primary minimum is associated with a large attractive energy, and this leads to higher values of  $E_c$  when compared with the values obtained for secondary minimum flocculation. For a weakly flocculated suspension, such as the case with secondary minimum flocculation of an electrostatically stabilized suspension, the deeper the secondary minimum, the higher the value of  $E_c$  (at any given volume fraction and particle size distribution of the suspension). With a sterically stabilized suspension, weak flocculation can also occur when the thickness of the adsorbed layer decreases. Again, the value of  $E_c$  can be used as a measure of the flocculation; the higher the value of  $E_c$ , the stronger the flocculation. If incipient flocculation occurs (on reducing the solvency of the medium for the change to worse than  $\theta$ -condition), a much deeper minimum is observed and this is accompanied by a much larger increase in  $E_c$ . To apply this analysis, one must have an independent method for assessing

the nature of the flocculation. Rheology is a bulk property that can give information on the interdroplet interaction (whether repulsive or attractive), and to apply it in a quantitative manner, one must know the nature of these interaction forces. However, rheology can be used in a qualitative manner to follow the change of the suspension on storage. Providing the system does not undergo any Ostwald ripening, the change of the moduli with time and in particular the change of the linear viscoelastic region may be used as an indication of flocculation. Strong flocculation is usually accompanied by a rapid increase in  $G'$ , and this may be accompanied by a decrease in the critical strain above which the “structure” breaks down. This may be used as an indication of formation of “irregular” flocs which become sensitive to the applied strain. The floc structure will entrap a large amount of the continuous phase, and this leads to an apparent increase in the volume fraction of the suspension and hence an increase in  $G'$ .

In the oscillatory sweep experiment, the strain amplitude is kept constant in the linear viscoelastic region (one usually takes a point far from  $\gamma_{cr}$  but not too low, that is, in the midpoint of the linear viscoelastic region) and measurements are carried out as a function of frequency. This is schematically represented in Fig. 50 for a viscoelastic liquid system.

Both  $G^*$  and  $G'$  increase with increase in frequency, and ultimately above a certain frequency, they reach a limiting value and show little dependence on frequency.  $G''$  is higher than  $G'$  in the low frequency regime; it also increases with increase in frequency, and at a certain characteristic frequency  $\omega^*$  (that depends on the system), it becomes equal to  $G'$  (usually referred to as the crossover point); after which, it reaches a maximum and then shows a reduction with further increase in frequency. In the low frequency regime, that is, below  $\omega^*$ ,  $G'' > G'$ ; this regime corresponds to longer times (remember that the time is reciprocal of frequency), and under these conditions, the response is more viscous than elastic. In the high-frequency regime, that is, above  $\omega^*$ ,  $G' > G''$ ; this regime corresponds to short times, and

under these conditions, the response is more elastic than viscous. At sufficiently high frequency,  $G''$  approaches zero and  $G'$  becomes nearly equal to  $G^*$ ; this corresponds to very short time scales whereby the system behaves as a near elastic solid. Very little energy dissipation occurs at such high frequency.

The characteristic frequency  $\omega^*$  can be used to calculate the relaxation time of the system  $t^*$ :

$$t^* = \frac{1}{\omega^*} \quad (95)$$

The relaxation time may be used as a guide for the state of the suspension. For a colloidally stable suspension (at a given particle size distribution),  $t^*$  increases with increase of the volume fraction of the oil phase,  $\phi$ . In other words, the crossover point shifts to lower frequency with increase in  $\phi$ . For a given suspension,  $t^*$  increases with increase in flocculation providing the particle size distribution remains the same (i.e., no Ostwald ripening). The value of  $G'$  also increases with increase in flocculation, since aggregation of particles usually result in liquid entrapment and the effective volume fraction of the suspension shows an apparent increase. With flocculation, the net attraction between the droplets also increases, and this results in an increase in  $G'$ .  $G'$  is determined by the number of contacts between the particles and the strength of each contact (which is determined by the attractive energy). It should be mentioned that in practice, one may not obtain the full curve, due to the frequency limit of the instrument and also measurement at low frequency is time-consuming. Usually, one obtains part of the frequency dependence of  $G'$  and  $G''$ . In most cases, one has a more elastic than viscous system. Most suspension systems used in practice are weakly flocculated, and they also contain “thickeners” or “structuring” agents to reduce sedimentation and to acquire the right rheological characteristics for application. The exact values of  $G'$  and  $G''$  required depends on the system and its application. In most cases, a compromise has to be made between acquiring the right rheological characteristics for application and the optimum

rheological parameters for long-term physical stability. Application of rheological measurements to achieve the above conditions requires a great deal of skill and understanding of the factors that affect rheology.

## Microemulsions in Agrochemical Formulations

Microemulsions are a special class of “dispersions” (transparent or translucent) which actually have little in common with emulsions. They are better described as “swollen micelles.” The term microemulsion was first introduced by Hoar and Schulman (Hoar and Schulman 1943; Prince 1977) who discovered that by titration of a milky emulsion (stabilized by soap such as potassium oleate) with a medium chain alcohol such as pentanol or hexanol, a transparent or translucent system was produced. A schematic representation of the titration method adopted by Schulman and coworkers is given below:

O/W emulsion	→	Add cosurfactant	→	Transparent
Stabilised by		e.g. $C_5H_{11}OH$		or Translucent
Soap		$C_6H_{13}OH$		System

The final transparent or translucent system is a W/O microemulsion.

A convenient way to describe microemulsions is to compare them with micelles. The latter which are thermodynamically stable may consist of spherical units with a radius that is usually less than 5 nm. Two types of micelles may be considered: normal micelles with the hydrocarbon tails forming the core and the polar head groups in contact with the aqueous medium and reverse micelles (formed in nonpolar media) with a water core containing the polar head groups and the hydrocarbon tails now in contact with the oil. The normal micelles can solubilize oil in the hydrocarbon core forming O/W microemulsions, whereas the reverse micelles can solubilize water forming a W/O microemulsion. A rough guide to the dimensions of micelles, micellar solutions and macroemulsions is as follows: Micelles,  $R < 5$  nm (they scatter little light and are transparent); macroemulsions,  $R > 50$  nm

(opaque and milky); and micellar solutions or microemulsions, 5–50 nm (transparent, 5–10 nm and translucent 10–50 nm).

Microemulsions are quite distinct from macroemulsions (EWs). With emulsions, increase of the mechanical energy and increase in surfactant concentration usually results in the formation of smaller droplets which become kinetically more stable. With microemulsions, neither mechanical energy nor increase in surfactant concentration can result in its formation. The latter is based on a specific combination of surfactants and specific interaction with the oil, and the water phases and the system is produced at optimum composition. Thus, microemulsions have nothing in common with macroemulsions, and, in many cases, it is better to describe the system as “swollen micelles.” The best definition of microemulsions is as follows (Danielsson and Lindman 1983): “System of water + oil + amphiphile that is a single optically isotropic and thermodynamically stable liquid solution.” Amphiphiles refer to any molecule that consists of hydrophobic and hydrophilic portions, for example, surfactants, alcohols, etc. The driving force for microemulsion formation is the low interfacial energy which is overcompensated by the negative entropy of dispersion term. The low (ultralow) interfacial tension is produced in most cases by combination of two molecules, referred to as the surfactant and cosurfactant (e.g., medium chain alcohol).

Microemulsions offer a very attractive alternative for formulation of agrochemicals when compared with EWs. As mentioned above, these are single optically isotropic and thermodynamically stable dispersions consisting of oil, water, and amphiphile (one or more surfactants). As mentioned above, the origin of the thermodynamic stability arises from the low interfacial energy of the system which is outweighed by the entropy of dispersion. These systems offer a number of advantages over *o/w* emulsions for the following reasons. Once the composition of the microemulsion is identified, the system is prepared by simply mixing all the components without the need of any appreciable shear. Due to their thermodynamic stability, these formulations

undergo no separation or breakdown on storage (within a certain temperature range depending on the system). The low viscosity of the microemulsion systems ensures their ease of pourability and dispersion on dilution, and they leave little residue in the container. Another main attraction of microemulsions is their possible enhancement of biological efficacy of many agrochemicals. This, as we will see later, is due to the solubilization of the pesticide by the microemulsion droplets.

The formulation of microemulsions is still an art, since understanding the interactions, at a molecular level, at the oil, and water sides of the interface is far from being achieved. However, some rules may be applied for selection of emulsifiers for formulating *o/w* and *w/o* microemulsions. These rules are based on the same principles applied for selection of emulsifiers for EWs described before. Two main methods may be applied for such selection, namely the hydrophilic-lipophilic balance (HLB) and the phase inversion temperature (PIT). As mentioned before, the HLB concept is based on the relative percentage of hydrophilic to lipophilic (hydrophobic) groups in the surfactant molecule. Surfactants with a low HLB number (3–6) normally form *w/o* emulsions, whereas those with high HLB number (8–18) form *o/w* emulsions. Given an oil to be microemulsified, the formulator should first determine its required HLB number. Several procedures may be applied for determining the HLB number depending on the type of surfactant that needs to be used. These procedures were described before. Once the HLB number of the oil is known, one must try to find the chemical type of emulsifier which best matches the oil. Hydrophobic portions of surfactants which are similar to the chemical structure of the oil should be looked at first.

The PIT system provides information on the type of oil, phase volume relationships, and concentration of the emulsifier. The PIT system is established on the proposition that the HLB number of a surfactant changes with temperature and that the inversion of the emulsion type occurs when the hydrophile and lipophile tendencies of

the emulsifier just balance. At this temperature, no emulsion is produced. From a microemulsion viewpoint, the PIT has an outstanding feature since it can throw some light on the chemical type of the emulsifier needed to match a given oil. Indeed, the required HLB values for various oils estimated from the PIT system compare very favorably with those prepared using the HLB system described above. This shows a direct correlation between the HLB number and the PIT of the emulsion.

The role of microemulsions in enhancement of biological efficiency can be described in terms of the interactions at various interfaces and their effect on transfer and performance of the agrochemical (Tadros 1994, 2009). The application of an agrochemical as a spray involves a number of interfaces, where interaction with the formulation plays a vital role. The first interface during application is that between the spray solution and the atmosphere (air) which governs the droplet spectrum, rate of evaporation, drift, etc. In this respect, the rate of adsorption of the surfactant at the air/liquid interface is of vital importance. Since microemulsions contain high concentrations of surfactant and mostly more than one surfactant molecule is used for their formulation, then on diluting a microemulsion on application, the surfactant concentration in the spray solution will be sufficiently high to cause efficient lowering of the surface tension  $\gamma$ . Two surfactant molecules are more efficient in lowering  $\gamma$  than either of the two components. Thus, the net effect will be production of small spray droplets, which as we will see later, adhere better to the leaf surface. In addition, the presence of surfactants in sufficient amounts will ensure that the rate of adsorption (which is the situation under dynamic conditions) is fast enough to ensure coverage of the freshly formed spray by surfactant molecules.

The second interaction is between the spray droplets and the leaf surface, whereby the droplets impinging on the surface undergo a number of processes that determine their adhesion and retention and further spreading on the target surface. The most important parameters that determine these processes are the volume of the droplets and their velocity, the difference

between the surface energy of the droplets in flight,  $E_o$ , and their surface energy after impact,  $E_s$ . As mentioned above, microemulsions which are effective in lowering the surface tension of the spray solution ensure the formation of small droplets which do not usually undergo reflection if they are able to reach the leaf surface. Clearly, the droplets need not to be too small, otherwise drift may occur. One usually aims at a droplet spectrum in the region of 100–400  $\mu\text{m}$ . The adhesion of droplets is governed by the relative magnitude of the kinetic energy of the droplet in flight and its surface energy as it lands on the leaf surface. Since the kinetic energy is proportional to the third power of the radius (at constant droplet velocity), whereas the surface energy is proportional to the second power, one would expect that sufficiently small droplets will always adhere. For a droplet to adhere, the difference in surface energy between free and attached drop ( $E_o - E_s$ ) should exceed the kinetic energy of the drop, otherwise bouncing will occur. Since  $E_s$  depends on the contact angle,  $\theta$ , of the drop on the leaf surface, it is clear that low values of  $\theta$  are required to ensure adhesion, particularly with large drops that have high velocity. Microemulsions when diluted in the spray solution usually give low contact angles of spray drops on leaf surfaces as a result of lowering the surface tension and their interaction with the leaf surface.

Another factor which can affect biological efficacy of foliar spray application of agrochemicals is the extent to which a liquid wets and covers the foliage surface. This, in turn, governs the final distribution of the agrochemical over the areas to be protected. Several indices may be used to describe the wetting of a surface by the spray liquid, of which the spread factor and spreading coefficient are probably the most useful. The spread factor is simply the ratio between the diameter of the area wetted on the leaf,  $D$ , and the diameter of the drop,  $d$ . This ratio is determined by the contact angle of the drop on the leaf surface. The lower the value of  $\theta$ , the higher the spread factor. As mentioned above, microemulsions usually give low contact angle for the drops produced from the spray.

The spreading coefficient is determined by the surface tension of the spray solution as well as the value of  $\theta$ . Again, with microemulsions diluted in a spray, both  $\gamma$  and  $\theta$  are sufficiently reduced, and this results in a positive spreading coefficient. This ensures rapid spreading of the spray liquid on the leaf surface.

Another important factor for control of biological efficacy is the formation of “deposits” after evaporation of the spray droplets, which ensure the tenacity of the particles or droplets of the agrochemical. This will prevent removal of the agrochemical from the leaf surface by the falling rain. Many microemulsion systems form liquid crystalline structures after evaporation, which have high viscosity (hexagonal or lamellar liquid crystalline phases). These structures will incorporate the agrochemical particles or droplets and ensure their “stickiness” to the leaf surface.

One of the most important roles of microemulsions in enhancing biological efficacy is their effect on penetration of the agrochemical through the leaf. Two effects may be considered, which are complimentary (Tadros 1994, 2009). The first effect is due to enhanced penetration of the chemical as a result of the low surface tension. For penetration to occur through fine pores, a very low surface tension is required to overcome the capillary (surface) forces. These forces produce a high pressure gradient that is proportional to the surface tension of the liquid. The lower the surface tension, the lower the pressure gradient and the higher the rate of penetration. The second effect is due to solubilization of the agrochemical within the microemulsion droplet. Solubilization results in an increase in the concentration gradient thus enhancing the flux due to diffusion. This can be understood from a consideration of Fick’s first law:

$$J_D = D \left( \frac{\partial C}{\partial x} \right) \quad (96)$$

where  $J_D$  is the flux of the solute (amount of solute crossing a unit cross section in unit time),  $D$  is the diffusion coefficient, and  $(\partial C/\partial x)$  is the concentration gradient. The presence of the

chemical in a swollen micellar system will lower the diffusion coefficient. However, the presence of the solubilizing agent (the microemulsion droplet) increases the concentration gradient in direct proportionality to the increase in solubility. This is because Fick’s law involves the absolute gradient of concentration which is necessarily small as long as the solubility is small but not its relative rate. If the saturation is noted by  $S$ , Fick’s law may be written as

$$J_D = D 100 S \left( \frac{\partial \%S}{\partial x} \right) \quad (97)$$

where  $(\partial \%S/\partial x)$  is the gradient in relative value of  $S$ . Equation 28 shows that for the same gradient of relative saturation, the flux caused by diffusion is directly proportional to saturation. Hence, solubilization will in general increase transport by diffusion, since it can increase the saturation value by many orders of magnitude (that outweighs any reduction in  $D$ ). In addition, the solubilization enhances the rate of dissolution of insoluble compounds, and this will have the effect of increasing the availability of the molecules for diffusion through membranes.

## Controlled-Release Formulations

Controlled-release formulation of agrochemicals offer a number of advantages of which the following is worth mentioning (Scher 1999; Kondo 1979): (1) improvement of residual activity, (2) reduction of application dosage, (3) stabilization of the core active ingredient (a.i.) against environmental degradation, (4) reduction of mammalian toxicity by reducing worker exposure, (5) reduction of phytotoxicity, (6) reduction of fish toxicity, and (7) reduction of environmental pollution. One of the main advantages of using controlled-release formulations, in particular microcapsules, is the reduction of physical incompatibility when mixtures are used in the spray tank. They also can reduce biological antagonism when mixtures are applied in the field. Several types of controlled-release systems can be identified: (1) Microcapsules with



particles in the size range 1–100  $\mu\text{m}$  that consist of a distinct capsule wall (mostly a polymer) surrounding the agrochemical core. (2) Microparticles (size range 1–100  $\mu\text{m}$ ) consisting of a matrix in which the agrochemical is uniformly dissolved or dispersed. (3) Granules with matrix particles of 0.2–2.0 mm with the agrochemical uniformly dissolved or dispersed within the matrix. In this section, I will give a brief account for the different types of slow release systems. For more detail, the reader can refer to the text edited by Scher (1999).

Microencapsulation of agrochemicals is mainly carried out by interfacial condensation, in situ polymerization and coacervation. Interfacial condensation (Scher 1999; Kondo 1979) is perhaps the most widely used method for encapsulation in industry. The a.i. which may be oil soluble, oil dispersible, or an oil itself is first emulsified in water using a convenient surfactant or polymer. A hydrophobic monomer A is placed in the oil phase (oil droplets of the emulsion), and a hydrophilic monomer B is placed in the aqueous phase. The two monomers interact at the interface between the oil and the aqueous phase forming a capsule wall around the oil droplet. Two main types of systems may be identified. For example, if the material to be encapsulated is oil soluble, oil dispersible, or an oil itself, an oil-in-water (O/W) emulsion is first prepared. In this case, the hydrophobic monomer is dissolved in the oil phase which forms the dispersed phase. The role of surfactant in this process is crucial since an oil-water emulsifier (with high hydrophilic-lipophilic balance, HLB) is required. Alternatively, a polymeric surfactant such as partially hydrolyzed polyvinyl acetate (referred to as polyvinyl alcohol, PVA) or an ethylene oxide-propylene oxide-ethylene oxide, PEO-PPO-PEO (Pluronic) block copolymer, can be used. The emulsifier controls the droplet size distribution and hence the size of capsules formed. On the other hand, if the material to be encapsulated is water soluble, a water-in-oil (W/O) emulsion is prepared using a surfactant with low HLB number or an A-B-A block copolymer of polyhydroxystearic acid-polyethylene oxide-polyhydroxystearic acid (PHS-PEO-PHS). In

this case, the hydrophilic monomer is dissolved in the aqueous internal phase droplets.

In interfacial polymerization, the monomers A and B are polyfunctional monomers capable of causing polycondensation or polyaddition reaction at the interface (Scher 1999; Kondo 1979). Examples of oil soluble monomers are polybasic acid chloride, bis-haloformate, and polyisocyanates, whereas water soluble monomers can be polyamine or polyols. Thus, a capsule wall of polyamide, polyurethane, or polyurea may be formed. Some trifunctional monomers are present to allow cross-linking reactions. If water is the second reactant with polyisocyanates in the organic phase, polyurea walls are formed. The latter modification has been termed in situ interfacial polymerization (Morgan and Kvolek 1947).

One of the most useful microencapsulation processes involves reactions that produce formation of urea-formaldehyde (UF) resins. Urea along with other ingredients such as amines, maleic anhydride copolymers, or phenols is added to the aqueous phase that contains oily droplets of the active ingredient that is to be encapsulated. Formaldehyde or formaldehyde oligomers are added, and the reaction conditions are adjusted to form UF condensates, sometimes referred to as aminoplasts, that should preferentially wet the disperse phase (Scher 1999). The reaction is continued to completion over several hours. Fairly high activity products can be obtained. A modification of this technique is the use of etherified UF resins. The UF prepolymers are dissolved in the organic phase, along with the active ingredient, through the use of protective colloids (such as PVA), and the reaction is initiated through temperature and acid catalyst. This promotes the formation of the shell in the organic phase adjacent to the interface between the bulk oil phase droplets and the aqueous phase solution (Scher 1999).

It should be mentioned that the role of surfactants in the encapsulation process is very important. Apart from their direct role in the preparation of microcapsule dispersions, surfactants can be used to control the release of the active ingredient (a.i) from the microcapsule

dispersion. For example, Wade et al. (Beetsman 1999) have shown that the efficacy of an edifenphos suspension can be improved by addition of a surfactant either to the aqueous medium or to the core. This was attributed to the possible solubilization of the a.i. by the surfactant micelles, thus increasing the release rate.

There are four types of encapsulation utilizing the system of phase separation from aqueous solution (Kondo 1979): (1) complex coacervation or phase separation resulting from two oppositely charged colloids neutralizing one another, (2) simple coacervation where a nonelectrolyte such as alcohol causes formation of a separate polymer-rich phase, (3) salt coacervation where a polymer separates as a result of salting-out process, and (4) precipitation and insolubilization of a polymer by changing the pH of the aqueous solution system.

Encapsulation of solid particles is by far the most challenging process of encapsulation since one has to coat the particles individually without any aggregation. These particles cover the size range 0.1–5  $\mu\text{m}$  with an average of 1–2  $\mu\text{m}$ . Clearly, when encapsulating these particles, one has to make sure that the smallest size fraction is retained without any aggregation. This is vital for biological efficacy since the smaller particles are more effective for disease control (due to their higher solubility when compared with the larger particles). Beeston (1999) suggested an injection treatment coating method for encapsulation of solid particles. This method utilizes air at sonic velocity to atomize the coating material and accelerate the particles in such a manner that they become coated on all surfaces. The liquid coating material may be melted wax or resins, solutions of polymers or coating materials, or suspensions of film-forming solids such as polymer latexes. Coating is accomplished by metering the solid particles in the shear zone concurrently with metering the liquid coating material into the air stream. The latter is accelerated to the speed of sound through a restriction zone to give a shear zone of sufficient intensity to affect coating. The mixing action within the shear zone coats the solid particles individually with the coating material. On-line particle size measurement of the encapsulated

solid particles showed that the particle size range of the solid particles remain virtually unchanged by this injection treatment coating process indicating that individual particles of all sizes are discretely coated.

Another method that can be applied to encapsulate solid particles is a modification of the coacervation process described above. In this method, a technique of solvent evaporation is used to precipitate the polymers as intact coatings. The solid particles are suspended in a solvent solution of the polymer and emulsified into a liquid. The emulsion is then heated to evaporate the solvent causing the polymer to insolubilize as a coating around the suspended particles. Alternatively, a non-solvent for the polymer is added to the suspension of particles in polymer solution, causing the solvent to phase separate and the polymers to insolubilize to coatings.

Another encapsulation technique is to use matrix-based microparticles. The latter are of three main types (Park et al. 1999): (1) Matrix powders where the active ingredient (a.i.) is dispersed throughout the matrix and the mixture is ground (if necessary to form a powder that can be applied as wettable powder. Surface active agents are incorporated to aid wetting and dispersion of the microparticles. The matrices used include polymers such as lignin, starch, and proteins; high molecular weight natural polymers such as waxes and cyclodextrin; and synthetic polymers such as urea formaldehyde resins or acrylic acid polymers. Inorganic materials such as glass, silica, or diatomaceous earth can also be used. These inorganic materials can also act as carriers. (2) Carriers plus matrix whereby the particles are based on a porous powder that is used as a carrier. Two types can be distinguished, namely co-loaded (where the a.i./matrix mixture is loaded into the carrier) and postcoated (where the a.i. is loaded into the carrier and the matrix is then loaded separately). (3) Matrix emulsions whereby the microparticles are made by emulsifying a hot solution of the a.i. plus matrix, typically in water. On cooling, the emulsion droplets solidify producing an aqueous suspension of the microparticles.

Generally speaking, one component of the formulation, the “matrix,” will be responsible for the controlled release of the formulation. It is convenient to consider the controlled release as being due to interaction among the a.i., the matrix, and the environment. Matrix systems where the a.i. is uniformly dispersed through a matrix material are the basis of commercial formulations (Bahadir and Pfister 1990). Three models may be used for describing the behavior of such systems. The first two mechanisms apply where the a.i. is uniformly dispersed throughout the matrix and is essentially impermeable to water or the external environment. Leaching of the a.i. occurs at the edge of the particle, setting up a concentration gradient within the particle that provides the driving force for diffusion of the a.i. to the edge of the particle and into the external environment. In such a system, the rate of release is governed by the solubility of the a.i. in the matrix, the diffusion coefficient for the transport of the a.i. through the matrix, and the geometry of the particle. Matrix particles usually contain pores and cracks thus increasing the effective surface area between the particle and the external environment and hence the release rate. The second mechanism applied to rigid, often glassy matrices where diffusion of the a.i. within the matrix of the active is negligible. Leaching is controlled by surface exposure, the a.i. through biological or chemical degradation of the matrix. The third mechanism applies to systems where the matrix material is permeable to the external environment, for example, water. This corresponds to a system where the a.i. is dispersed in a latex. In this case, water permeates the matrix through a combination of capillary and osmotic effects. The a.i. dissolves and diffuses to the edge of the particle into the surrounding medium. The process is diffusion controlled and is governed by the solubility and diffusion coefficient of the a.i. in water.

Controlled release can also be achieved from granules. Many agrochemicals are formulated as water dispersible granules (WGs) which disperse quickly and completely when added to water. The main advantage of WGs is that they avoid the use of solvents thus reducing the risk during

manufacture and to farm workers during application. In addition, they can be applied for slow release as will be discussed below. Several processes can be applied to produce WGs of insoluble a.i.: (1) Those in which the starting materials are essentially dry and are subsequently making them wet and then redrying. (2) Those in which the starting materials are wet and are granulated and dried. A typical composition of a WG is one or two a.i.s, dispersing agent, suspending agent, wetting agent, binder (such as lignosulphonate or a gum), and a filler (mineral filler or water soluble salt). As mentioned before, granulation is carried out using a dry or wet route process. Several dry route processes are possible such as pan granulation, fluid-bed granulation, Schugi granulator, extrusion, and peg or pin granulator (Woodford 1998). The wet route process can be carried out by spray drying or spray granulation (Woodford 1998).

Approaches to achieve controlled release in granules fall into two main categories: (1) The matrix (monolith) with the a.i. dispersed throughout the structure. (2) The reservoir in which a polymeric coating entraps the a.i. with or without a support. (Wilkins 1990). Particle size and uniformity are very important especially in applications where the duration of release is critical. Three types of granule dimensions can be distinguished, namely fine granules 0.3–2.5 mm in diameter, microgranules 0.1–0.6 mm, and macrogranules 2–6 mm. A formulation containing a range of particle sizes from dusts to macrogranules will have an extended period of effectiveness. A controlled-release system based on a monolithic polymer granule made from extruding the a.i. with a release-rate-modifying inert material (“porisogen”) in a thermoplastic matrix can play an important role for pest management for periods (following a single treatment of a nonpersistent agrochemical) up to 2–3 years.

Although the above approach based on synthetic polymers is the most successful of the controlled-release granules, natural polymers showed great success in matrix formulations for a.i. delivery. Examples of natural polymers are cross-linked starch, polysaccharides, cross-linked

alginates, and cellulose derivatives. To provide effective delay of release, alginate gels cross-linked with calcium require the incorporation of absorbents such as silica, alumina, clays, or charcoal. Further control of the release rate could be achieved by combining kaolin clay with linseed oil in the granule. Other gel forming polymers include carboxymethylcellulose stabilized with gelatin and cross-linked with cupric or aluminum ions. Coating of granules with rate-controlling polymer film can also be applied. Controlled delivery of agrochemicals has also been obtained with superabsorbent acrylamide and acrylate polymers.

The biodegradability of the formulating material is an important aspect of controlled release for environmental applications. Several synthetic and natural polymers used for formulating granules are biodegradable. The delivery of bioactives from controlled-release granules can be enhanced by inclusion of biosurfactants.

Several lignin-based granules have been introduced for controlled release of several a.i.s. Lignin is a polyphenolic material that occurs in the cell wall of most terrestrial plants, where it is strongly associated with carbohydrates. It is a polymer produced by random dehydrogenation of a number of phenolic precursors linked to the polysaccharide component of the plant cell. This produces a complex structure without any regular repeating monomer. Lignin is separated from lignocellulosic plants by physical or chemical means.

Several agrochemicals are formulated as granules using lignin, in particular for soil application. The a.i. is characterized by some physicochemical properties such as moderate sorption on soil components, low volatility, moderate to high melting points, crystallinity, and low to moderate water solubility. Such properties make them compatible with alkali lignins for preparing matrices by melting the components together. This produces a glassy matrix upon cooling.

The compatibility of a lignin and an agrochemical can be assessed by observing a film of the melt mixture under the microscope for presence of unsolvated lignin particles. Where

solvation occurs, the melting point of the agrochemical is depressed, and this can be determined using differential scanning calorimetry (DSC). The density of the glassy adhesive matrix is usually lower than that of the lignin and often less than that of the a.i. This can be explained by the presence of voids or pores that cannot be observed by microscopy.

The effect of water on the matrix formulation varies according to the agrochemical compatibility with the lignin and the ratio of a.i. to lignin. With highly compatible a.i. such as diuron, the surface of the matrix changes from dark brown to dull light brown on exposure to water. With further exposure, some swelling occurs and the outer region is very porous. Diffusion of diuron is enhanced compared to that in the unswollen glassy interior. The swelling and water uptake depend to a large extent on the lignin type used.

The mechanism of release from lignin matrix granules intended for use in soil and aqueous media is studied by immersing the granule in water under static, stirred, or flowing conditions. Granules prepared from various lignin types always show release rates that decrease with time.

## References

- Abele F (1964) In: Passaglia E, Stromberg RR, Kruger J (eds) Ellipsometry in the measurement of surfaces and thin films. Nat Bur Stand Misc Publ 256
- Adam NK (1925) *J Phys Chem* 29:87
- Asakura A, Oosawa F (1954) *J Chem Phys* 22:1235; *J Polymer Sci* 93:183 (1958)
- Bahadir M, Pfister G (1990) Controlled release formulations of pesticides. In: Bowers WS, Ebing W, Martin D (eds) Controlled release, biochemical effects of pesticides and inhibition of plant pathogenic fungi. Springer, Berlin, pp 1–64
- Barnett KG, Cosgrove T, Vincent B, Burgess A, Crowley TL, Kims J, Turner JD, Tadros THF (1981) *Disc Faraday Soc* 22:283
- Batchelor GK (1972) *J Fluid Mech* 52:245
- Becher P (1987) In: Schick MJ (ed) Nonionic surfactants, vol 1, Surfactant science series. Marcel Dekker, New York
- Beetsman GB (1999) In: Scher HB (ed) Controlled-release delivery systems for pesticides. Marcel Dekker, New York
- Bijsterbosch BH (1987) Stability of solid/liquid dispersions. In: Tadros THF (ed) Solid/liquid dispersions. Academic, London

- Buestein BR, Hilton CL (1982) Amphoteric surfactants. Marcel Dekker, New York
- Buscall R, Goodwin JW, Ottewill RH, Tadros TF (1982) *J Colloid Interface Sci* 85:78
- Clunie JS, Ingram BT (1983) In: Parfitt GD, Rochester CH (eds) Adsorption from solution at the solid/liquid interface. Academic, London, p 105
- Cohen-Stuart MA, Fleer GJ, Bijsterbosch J (1982) *Colloid Interface Sci* 90:321
- Cohen-Stuart MA, Mulder JW (1985) *Colloids and Surfaces* 15:49
- Conner P, Ottewill RH (1971) *J Colloid Interface Sci* 37:642
- Cosgrove T, Crowley TL, Ryan T (1987) *Macromolecules* 20:2879
- Danielsson I, Lindman B (1983) *Colloids Surf* 3:391
- Davies JT (1959) *Proc Int Congr Surf Act* 1:426; Davies JT, Rideal EK (1961) *Interfacial phenomena*. Academic, New York
- Davies JT, Rideal EK (1969) *Interfacial phenomena*. Academic, New York
- Day RE, Greenwood FG, Parfitt GD 4th (1967) *Int Congr Surface Active Subst* 18:1005
- Debye P, Anaker EW (1951) *J Phys Colloid Chem* 55:644
- Deryaguin BV, Landau L (1941) *Acta Physico Chem* 14(633)
- Deryaguin BV, Scherbaker RL (1961) *Kolloid Zh* 23:33
- Dukhin SS, Kretzschmar G, Miller R (1995) *Dynamics of adsorption at liquid interfaces*. Elsevier, Amsterdam
- Elworthy PH, Florence AT, Macfarlane CB (1968) *Solubilization by surface active agents*. Chapman and Hall, London
- Fischer EW (1958) *Kolloid Z* 160:120
- Fleer GJ, Cohen-Stuart MA, Scheutjens JM, Cosgrove T, Vincent B (1993) *Polymers at interfaces*. Chapman and Hall, London
- Flory PJ, Krigbaum WR (1950) *J Chem Phys* 18:1086
- Fontana BJ, Thomas JR (1961) *J Phys Chem* 65:480
- Friberg S, Jansson PO, Cederberg E (1976) *J Colloid Interface Sci* 55:614
- Fuerstenau DW (1971) In Hair ML (ed) *The chemistry of biosurfaces*. Marcel Dekker, New York, p 91
- Fuerstenau DW, Healy TW (1972) In: Lemlich R (ed) *Adsorptive bubble separation techniques*. Academic, London, p 91
- Garvey MJ, Tadros THF, Vincent B (1974) *J Colloid Interface Sci* 49:57
- Garvey MJ, Tadros TF, Vincent B (1976) *J Colloid Interface Sci* 55:440
- Gaudin AM, Fuerstenau DW (1955) *Trans AIME* 202:958
- Gibbs JW (1928) *Collected works*, 1. Longman, New York, p 219
- Goodwin JW, Hughes R (2000) *Rheology for chemists*. Royal Society of Chemistry Publication, Cambridge
- Greenwood FG, Parfitt GD, Picton NH, Wharton DG (1968) *Adv Chem Ser No.* 79:135
- Griffin WC (1949) *J Cosmet Chemists* 1:311; 5:249 (1954)
- Hamaker HC (1937) *Physica* 4:1058
- Harkins WD, Mattoon WD, Corrin ML (1946) *J Am Chem Soc* 68: 220; *J Colloid Sci* 1:105
- Hartley GS (1936) *Aqueous solutions of paraffin chain salts*. Hermann and Cie, Paris
- Healy TW (1974) *J Macromol Sci Chem* 118:603
- Hesslink FT, Vrij A, Overbeek JTG (1971) *J Phys Chem* 75:2094
- Higuchi WI, Misra J (1962) *J Pharm Sci* 51:459
- Hirst EL, McGilvary DI, Percival EG (1950) *J Chem Soc*:1297
- Hoar TP, Schulman JH (1943) *Nature (London)* 152:102
- Hoeve CA (1970) *J Polym Sci* 30: 361; (1971) 34:1
- Holmberg K, Jonsson B, Kronberg B, Lindman B (2003) *Surfactants and polymers in solution*, 2nd edn. Wiley, Chichester
- Hough DB, Randall HM (1983) In: Parfitt GD, Rochester CH (1983) *Adsorption from solution at the solid/liquid interface*. Academic, London, p 247
- Hunter RJ (1981) *Zeta potential in colloid science; principles and applications*. Academic, London
- Istraelachvili J (1985) *Intermolecular and surface forces, with special applications to colloidal and biological systems*. Academic, London, p 251
- Jungerman E (1970) *Cationic surfactants*. Marcel Dekker, New York
- Kabalanov AS, Shchukin ED (1992) *Adv Colloid Interface Sci* 38:69; Kabalanov AS (1994) *Langmuir* 10:680
- Killmann E, Eisenlauer E, Korn MJ (1977) *Polymer Sci Polymer Symp* 61:413
- Kloubek J, Friml K, Krejci F (1976) *Check Chem Commun* 41:1845
- Kondo A (1979) *Microcapsule processing and technology*. Marcel Dekker, New York
- Lifshitz IM, Slesov VV (1959) *Sov Phys JETP* 35:331
- Lindman B (1984) In: Tadros THF (ed) *Surfactants*. Academic, London. Holmberg K, Jonsson B, Kronberg B, Lindman B (2003) *Surfactants and polymers in aqueous solution*, 2nd edn. Wiley, New York
- Linfield WM (ed) (1967) *Anionic surfactants*. Marcel Dekker, New York
- Lucassen-Reynders EH (1994) *Colloids Sur* A91:79
- Lucassen-Reynders EH (1981) *Anionic surfactants—physical chemistry of surfactant action*. Marcel Dekker, New York
- Lyklema J (1987) *Structure of the solid/liquid interface and the electrical double layer*. In: Tadros THF (ed) *Solid/liquid dispersions*. Academic, London
- Mackor EL, van der Waals JH (1951) *J Colloid Sci* 7:535
- McBain JW (1913) *Trans Faraday Soc* 9:99
- McBain JW (1950) *Colloid science*. Heath, Boston
- McCutcheon. *Detergents and emulsifiers*. Allied, New Jersey, published annually
- Miller R, Hoffmann A, Hartmann R, Schano KH, Halbig A (1992) *Adv Mater* 4:370
- Morgan PW, Kvolek SL (1947) *J Polym Sci* 2:90



- Mukerjee P, Mysels KJ (1971) Critical Micelle concentrations of aqueous surfactant systems. National Bureau of Standards Publication, Washington, DC
- Napper DH (1981) Polymeric stabilisation of colloidal dispersions. Academic, London
- Norrish K (1954) Disc Faraday Soc 18:120
- Ottewill RH (1987) Properties of concentrated suspensions. In: Tadros THF (ed) Solid/liquid dispersions. Academic, London
- Parfitt GD (1977) Dispersion of powders in liquid. Applied Science, London
- Park DJ, Jackson WR, McKinnon IR, Marshall M (1999) In: Scher HB (ed) Controlled-release delivery systems for pesticides. Marcel Dekker, New York
- Piirma I (1992) Polymeric surfactants, Surfactant science series, No.42. Marcel Dekker, New York
- Porter MR (1994) Handbook of surfactants. Chapman and Hall, Blackie
- Prince LM (1977) Microemulsion theory and practice. Academic, New York
- Pusey PN (1973) In: Green JHS, Dietz R (eds) Industrial polymers : characterisation by molecular weights. Transcrip Books, London
- Reynders L (1996) In: Becher P (ed) Encyclopedia of emulsion technology. Marcel Dekker, New York
- Rideal EK (1922) Phil Mag 44:1152
- Robb ID, Smith R (1974) Eur Polym J 10:1005
- Roe RJ (1974) J Chem Phys 60:4192
- Rubingh N, Holland PM (eds) (1991) Cationic surfactants – physical chemistry. Marcel Dekker, New York
- Saleeb FZ, Kitchener JA (1965) J Chem Soc 911
- Scher HB (1999) Controlled-release delivery systems for pesticides. Marcel Dekker, New York
- Scheutjens JMHM, Flerer GJ (1979) J Phys Chem 83:1919
- Scheutjens JMHM, Flerer GJ (1980) J Phys Chem 84:178
- Scheutjens JMHM, Flerer GJ (1982) Adv Colloid Interface Sci 16:341
- Schick MJ (ed) (1966) Nonionic surfactants. Marcel Dekker, New York
- Schick MJ (ed) (1987) Nonionic surfactants: physical chemistry. Marcel Dekker, New York
- Schonfeldt N (1970) Surface active ethylene oxide adducts. Pergamon, Elmsford
- Shinoda K (1967) J Colloid Interface Sci 25:396
- Shinoda K, Saito H (1969) J Colloid Interface Sci 30:258
- Shinoda K, Nagakawa T, Tamamushi BI, Isemura T (1963) Colloidal surfactants, some physicochemical properties. Academic, London
- Silberberg A (1968) J Chem Phys 48:2835
- Smolders CA (1960) Rec Trav Chim 80:650
- Somasundaran P, Goddard ED (1979) Modern Aspects Electrochem 13:207
- Somasundaran P, Hannah HS (1979) In: Shah DO, Schechter RS (eds) Improved oil recovery by surfactant and polymer flooding. Academic, London, p 205
- Stevens CV, Meriggi A, Peristerpoulou M, Christov PP, Booten K, Levecke B, Vandamme A, Pittevels N, Tadros TF (2001) Biomacromolecules 2:1256
- Suzuki M (1993) In : Suzuki M, Chatterton NJ (eds) Science and technology of fructans. CRC Press, Boca Raton, p 21
- Tadros TF (1980) Adv Colloid Interface Sci 12:141
- Tadros ThF (1985) In: Buscall R, Corner T, Stageman JF (eds) Polymer colloids. Appl Sci London, Elsevier, p 105
- Tadros THF (1987) Solid/liquid dispersions. Academic, London
- Tadros TF (1994) Surfactants in agrochemicals. Marcel Dekker, New York
- Tadros TF (2005) Applied surfactants. Wiley-VCH, Germany
- Tadros T (2009) Colloids in agrochemicals. Wiley-VCH, Weinheim
- Tadros TH (2010) Rheology of dispersions. Wiley-VCH, Germany
- Tadros Th F (1973) In: Smith AL (ed) Particle growth in suspensions. Academic, London
- Tadros Th F (1983) In: Poehlein GW, Ottewill RH (eds) Science and technology of polymer colloids, vol II. Marinus Nish of Publishing, Boston
- Tadros Th F, Vincent B (1983) In: Becher P (ed) Encyclopedia of emulsion technology. Marcel Dekker, New York
- Tadros ThF, Booten K, Levecke B, Vandamme A to be published
- Tadros THF, Vincent B (1978) J Colloid Interface Sci 72:505
- Th.F. Tadros, "Polymer adsorption and Dispersion Stability", in "the Effect of Polymers on Dispersion Properties", Editor Th.F. Tadros, Academic Press, London (1981)
- Thompson (Lord Kelvin) W (1871) Phil Mag 42(448)
- van den Boomgaard T, King TA, Tadros THF, Tang H, Vincent B (1978) J Colloid Interface Sci 61:68
- van den Tempel M (1960) Proc Int Congr Surf Act 2:573
- van Olphen H (1963) Clay colloid chemistry. Wiley, New York
- van Os NM, Haak JR, Rupert LAM (1993) Physicochemical properties of selected anionic, cationic and nonionic surfactants. Elsevier, Amsterdam
- Verwey EJW, Overbeek JTG (1948) Theory of stability of lyophobic colloids. Elsevier, Amsterdam
- von Smoluchowski (1914) Handbuch der Electricitat und des Magnetismus, vol II, Barth, Leipzig
- Wagner C (1961) Z Electrochem 35:581
- Wakamatsu T, Fuerstenau DW (1968) Adv Che Ser 71:161
- Walstra P (1983) In: Becher P (ed) Encyclopedia of emulsion technology, vol I. Marcel Dekker, New York
- Walstra P (1996) In: Becher P (ed) Encyclopedia of emulsion technology, vol 4. Marcel Dekker, New York
- Walstra P, Smolders PEA (1998) In: Binks BP (ed) Modern aspects of emulsions. The Royal Society of Chemistry, Cambridge
- Ward AFH, Tordai L (1946) J Phys Chem 14:453



Washburn ED (1921) *Phys Rev* 17:273

Whorlow RW (1980) *Rheological techniques*. Ellis Horwood, Chister

Wilkins RM (ed) (1990) *Controlled Delivery of Crop Protection Agents*. Taylor and Francis, London

Woodford AR (1998) *Dispersible granules*. In: Van Valkenberg W, Sugavanan B, Khetan SK (eds) *Pesticide formulation*. UNIDO, Vienna, New Age International (P) Ltd., New Delhi, India, Chapter 9

---

## Attachment

- ▶ [Deposition](#)
- ▶ [Particle Deposition](#)

---

## Air-Liquid Interface

- ▶ [Interface, Air-liquid](#)

---

## Attractive Forces

- ▶ [Van der Waals Attraction](#)